measurements in this study are conducted after twenty minutes of exposure to CO/H_2 in order to let the reaction reach steady state. It is likely that the C_β already exists on the surface. Bell et al.[41] indicated that C_β does not deactivate the catalysts. The location of C_β has been suggested to be between the metal and the support interface.[41] It is possible that some C_β may occupy active sites for C_{ad}. High P_{H_2} varies the low level of C_{irr}, which results in k_1 increasing with P_{H_2}. An alternative explanation for the observed increase of k_1 with P_{H_2} is "slow oxygen removal." Whenever the steady-state level of O_{ad} is sufficiently high to impair CO dissociation, a varying level of O_{ad} would translate into a varying rate constant, k_1. As $\Theta_{O_{ad}}$ is expected to decrease with increasing P_{H_2}, this also will result in k_1 increasing with P_{H_2}.

From the study of H/D isotope effect (Chapter 5), we found an inverse H/D isotope effect ($R_{CD_4} > R_{CH_4}$) with $\Theta_{CD_x} > \Theta_{CH_x}$ and $k_{CH_x} \simeq k_{CD_x}$. If one of the hydrogenation steps of surface carbon is rate limiting, then one would expect $k_{CH_x} > k_{CD_x}$ since light H_2 generally reacts faster than D_2. However, the observation of $k_{CH_x} \simeq k_{CD_x}$ seems incompatible with what would have been observed if k_2 was a hydrogenation step. The observation of $\Theta_{CD_x} > \Theta_{CH_x}$, implies that in D_2 atmosphere, CO "dissociates" more rapidly than in H_2 atmosphere. This seems consistent with H-assisted CO dissociation. With regard to k_2, it is suspected that a carbon "depolymerization" step or a change in carbon-metal coordination rather than a hydrogen-addition step is rate

determining. Since hydrogen is not involved in rate-limiting step, it will result in $k_{CD_x} \simeq k_{CH_x}$.

With respect to k_1, the possibility of a thermodynamic effect, i.e., a difference in steady-state level of CO dissociation-impairing species such as OH or $C_\beta Hy$ (respectively OD or $C_\beta Dy$) is considered. Additional evidence which suggests the H may not be involved in the rate limiting step is presented in Figure 4-24a.

A special experiment was conducted at one particular reaction condition (T = 230°C, H_2/CO = 3.3, 60 wt % Ni/SiO_2) with $R_{CD_4} = R_{CH_4}$. The ingrowth of $^{12}CH_4$ transient reponses was compared: the ingrowth of $^{12}CH_4$ from $^{13}CO + H_2 \rightarrow {}^{12}CO + H_2$; and the ingrowth of $^{12}CH_4$ from $^{12}CO + D_2 \rightarrow {}^{12}CO + H_2$. The $^{12}CH_4$ transient (from $^{13}CO \xrightarrow{H_2} {}^{12}CO$) represents the carbon involving reaction pathways. The $^{12}CH_4$ transient (from $D_2 \xrightarrow{^{12}CO} H_2$) represents the H involving reaction pathways. As seen in Figure 4-24a, the H involving reaction pathways are much faster than the carbon involving pathways. This observation indicated that the hydrogenation of surface carbon is a fast process. H assisted CO dissociation or hydrogenation of surface active carbon may not involve in rate-limiting step. The result further suggested that the hydrogenation of surface carbon is a process involving a fast equilibrium between each addition of H steps.

The apparent activation energy obtained from TOF of CH_4 and from Θ_C may also bear relevant information regarding the rate-limiting step. The apparent activation energy of the hydrogenation of surface active carbon, C_{ad} ($\simeq$ 10 kcal/g mole Figure 4-8), differs from that of the

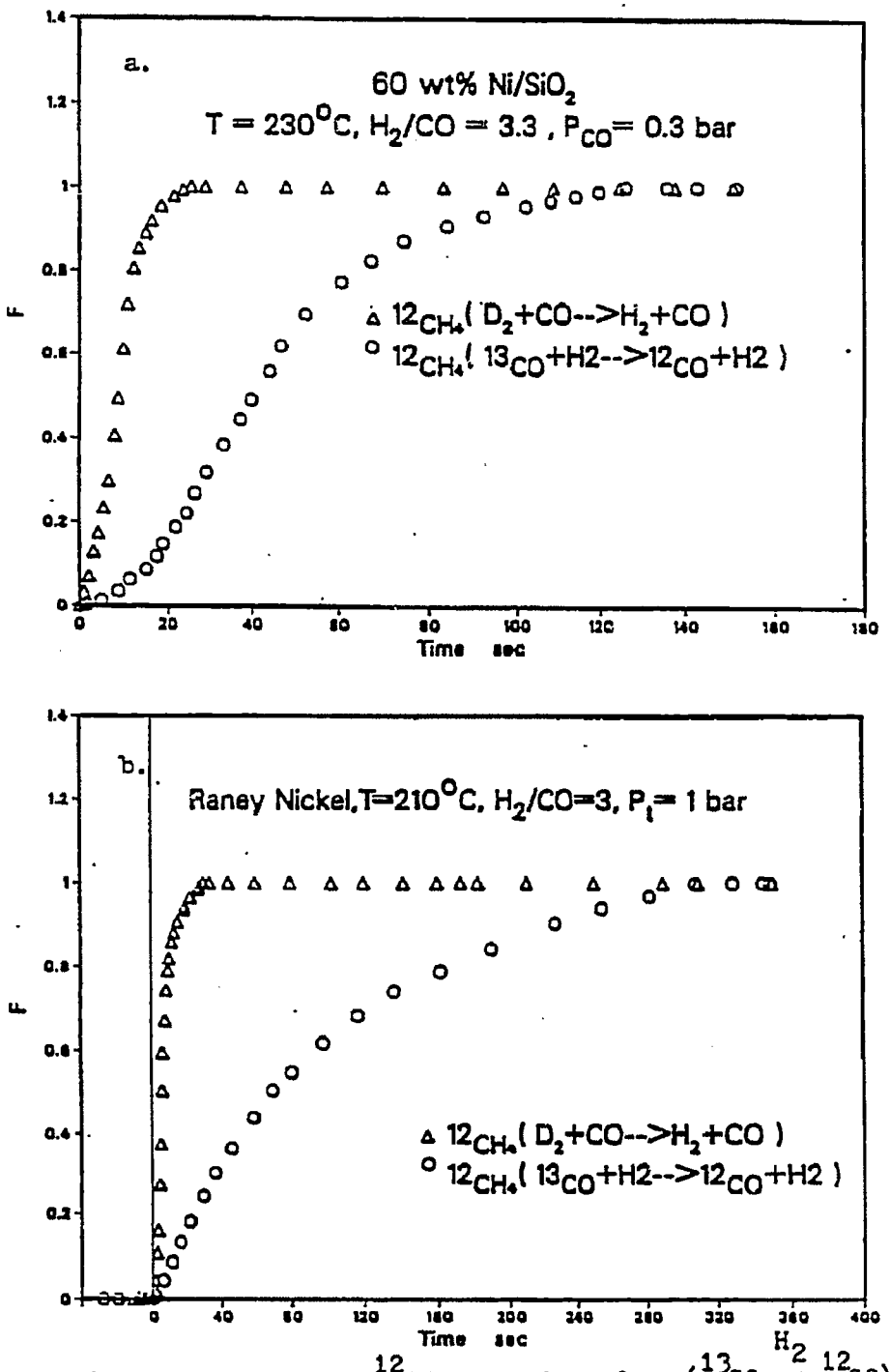

Figure 4-24 Comparsion the $^{12}CH_4$ transient from ($^{13}CO \xrightarrow{H_2} {}^{12}CO$) with the $^{12}CH_4$ transient from ($D_2 \xrightarrow{^{12}CO} H_2$).

methanation reaction (25 - 32 kcal/g mole Table 4-2). This finding suggests that the hydrogenation of surface active carbon does not seem to be rate controlling. Taken together, a simplified reaction scheme is proposed as shown in Figure 4-25. The slow step is either C-C depolymerization or change in C-M coordination.

Literature regarding the C-C depolymerization and change in C-M coordination will be discussed below. Tamaru and coworkers[94,95] have suggested that a part of the carbon inventory on the catalyst is in the form of C chains attached to the metal surface. It was proposed that these species can resupply the catalyst surface with single carbon atom units by scission of the C-C bonds in the chains.

Goddard et al.[96] tried to estimate the energetics of the carbide route to CH_4 on nickel by theoretical methods. Goddard et al.[96] concluded that deposited carbon is not monoatomic, but for a C-C species bonded to 4 nickels in a distorted ethylenic type structure. They also suggest that the following steps are favorable:

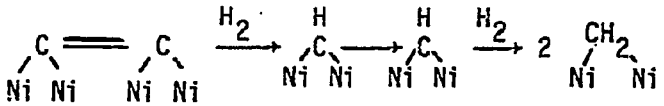

(4-7)

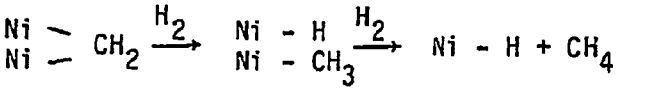

(4-8)

A change in C-M coordination as a rate determining step is also proposed by Hadjigeorghious and Richardson:[17] (i.e.) $(M\text{-}C + M \xrightarrow{RDS} M_2\text{-}C)$.

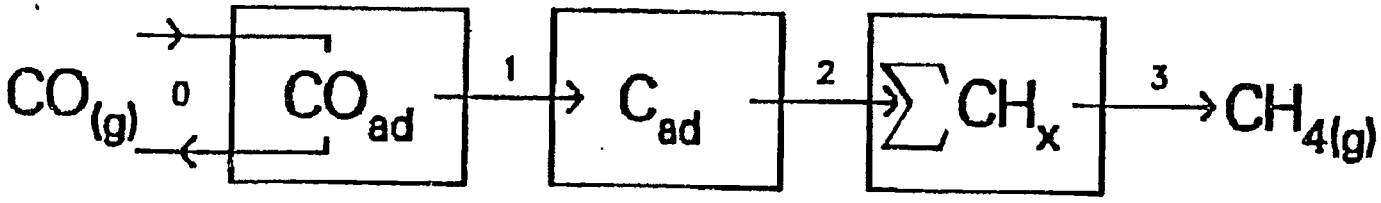

Figure 4-25 Proposed reaction pathway scheme for methanation

The mechanism of methanation can be described as follows. Both H_2 and CO in the gas phase are virtually in equilibrium with adsorbed H atoms (Chapter 6) and CO. The dissociation of CO is essentially irreversible. The reaction of surface carbon proceeds through a slow step (C-C depolymerization or change in the C-M coordination) and then reacts very rapidly via a reversible sequence of steps to form a CH_x (x = 1 - 3) group. The $CH_{3_{ad}}$ species further reacts with H_{ad} to form CH_4. The proposed mechanism included the following elementary reaction steps.

(1) $CO_{(g)} \longleftrightarrow CO_{ad}$ k_{co}

(2) $H_{2(g)} \longleftrightarrow 2\ H_{ad}$ k_{H_2}

(3) $CO_{ad} + C_{ad} + O_{ad}$ k_1

(4) $C_{n_{ad}} \xrightarrow{RDS} C_{n-1_{ad}} + C_{ad*}$ (C-C depolymerization) k_2

or

(4) $C_{ad} \xrightarrow{RDS} C_{ad*}$ (change in C-M coordination) k_2

(5) $C_{ad*} + H_{ad} \rightarrow CH_{ad}$ k_3

(6) $C_{ad} \rightarrow C_{irreact}$ k_4

(7) $O_{ad} + H_{ad} \rightarrow OH_{ad}$ k_5

(8) $OH_{ad} + H_{ad} \rightarrow H_2O$ k_6

(9) $CH_{ad} + H_{ad} \longleftrightarrow CH_{2\ ad}$ k_7

(10) $CH_{2\ ad} + H_{ad} \longleftrightarrow CH_{3\ ad}$ k_8

(11) $CH_{3_{ad}} + H_{ad} \rightarrow CH_{4(g)}$ k_{CH}

4.4.5 Reactivity and Coverage of Reaction Intermediates

The $\Theta_{C_{ad}}$ follows a general trend; it increases with increasing temperature (Figures 4-8). This phenomenon can be explained in two ways.

1. With increasing temperature, a larger part of the catalyst surface participates in catalysis as the result of surface heterogeneity.
2. Higher temperature favors CO dissociation, resulting in more formation of C_{ad}.

Goodman [36] also indicated that at fixed reaction condition (H_2/CO ratio and total pressure), increasing the temperature results in a progressive increase in the "carbidic" carbon species on the surface

until a mixed carbide/graphite carbon is observed. On further heating this produces multilayer graphite and deactivation.

The $\Theta_{C_{ad}}$ varies with H_2/CO ratio as shown in Figure 4-9. Different trends are observed. For Raney nickel and Ni/SiO_2, $\Theta_{C_{ad}}$ increases with H_2/CO ratio. The observation can be explained by a varying low level of C_{irr} and O_{ad} on the surface. However, the Ni powder showed an opposite trend; this difference trend is probably due to the nature of Ni powder (See 4.4.9.). The low-surface-area metal powders are difficult to prepare and to maintain in a clean state.

The surface oxygen may also affect the Θ_{Cad}. Recently, a study of Raney nickel by ESCA[97] indicated a high concentration of oxygen on the catalyst surface. The results of this study also suggest that the surface has a high level of oxygen (Figures 4-21,4-22). It is clear that for Raney nickel and Ni/SiO_2, the surface oxygen has an effect on Θ_C. For Ni powder, a similar result is not observed (Figure 4-23), indicating that surface oxygen containing species on Ni powder is low. Goodman et al.[36] also reports no detectable oxygen species on Ni(100) surface through a study by AES. Different oxygen levels on the surface may result in different behavior of Θ_{Cad}.

The reactivity of all the nickel catalysts in this study displayed the same trend (Figure 4-11~15), increasing with increasing temperature at constant H_2/CO ratio. It also increases with H_2/CO ratio at constant temperature. For Ni/SiO_2, the reactivity is a strong function of reaction conditions. When P_{CO} is maintained constant, it will increase with P_{H_2}. When P_{H_2} remains constant, it will decrease as the Pco

increases. Figure 4-15 (k vs. T) and Figure 4-14 (k vs. H_2/CO ratio with different catalysts) show that the overall trend for k is similar. However, by comparing different catalysts, significant differences are observed (Figure 4-15). The reactivity of intermediates depend on the nature of nickel. Different catalysts have different distribution of step sites and smooth planes. The binding of carbon atoms to steps is stronger than on smooth planes[100]. The measured k_2 is either breaking carbon-carbon bonds or breaking carbon-metal bonds. For the later case of breaking carbon-metal bonds, different catalysts will have different k's. The k can also represent the ease of breaking carbon-carbon bonds or breaking carbon-metal bonds. High temperatures may increase the mobility of carbon (change in C-M coordination) and increase the vibration between carbon-carbon bonds (C-C depolymerization). This results in an increase in k increase with temperature. An alternative explanation for the observed increase of k with temperature is that with a temperature increase, not only more intermediates are formed, but also the reactivity of the intermediate increases.

Data presented in Figure 6-14 indicates that the amount of adsorbed hydrogen increases with P_{H_2}. Also, the observation that k increases with P_{H_2} is shown in Figure 4-10. Taken together, the variation in k with P_{H_2} may be explained by the nature of carbon condition which is a function of P_{H_2}. The increasing P_{H_2} may favor the mobility of carbon (change in C-M coordination) and increase the vibration between carbon-carbon bonds (C-C depolymerization). This will result in a higher k

with higher P_{H_2}. However, the details of how P_{H_2} affects the carbon-carbon bonding or carbon-metal bonding are unclear so far.

4.4.6 Active Sites for Methanation

Ponec[87] presented evidence that the dissociation of CO_{ad} requires sites which are multiply coordinated (multisites) by suitable metal atoms. CO dissociation has also been shown to require a large ensemble of surface atoms [18,22,87].

Biloen and Sachtler[8] suggested that dissociation of CO occurs on the sites coordinated by several metal atoms. The undissociated CO_{ad} molecule is occupied on the on-top sites. As soon as a multisite becomes available, it is rapidly filled with CO_{ads}. The carbidic intermediates may also occupy the multisites. Somorjai et al.[99] suggest that CO dissociation proceeds preferentially on various defects like steps, kinetic, etc. Ordered defects appear to adsorb CO easier and may activate CO more strongly. Various reports have reported the locations of Cα (reactive) and Cβ (unreactive).

Schouten et al.[100] suggest that adsorbed, atomic carbon (Cα) is more stable on Ni (100) than Ni (110), which in turn is much more stable than adsorbed carbon on Ni(111). Rostrup-Nielsen[101] report that carbon was formed in the Boudard reaction on Ni(111) but could not be observed on Ni(100) and (110).

The dispersed carbon phase (Cα) on Ni (001) is considered to be made up of single carbon atoms bonded to the Ni lattice at a high

coordination number on both flat[102] and stepped[103] (001) surfaces. It has been suggested that on Ni(110), the dispersed form of chemisorbed carbon is composed of diatomic carbon species.[104,105] Bell and Winslow [41] indicate that both the structure of C_β, and its location relative to the surface of the catalyst, are difficult to define. They propose that C_β attaches to the support and/or is held in the pores between the metal particles. Wise's[35] remark may well clarify the exact location of carbon. Wise indicates the local surface structure of Ni crystallite governs the type of surface carbon formed. In other words, one crystal face may produce C_α and the other may produce C_β.

It is speculated that carbidic active carbon bounds to nickel through three or more atoms. The unreactive carbon is most probably located either between the metal and support interface, or between the pores and metal particles. The adsorbed CO is probably located on top of the sites.

It appears that the sites for CO dissociation and for surface carbon depend on the chemical and physical state of the metal. The reaction condition may also affect the chemical and physical state of the metal. Factors such as support, promoter, particle size, and impurity may also affect the state of metal catalysts.

Figure 4-16 shows the Arrhenius plots for different Ni catalysts. The difference in TOF for different catalysts is less than a factor of 10. A difference of at least a factor ten is the criterion for a structure-sensitive reaction.[49-51] Methanation is, according to this definition, a structure-insensitive reaction. However, Figures 4-15 and

4-8 show significant differences in k and Θ for different Ni catalysts. The TOF, Θ, k from Raney nickel were compared at one typical reaction condition (210°C, $H_2/CO = 3$) with that of 60 wt % Ni/SiO_2. The values of $TOF_{Raney\ nickel}/TOF_{Ni/SiO_2}$, $\Theta_{Raney\ nickel}/\Theta_{Ni/SiO_2}$ and $k_{Raney\ nickel}/k_{Ni/SiO_2}$ are 4.4, 6 and 0.73, respectively. It is concluded that the k and Θ are significantly more structure/catalyst sensitive than what is indicated by their algebraic product

$$k \cdot \Theta = TOF$$

Various factors which may affect the k and Θ are discussed in the following sections.

4.4.7 Particle Size Effect

Coenen et al.[55] suggest that the larger crystallites are particularly active in the reaction, and a maximum activity is found within the appropriate particle size range. Coenen et al.[106] also report that, with silica supported Ni, a trend in activity seems to occur; the small Ni crystallites (45 Å) have a lower TOF_{CH_4} than larger crystallites of 130 Å particles. However, large unsupported Ni crystallites also exhibit a low specific activity.

Maximum activity occurs over a specific range of crystallite sizes. It can be expected that, as the size of the metal particles varies, the relative population of atoms in the plane and atoms on edges, corners (or those near to these or other defects) would vary correspondingly. The concentration of sites with both an exceptionally

low coordination numbers, such as edges and corners or an exceptionally high coordination number, as occurs at sites in the transition zones between various crystallographic planes, can further vary due to the fact that small particles favor special particle shapes. It is possible that a particle size range exists which has the most favorable conditions for methanation.

How does the particle size effect translate into k and θ effects? The particle sizes measured by H_2 TPD for Ni/SiO_2, Raney nickel and Ni powder are 62 Å, 188 Å and 900 Å respectively (Table 2-1). In view of the particle size, Raney nickel seems to be in the size range which favors methanation (see Figure 1 in Ref. 55). Ni/SiO_2 has the smallest particle size which may result in low methanation activity. Ni powder has the largest particle size of the catalysts investigated, that may still have higher methanation activity than the Ni/SiO_2. From Figure 4-8 and 4-9 the order of θ_C is Raney nickel > Ni powder > Ni/SiO_2. The order of θ_C seems consistent with the particle size. Many possibile explanations can be formulated.

As smaller particles bind oxygen from CO dissociation more firmly than larger particles, the θ_C (coverage of reaction intermediates) is lower since O_{ad} may inhibit CO dissociation. Smaller particles allow a faster deactivation of carbon, resulting in a lower steady state θ_C. Also, small particles may bind carbon more firmly causing its lower θ_C value. It is more difficult to remove carbon from small particles as the steady state θ_C is low.

However, the trend observed for k seems to vary significantly with reaction conditions (Figures 4-14 and 4-15). At high temperatures and high H_2/CO ratios, a different trend is found: $k_{Ni/SiO_2} > k_{Raney\ nickel} > k_{Ni\ powder}$. For Ni/SiO_2, Ni is highly dispersed on the support SiO_2. High temperatures and high H_2/CO ratios may favor the C-C depolymerization or change in the C-M coordination. Ni powder is a highly packed bulk structure on which C-C depolymerization and change in C-M coordination may not be favorable. For Raney nickel the particle size falls in between those sizes of Ni/SiO_2 and Ni powder, as does k_2. The effect of reaction conditions (T and H_2/CO ratio) on k_2 is more pronounced on Ni/SiO_2 than other Ni catalysts. This is probably due to the support effect.

4.4.8 Support Effect

Recent investigations[91,107] have provided evidence that supports can significantly influence the adsorption and CO hydrogenation activity/selectivity properties of Ni.

The activity for methanation on different supported Ni catalysts was reported by Vannice.[108] The relative order is $Ni/TiO_2 > Ni/Al_2O_3 > Ni\ powder > Ni/SiO_2$. Bartholomew and Vance[107] also showed that support significantly influences the specific activity and kinetics of carbon hydrogenation on Ni with the order of $Ni/TiO_2 > Ni/Al_2O_3 > Ni/SiO_2$. As presented in Figure 4-16, the order of specific activity is Raney nickel > Ni powder > Ni/SiO_2. It seems that the support effect

can be directly translated to a Θ_C effect. Figure 4-8 indicates that the order of Θ_C is Raney nickel > Ni powder > Ni/SiO_2. However, the k effect on support shows different trend - Ni/SiO_2 > Raney nickel > Ni powder. It appears that the k effect cannot be satisfactorily explained by the support effect only.

4.4.9 Effect of Nature of Nickel Catalysts on k and on Θ

The higher specific activity of Raney nickel relative to Ni powder and Ni/SiO_2 found in this study suggests that aluminum metal or Al_2O_3 at the surface is a chemical promoter for methanation, presumably as a result of an electronic interaction in the Ni-Al alloy.

It has been reported that the electron density of Ni metal is modified by the additives Al. The change in the electron density of Ni metal remarkably alters the specific activity of methanation.[109,110] The high electron density of the Ni metal in Raney nickel catalyst facilitates the dissociation of adsorbed CO by enhanced $d\pi$-$P\pi^*$ back bonding. This increases the extent of π-back bonding in the Ni-CO complex, resulting in an increased Ni-CO bond strength and a decreased C-O bond strength. Our observation of Θ_C Raney nickel > Θ_C Ni powder > Θ_C Ni/SiO_2 is consistent with the electronic interaction in the Raney nickel. Bartholomew and Mustard[111] have shown that the reductive behavior of metal on various supports depends, among other things, on the degree of dispersion of the metal, with smaller crystallites being harder to reduce. The reduction of silica supported catalysts is a very

complex process. Due to the presence of basic silicates, complete reduction can only be achieved at temperatures of 700°C or higher.[106] Then serious sintering of the resulting Ni metal occurs so that the high degree of dispersion, which is the salient feature of this type of catalysts, is lost. Therefore, incomplete reduction (70-80% according to manufacturers' information) at 350°C is expected. The unreduced Ni^{x+} species may cause the low Θ_C values in Ni/SiO_2.

This is explained by the presence of the less reducible solid Ni species, which can withdraw electrons from the surrounding Ni^0 atoms. Since the C-O bond of the CO species adsorbed on these electron-deficient Ni^0 atoms is not broken under the conditions of the reaction, less Θ_C is expected. These inactive particles (Ni^+ and neighboring Ni^0 atoms) result in a geometric dilution effect of the active unperturbed Ni^0 phase, leading to a lower Θ_C values.

The Ni^{2+} may also trap hydrogen and at high H_2/CO and/or high temperature the redox equilibrium might shift to the right.[112]

$$Ni^{2+} + H_2 \rightleftharpoons 2\ H^+ + Ni^0 \qquad (4\text{-}9)$$

This results in an increasing Θ_C and k_2. For Θ_C, the results can be attributed to the presence of more available Ni^0 sites. The increasing k_2 may be explained by the presence of additional H^+ species that may tend to facilitate the C-C depolymerization and the change in C-M

coordination. The behavior of Ni powder as shown in Figure 4-9 (Θ_C decreases as H_2/CO ratio is increased) may be explained by the following hypothesis.

According to the report by Goodman et al.[36], the Ni surface has no detectable oxygen. Results from the study (Figure 4-23) also indicate that the oxygen level is very low. The "slow oxygen removal" may not affect Θ_C in nickel powder. Ni powder is composed of bulk Ni particles. It is speculated that during the methanation, the C_{irr} continuously and irreversibly blocks the active sites. The experimental sequences for measuring Θ_c on Ni powder followed a variation of H_2/CO ratio from low to high, at constant temperature, which may cause a decrease in Θ_C as H_2/CO is increased (C_{irr} blocks the sites during the measurements of Θ_c). Θ_{CO} data indicates that it remains essentially constant during the reaction. Besides, Ni powder has no support metal interface available for C_{irr} deposited. The C_{irr} may deposit on active sites. This site blocking in Ni powder will not affect k. The k behavior seems normal (Figures 4-14, 4-15). Another hypothesis is the impurity in Ni powder. It is likely that high P_{H_2} favors the mobility of those impurities toward active sites. This also results in the decrease in Θ_C as H_2/CO ratio is increased. However, knowledge of the crystal orientation and the distribution of impurities, as well as their electronic state, is poor.

It appears that factors such as effect of support, reducibility, electronic properties, particle size, impurity and reaction conditions may complicate the overall observed effect on the k and Θ. It is,

therefore, extremely difficult to correlate the effect of these factors on k and Θ. However, it is clear that the nature of nickel catalyst has a significant effect on k and Θ. The production of carbidic carbon and the removal of carbidic carbon is a structure/catalyst sensitive process.

4.5 Conclusions

1. A low coverage in reaction intermediates are not due to the fact that a carbidic adlayer blocks a large fraction of the catalyst surface.

   Small coverages in C_{irr} and oxygen appear to inhibit the CO dissociation, thereby limiting the steady-state production of carbidic reaction intermediates.

2. A proposed mechanism is shown in Figure 4-25 (p. 113).

   H_2 and CO in the gas phase are in equilibrium with adsorbed H atoms and CO. The dissociation of CO is essentially irreversible. The reaction of surface carbon proceeds through a slow step (change in the C-M coordination or C-C depolymerization). The reaction then proceeds very rapidly via a reversible sequence of steps to form a CH_x (x = 1 - 3) group. The CH_{3ad} species further reacts with H_{ad} to form of $CH_{4(g)}$.

3. The production and consumption of carbidic intermediates is a sensitive function of the nature of the catalyst surface. The k_2 and $\Theta_{C_{ad}}$ are significantly more structure/catalyst sensitive than what is being indicated by their algebraic product $k_2\Theta_{C_{ad}} = TOF_{CH_4}$.

5.0 H/D ISOTOPE EFFECT ON RANEY NICKEL, Ni/SiO_2 AND NICKEL POWDER

5.1 Background

Isotopic transient methods provide an excellent way to study the H/D isotope effect in methanation. The study of H/D isotope effect in methanation as a function of reaction condition and different nickel catalysts provided a deeper understanding of the H/D isotope effect. The H/D effect experiments were conducted at P_{tot} = 1 bar for Raney nickel and nickel powder. For 60 wt % Ni/SiO_2, P_{tot} = 4 bar instead of 1 bar was used.

5.2 Results

By conducting $H_2/^{12}CO \rightarrow H_2/^{13}CO$ and $D_2/^{12}CO \rightarrow D_2/^{13}CO$ transients the (k, Θ) of CD_x intermediates could be compared with (k, Θ) of CH_x intermediates. The steady state CD_4 and CH_4 production was also compared at the same reaction conditions, in order to determine the overall H/D isotope effect. The dependence of overall H/D isotope effect (R_{CD_4}/R_{CH_4}) on the H_2/CO ratio with Raney nickel at 192°C is shown in Figure 5-1. The inverse H/D isotope effect ($R_{CD_4}/R_{CH_4} > 1$) is found on Raney nickel and increases with the H_2/CO ratio. Figures 5-1 also displays the k_{CD_x}/k_{CH_x} and $\theta_{CD_x}/\theta_{CH_x}$ vs. H_2/CO ratio respectively

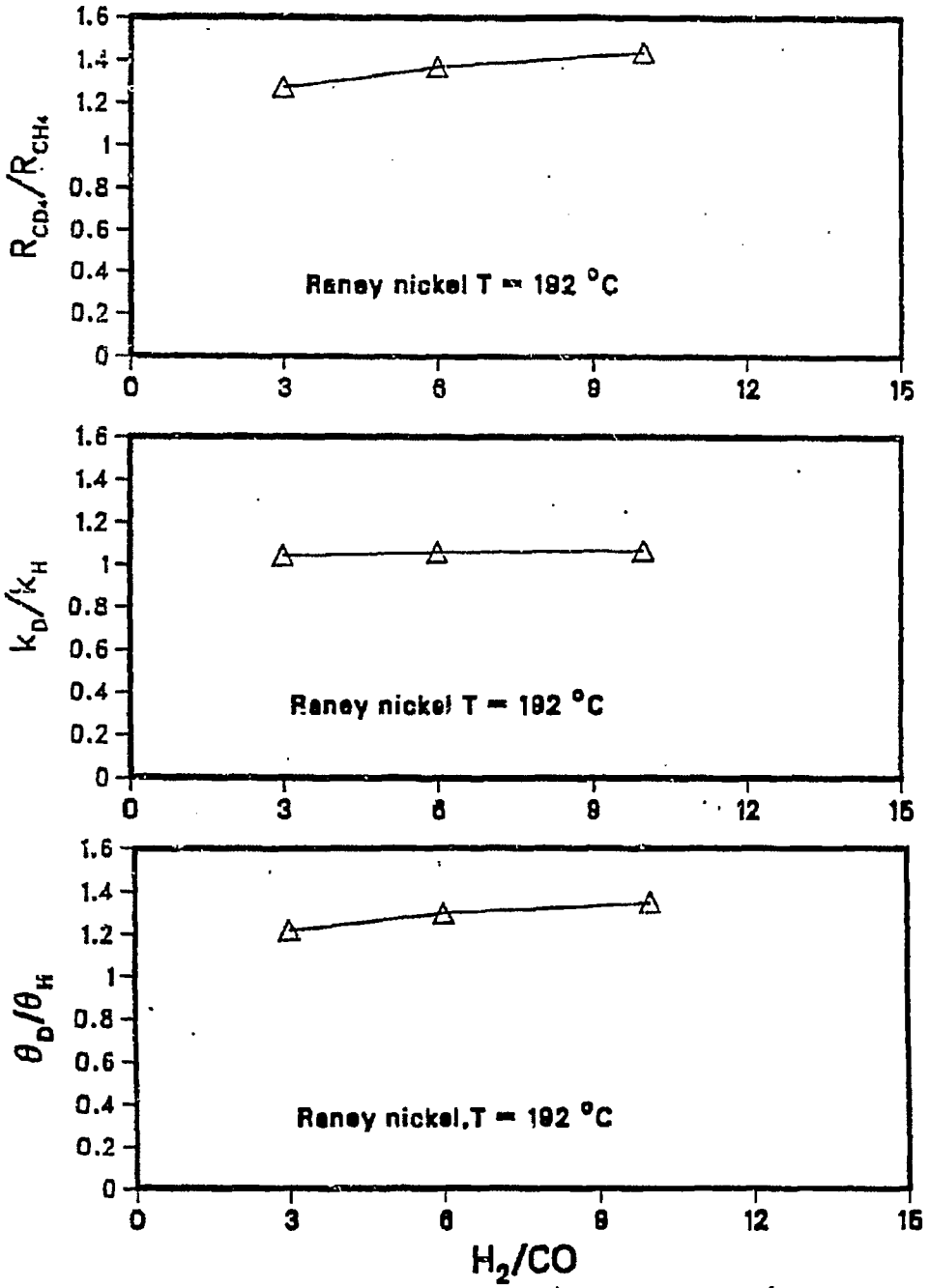

Figure 5-1 Dependence of the kinetic H/D effect on H_2/CO ratio (Raney nickel)

on Raney nickel. The k_{CD_x}/k_{CH_x} values shown are highly independent of H_2/CO ratios and $k_{CD_x} \simeq k_{CH_x}$. As seen in Figure 5-1, the result clearly indicate that the overall H/D isotope effect on Raney nickel is merely a Θ effect. The trend in $\frac{\Theta_{CD_x}}{\Theta_{CH_x}}$ is similar to that observed for $\frac{R_{CD_4}}{R_{CH_4}}$. The data presented in Figure 5-1 indicates that the origin of H/D isotope effect in Raney nickel is due to the difference of coverages in reaction intermediates. At higher temperature, similar behavior is also observed, but the overall H/D isotope effect is less pronounced. The details are listed in Table 5-1. Table 5-1 also presents the temperature dependence of the H/D isotope effect over Raney nickel at constant H_2/CO ratio. The data indicated that the inverse H/D effect decreased as temperature increased, however, $k_{CD_x} \simeq k_{CH_x}$ was observed. The overall H/D isotope effect again is due to the Θ effect. The overall inverse H/D effect obtained from Raney nickel is close to the results reported in literature.[9,7]

In 60 wt % Ni/SiO_2, the H/D isotope effect study was conducted in a different way. By using a buffering gas He and maintaining the total pressure constant (4 bar), P_{CO}, P_{H_2} and P_{D_2} were independently changed. The results of H/D isotope effect are presented in Figures 5-2 and 5-3.

Figure 5-2 shows the $\frac{R_{CD_4}}{R_{CH_4}}$, k_{CD_x}/k_{CH_x} and $\Theta_{CD_x}/\Theta_{CH_x}$ as a function of P_{H_2}. As indicated from Figure 5-2, the overall H/D isotope effect increases with the P_{H_2}. The $k_{CD_x} \simeq k_{CH_x}$ is also shown in Figure 5-2. The result suggests that the overall H/D effect is merely a Θ effect.

Table 5-1

Effect of Reaction Conditions on
H/D Isotope Effect in Raney Nickel

T	H_2/CO	TOF $x10^{-4}$	k $x10^{-3}$	Θ $x10^{-2}$
212	3	20.32	12.006	16.93
212	6	31.49	13.82	22.78
212	10	43.223	20.52	21.66
212	20	81.16	25.84	31.4
212	30	106.21	32.16	33.02

T	D_2/CO	TOF $x10^{-4}$	k $x 10^{-3}$	Θ $x10^{-2}$
212	3	21.95	12.13	18.08
212	6	34.74	13.95	24.9
212	10	48.68	21.626	22.51
212	20	92.6	24.06	38.48
212	30	123.65	29.4	41.94

T		R_D/R_H	H_K/D_K	H_Θ/D_Θ
212	3	1.08	1.01	1.0679
212	6	1.103	1.009	1.093
212	10	1.126	1.053	1.068
212	20	1.1408	0.931	1.22
212	30	1.164	0.914	1.27

T	H_2/CO	TOF $x10^{-4}$	k $x10^{-3}$	Θ $x10^{-2}$
192	3	5.195	9.725	5.34
212	3	20.32	12.006	16.93
232	3	92.318	24.1	38.3
252	3	323.39	51	63.41

	D_2/CO			
192	3	6.603	10.14	6.509
212	3	21.95	12.13	18.08
232	3	98.177	28.0	36.1
252	3	333.1	53.7	63.18

T		R_D/R_H	D_K/H_K	D_Θ/H_Θ
192	3	1.27	1.0429	1.218
212	3	1.08	1.01	1.0679
232	3	1.063	1.16	0.915
252	3	1.03	1.033	0.9963

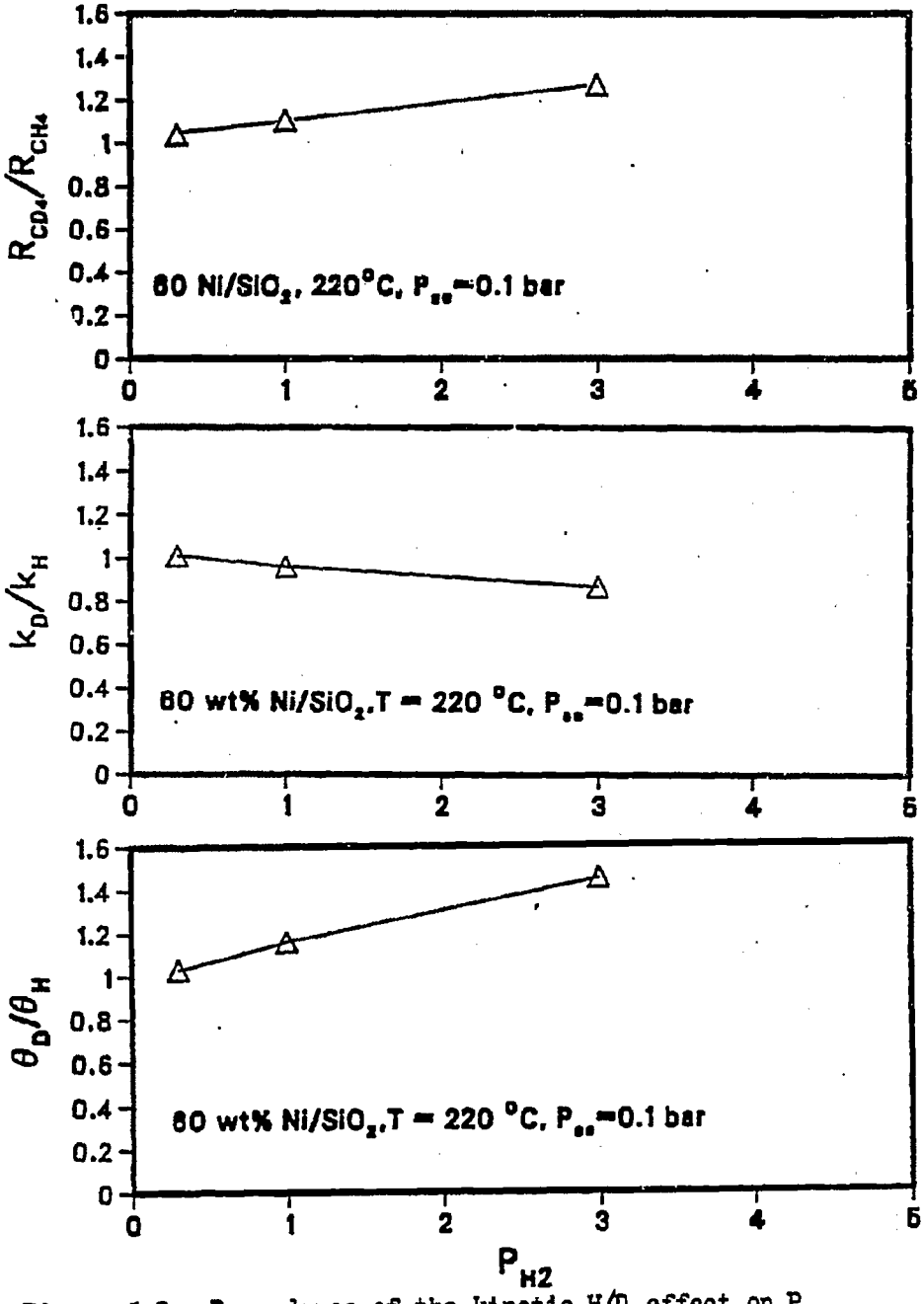

Figure 5-2 Dependence of the kinetic H/D effect on P_{H_2} (60 wt % Ni/SiO_2)

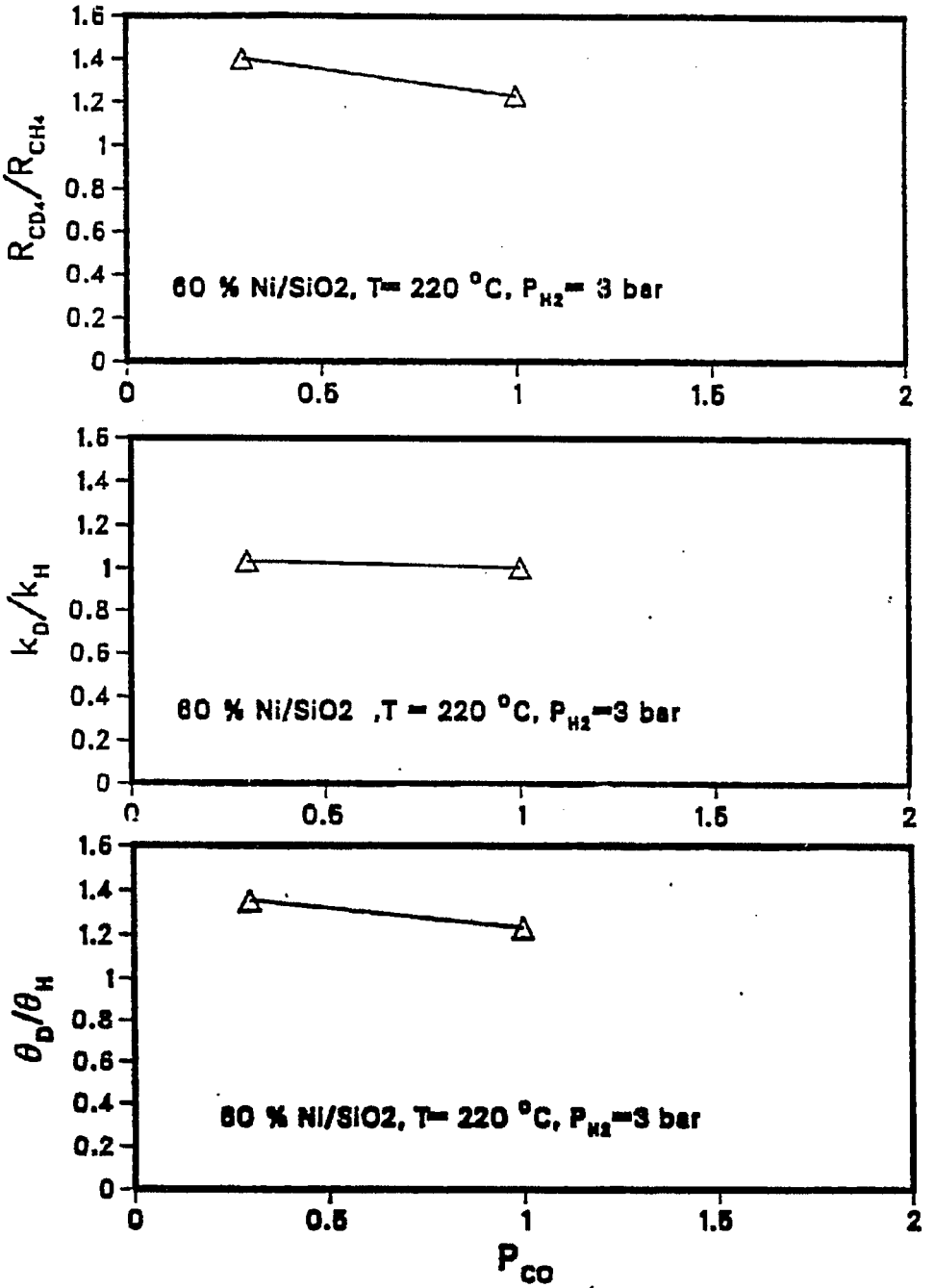

Figure 5-3 Dependence of the kinetic H/D effect on P_{CO} (60 wt % Ni/SiO_2)

The R_{CD_4}/R_{CH_4}, k_{CD_x}/k_{CH_x} and $\Theta_{CD_x}/\Theta_{CH_x}$ ratios are displayed as a function of Pco in Figure 5-3. The inverse H/D isotope effect decreases as Pco increases. k_{CD_x} is close to k_{CH_x}, as shown in Figure 5-3. The $\Theta_{CD_x}/\Theta_{CH_x}$ also decreased with increasing Pco.. The values are listed in Table 5-2. A typical result at Pco = 0.3 bar, P_{D_2} or P_{H_2} = 3 bar and T = 220°C is shown in Figure 5-4. As seen in Figure 5-4, the decay of transient responses CD_4 and CH_4 are indistinguishable and $k_{CD_x} \simeq k_{CH_x}$. At this particular condition, the data confirms $k_{CD_x} \simeq k_{CH_x}$. The R_{CD_4}/R_{CH_4} and k_{CD_x}/k_{CH_x} are 1.4 and 1.03, respectively. This results in $\Theta_{CD_x}/\Theta_{CH_x}$ = 1.35. The H/D effect is due to a Θ effect.

The influence of temperature on the H/D isotope effect on 60 wt % Ni/SiO_2 is shown in Table 5-2. The overall H/D isotope effect decreases as temperature is increased. The Θ effect also decreases as temperature increases. The observed inverse H/D isotope effect ($R_{CD_4} > R_{CH_4}$) on 60 wt % Ni/SiO_2 is consistent with the result reported by Coenen.[9]

Similar experiments were conducted on Ni powder at P_{tot} = 1 bar and T = 210°C. The results are shown in Table 5-3. Several features are noteworthy. First, no appreciable H/D isotope effect is found. Secondly, the $k_{CD_x} \simeq k_{CH_x}$.

The amount of CO_{ad} on the catalyst surface can also be determined during the transient experiments. The amount of adsorbed CO in H_2 is close to that in D_2 (i.e., CO_{ad} in $H_2 \simeq CO_{ad}$ in D_2). (Figure 4-4, Figure 4-5.)

A summary of the important results in H/D isotope effect study is given below:

Table 5-2

Effect of Reaction Conditions on H/D Isotope Effect on 60 wt % Ni/SiO_2

Ni/SiO_2

T	P_{CO}	P_{H_2}	H_2/CO	TOF $x10^{-4}$	k $x10^{-3}$	Θ $x10^{-2}$
220	0.1	0.3	3	7.101	17.13	4.1434
220	0.1	1	10	13.421	22.20	6.044
220	0.1	3	30	30.13	31.08	7.33
220	0.3	3	10	18.371	41.08	4.188
220	1	3	3	8.842	15.68	5.63

T	P_{CO}	P_{D_2}	D_2/CO	TOF $x10^{-4}$	k $x10^{-3}$	Θ $x10^{-2}$
220	0.1	0.3	3	7.387	17.31	4.267
220	0.1	1	10	14.856	21.05	7.0568
220	0.1	3	30	38.38	35.89	10.69
220	0.3	3	10	25.739	41.47	6.205
220	1	3	3	10.92	15.75	6.93

T	P_{CO}	P_{H_2}		R_D/R_H	D_k/H_k	D_Θ/H_Θ
220	0.1	0.3	3	1.04	1.01	1.03
220	0.1	1	10	1.106	0.948	1.16
220	0.1	3	30	1.27	0.8736	1.45
220	0.3	3	10	1.40	1.032	1.35
220	1	3	3	1.23	1.004	1.23

Table 5-2 (Continued)

Effect of Reaction Conditions on H/D Isotope Effect
in 60 wt % Ni/SiO_2

T	H_2/CO	TOF $x10^{-4}$	k $x10^{-3}$	Θ $x10^{-2}$
180	3.3	0.947	2.5764	3.674
200	3.3	2.736	5.9637	4.588
220	3.3	9.19	19.113	4.808

T	D_2/CO	TOF $x10^{-4}$	k $x10^{-3}$	Θ $x10^{-2}$
180	3.3	1.084	2.398	4.52
200	3.3	3.168	6.428	4.927
220	3.3	9.676	18.69	5.176

T		R_D/R_H	D_K/H_K	D_Θ/H_Θ
180	3.3	1.144	0.9307	1.23
200	3.3	1.157	1.077	1.074
220	3.3	1.05	0.978	1.07

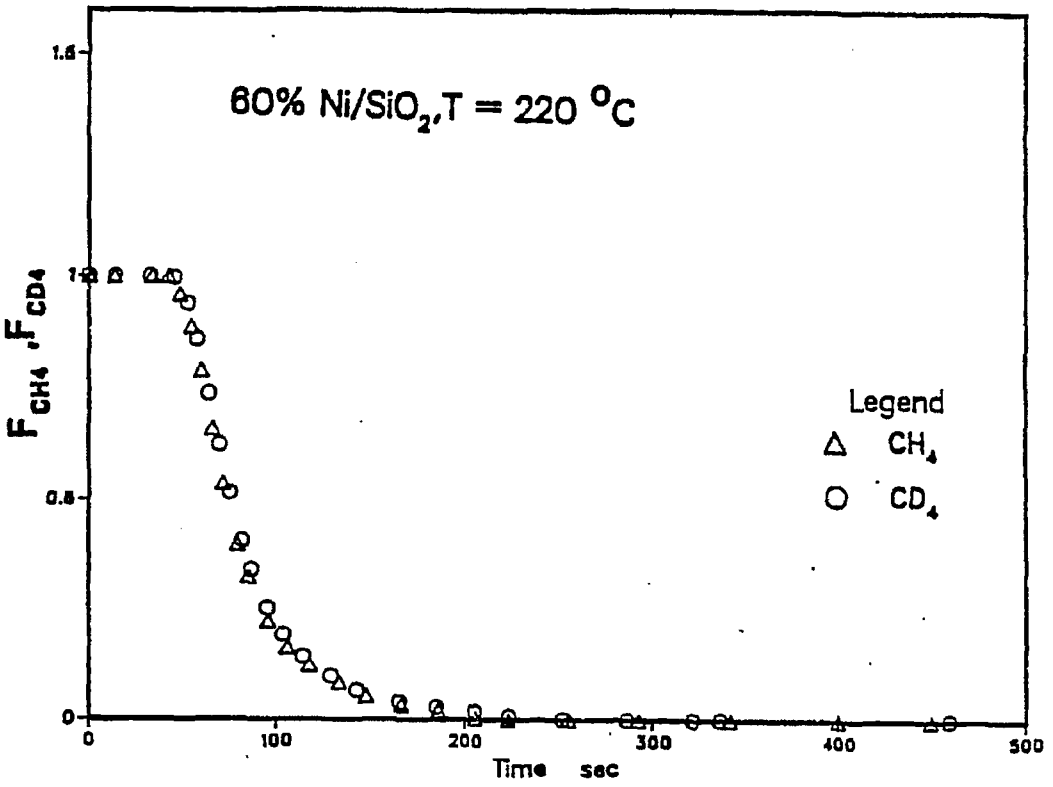

Figure 5-4 The decay of CH_4 and CD_4 transients at P_{CO} = 0.3 bar , P_{H_2} = 3 bar in 60 wt% Ni/SiO_2

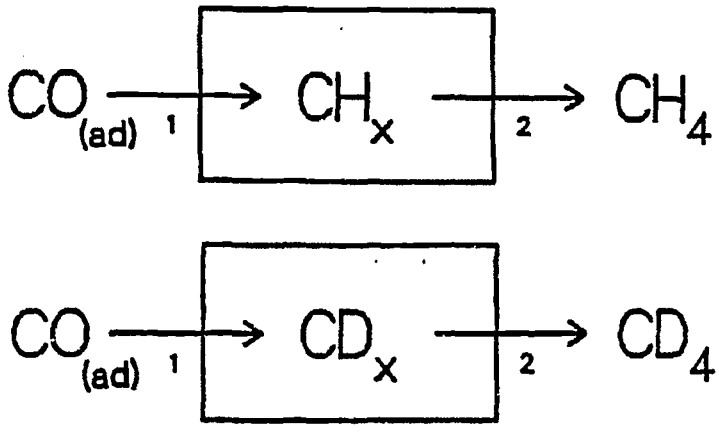

Figure 5-5 Simplified reaction pathway scheme for H/D isotope effect study

Table 5-3

Effect of Reaction Conditions on H/D Isotope Effect in Nickel Powder

T	H_2/CO	TOF $x10^{-4}$	k $x10^{-3}$	Θ $x10^{-2}$
210	3	7.82	6.76	11.55
210	10	12.63	10.63	11.87
210	25	15.45	25.56	6.04
T	D_2/CO	TOF $x10^{-4}$	k $x10^{-3}$	Θ $x10^{-2}$
210	3	8.258	6.639	12.43
210	10	12.984	10.75	12.07
210	25	15.334	22.06	6.94
T		R_D/R_H	D_K/H_K	D_Θ/H_Θ
210	3	1.056	0.98	1.076
210	10	1.028	1.01	1.016
210	25	0.99	0.86	1.149

- Raney-nickel and Ni/SiO_2 showed an inverse H/D isotope effect. It is a function of the (H_2/CO (P_{CO} and P_{H_2})), and it decreases as the temperature increases.
- The origin of H/D isotope from Raney nickel and Ni/SiO_2 is due to the Θ effect (coverage of reaction intermediate effect) with $\Theta_{CD_x} > \Theta_{CH_x}$.
- No appreciable H/D isotope effect on unsupported Ni powder is observed, while a pronounced H/D inverse isotope effect on Raney nickel and Ni/SiO_2 is found.

5.3 Discussion

There is some debate as to whether the slow step (RDS) in methanation is CO dissociation (H-assisted or H-unassisted), or one of the hydrogenation steps of surface carbon (formation CH_x, or further reaction of CH_x).[2-16]

No matter whether the slow step involves CH_x or CH_nO, the inclusion of H should lead to a signficant H/D isotope effect where hydrogen is replaced by deuterium. However, both Mori et al[7] and Coenen et al.[9] reported inverse H/D isotope effects on Ni/SiO_2 but with different slow steps (CH_nO vs. CH_x). The advantages of using isotopic transient method in study of H/D effect are that not only can the steady-state rate be observed, but the k and Θ under reaction conditions in H_2 and in D_2 can

be determined. The study of H/D isotope effect in this investigation gives us a greater understanding of the slow step.

Figure 5-5 is the simplified reaction scheme; the k_2 and Θ_{CH_x} are what we measured in this study.

At steady-state condition

$$k_1\Theta_{CO_{ad}} = k_2\Theta_{CH_x} \qquad (5\text{-}1)$$

From Chapter 4, Figures 4-4 and 4-5, it can be concluded that the amount of CO_{ad} is highly independent of reaction condition.

$\Theta_{CO} \simeq$ constant (independent of H_2/CO ratio, or P_{co} and P_{H_2})

Θco (in D_2) $\simeq$ Θco (in H_2) at the same reaction condition (Figures 4-4 and 4-5) was also observed. As shown in Figure 4-10, k_2 increases with P_{H_2}, $\frac{\partial k_2}{\partial P_{H_2}} > 0$. This formula implies that the methanation may involve a slow step in one of hydrogenation steps in surface carbon. If this is the case, then substituting H_2 by D_2 should lead to a significant difference in D_{k_2} and H_{k_2} probably $H_{k_2} > D_{k_2}$, since the lighter H_2 may react faster than the heavier D_2. $\frac{D_{k_2}}{H_{k_2}}$ may be < 1. However, results obtained from H/D study showed interesting results ($D_{k_2} \simeq H_{k_2}$).

A significant inverse H/D isotope effect was observed and is documented in Table 5-2. A $\Theta_{CD_x} > \Theta_{CH_x}$ and $D_{k_2} \simeq H_{k_2}$ was also found. Having $D_{k_2} \simeq H_{k_2}$ suggests that the slow step may not be one of the

hydrogenation steps on surface carbon. Since k_2 is a function of P_{H_2} (Figure 4-10), the amount of H_{ad} adsorbed on the surface is also a function of P_{H_2} (Figure 6-14). So $H_{k_2} \simeq D_{k_2}$, implying that the amount of H_2 and D_2 on the catalyst surface are nearly the same. Independent measurements showed that the amount of hydrogen on the surface is close to that of deuterium (Chapter 6). If the hydrogenation of surface carbon is not the slow step, then the hypothesis proposed that either the carbon-carbon "depolymerization" step or a change in carbon-metal coordination is rate determining. The C-C depolymerization mechanism has also been proposed by many investigators.(94 ~ 96). Furthermore, Hadjigeorgbious and Richardson(17) indicate that a change of C-M coordination may be involved in RDS. The proposed hypothesis explains why $D_{k_2} \simeq H_{k_2}$. For $k_2 = f(P_{H_2})$, our explanation is that the nature of carbon condition (with carbon or metal) is a function of P_{H_2} (Chapter 4). If C-C depolymerization or a change in C-M coordinates is the slow step, then substitution of H_2 by D_2 should not have any effect on k_2, and $H_{k_2} \simeq D_{k_2}$. The basis behind $\frac{R_{CD_4}}{R_{CH_4}} > 1$ is concentrated on Θc ($\Theta_{CD_x} > \Theta_{CH_x}$). This can be explained by the different oxygen levels present on the surface with H_2 and with D_2. This results in a different Θ_c in D_2, and Θ_c in H_2. A detailed discussion will be presented later. As indicated in Figure 4-6, Θ_{CH_x} increased with P_{H_2}. From Equation 5-1, $\partial\Theta_{CH_x}/\partial P_{H_2} > 0$, with $\frac{\partial k_2}{\partial P_{H_2}} > 0$, and Θco = constant. $\frac{\partial k_1}{\partial P_{H_2}} > 0$ is obtained. From H/D isotope effect study, we have $\Theta_{CD_x} > \Theta_{CH_x}$, but $D_{k_2} \simeq H_{k_2}$, with Θ_{co} in $D_2 \simeq \Theta_{co}$ in H_2. $D_{k_1} > H_{k_1}$ is obtained. $\partial k_1/\partial P_{H_2} > 0$,

suggesting an H-assisted CO dissociation. The observation of $\Theta_{CD_x} > \Theta_{CH_x}$, implies that CO "dissociates" more rapidly in D_2 atmosphere than in H_2 atmosphere. Assuming that H-assisted CO dissociation is the slow step seems inconsistent with the literature findings[4,5,8-12,22-23,25-28] and conclusions from Chapter 4. Additionally, no observed evidence of the CH_nO species on the nickel surface has been reported in the literature. The observed $\partial k_1/\partial P_{H_2} > 0$ is probably due to "C_{irr} or O_{ad}."

Bell and Winslow[41] recently reported that low levels of "C_β" build up during the first few hundred seconds of exposure of the clean ruthenium surface. The fast build-up of C_β before the steady state methanation rate is reached may play an important role in affecting the active carbon. High P_{H_2} favors the removal of C_β, which results in more active carbon formation. The H_2 or D_2 may also affect the level of C_β on the surface, which also contributes to the difference in Θ_{CD_x} and Θ_{CH_x}.

The "slow oxygen removal" effect on k_1 with P_{H_2} can be explained as follows. Whenever the steady-state level of O_{ad} is sufficiently high as to impair CO dissociation, then a varying level of O_{ad} would translate into a varying rate constant k_1. As O_{ad} is expected to decrease with P_{H_2} increased, k_1 would increase, conforming the observations. For $D_{k_1} > H_{k_1}$, a thermodynamic effect, i.e., a difference in steady-state level of CO dissociation-impairing species such as O, OH, C_β, $C_\beta H_x$ (respectively O, OD, C_β, $C_\beta D_x$) may be the cause.

The question arises that, if H is not involved in the RDS, what will the transient curves look like? To answer this, an experiment was

performed at one particular reaction condition in 60 wt % Ni/SiO_2, at T = 230°C, Pco = 0.3, P_{H_2}, P_{D_2} = 1 atm. At this condition, no H/D isotope effect is found (i.e., $R_{CD_4} \simeq R_{CH_4}$). The ingrowth $^{12}CH_4$ curve from ($^{13}CO + H_2 \rightarrow {}^{12}CO + H_2$) was compared to the ingrowth curve from ($^{12}CO + D_2 \rightarrow {}^{12}CO + H_2$). The result is shown in Figure 4-24. A significant difference is observed indicating that the H involving reaction steps are much faster than the carbon involving step. The hydrogenation of carbon or H-assisted CO dissocation may not be a slow step.

Our hypothesis for the mechanism of methanation is shown in Figure 4-25. The simplified scheme indicates that the adsorbed CO is in equilibrium with gas phase CO. The H-unassisted CO dissociation is fast and irreversible. The step $C_{ad} \rightarrow \Sigma CH_x$ is the slow step. There is a rapid equilibrium in $CH_x + H \longleftrightarrow CH_{x+1}$.[30,41] The formation of methane from CH_x is fast.

Step 2 is the slow step. Step 2 can either be carbon-carbon depolymerization or change in the carbon-metal coordination.

The above analysis is based on Ni/SiO_2. However, there are many similarities between Raney nickel and Ni/SiO_2. These behaviors are listed as follows:

A. the behaviors of k and Θ with reaction condition (Figures 4-9 and 4-14);

B. CO_{ad} and H_{ad} behavior (Figures 4-4, 4-5, 6-8, 6-10, 6-15, 6-16, 6-17);

C. H/D isotope effect behavior (Figures 5-1, 5-2, Table 5-1 and Table 5-2);

D. $^{12}CO + H_2 \rightarrow H_2$ behavior (switching off ^{12}CO, Figures 4-21 and 4-22);

E. A smililar result on Raney nickel by comparing the $^{12}CH_4$ (from $^{12}CO + D_2 \rightarrow {}^{12}CO + H_2$) with $^{12}CH_4$ (from $^{13}CO + H_2 \rightarrow {}^{12}CO + H_2$) is observed in Figure 4-24b.

Such remarkable similarities in so many critical parameters suggest that the reaction mechanism on the two catalysts (Raney nickel and Ni/SiO_2) must be essentially the same, involving either the depolymerization of carbon-carbon or the change of the carbon-metal coordination as the slow step. Ni powder seems to show different behavior compared to Ni/SiO_2 and Raney nickel. These behaviors are listed as follows. (1) $\frac{\partial \Theta_{CH_x}}{\partial P_{H_2}} < 0$ (Figure 4-9), (2) no appreciable H/D isotope effect (Table 5-3), (3) ^{12}CO (switching off) shows different behavior of H_2O (Figure 4-23). Are the discrepancies be due to different mechanisms; or due to the nature of catalyst?

The Θ_{CO} in Ni powder is also independent of reactions conditions. $\Theta_{CO} \simeq$ constant (Figures 4-4 and 4-5). Let us refer to Figure 5-5, the simplified reaction scheme

$$k_1 \Theta_{CO} = k_2 \Theta_{CH_x} \qquad (5\text{-}1)$$

$$\text{since } \frac{\partial \Theta_{CH_x}}{\partial P_{H_2}} < 0 \quad \text{(Figure 4-9)} \qquad (5\text{-}2)$$

$$\frac{\partial k_2}{\partial P_{H_2}} > 0 \quad \text{(Figure 4-14)} \qquad (5\text{-}3)$$

$\frac{\partial k_2}{\partial P_{H_2}} > 0$ suggests that H is involved in the slow step of hydrogenation of surface carbon. However, from the H/D isotope effect study, $D_{k_2} \simeq H_{k_2}$. This implies that the slow step is not hydrogenation of surface carbon. The $k_2 = f(P_{H_2})$ is probably due to the nature of carbon condition (associated with carbon or metal (Chapter 4)).

For

$$k_1\Theta co = k_2\,\Theta_{CH_x} = TOF \qquad (5\text{-}i)$$

since $\frac{\partial TOF}{\partial H_2/CO} > 0$ (Figure 4-18) $\Theta co = c$ (Figures 4-4,4-5) (5-4)

so $\frac{\partial k_1}{\partial P_{H_2}} > 0.$ (5-5)

This suggests H-assisted CO dissociation. However, from H/D isotope study $D_{k_2} \simeq H_{k_2}$, $D_{\Theta_C} \simeq H_{\Theta_C}$, and Θco in $D_2 \simeq \Theta co$ in H_2. It follows that $D_{k_1} \simeq H_{k_1}$. This contradicts H-assisted CO dissociation. So H-involving RDS is not the case for Ni powder.

For $\frac{\partial k_1}{\partial P_{H_2}} > 0 \qquad \frac{\partial k_2}{\partial P_{H_2}} > 0$ (5-6)

$$\frac{\partial \Theta_{CH_x}}{\partial P_{H_2}} < 0 \qquad (5\text{-}7)$$

From $D_{k_1} \simeq H_{k_1}$, $D_{k_2} \simeq H_{k_2}$ and $\frac{\partial k_1}{\partial P_{H_2}} > 0 \qquad \frac{\partial k_2}{\partial P_{H_2}} > 0$

It is inferred that the RDS in methanation over Ni powder does not involve H. The overall rate of CH_4 may be controlled by the balancing formation or removal of carbon. The variant behavior on nickel powder is probably due to the nature of nickel powder. For $\frac{\partial \Theta_C}{\partial P_{H_2}} < 0$, this observation is consistent with Goodman's result.[3] Goodman also reported no detectable oxygen levels on Ni(100). In this study, very low levels of oxygen on the Ni powder compared with Ni/SiO_2 and Raney nickel were observed (Figure 4-21, 4-22, 4-23). The hypothesis is that if the nature of Θc has a tendency to alter by increasing P_{H_2}, Θc will also be affected by oxygen and C_{irr}. High P_{H_2} affects oxygen level which, in turn, favors CO dissociation. If the oxygen level is very, very low, then an increase in P_{H_2} will not result in the increase in Θ_C. The Θ_C decreasing as H_2/CO increases has been discussed in 4.4.9. The H-assisted CO dissociation not involving the slow step is also indicated by $D_{k_1} \simeq H_{k_1}$. Therefore, on Ni powder, the hypothesis $CO_{ad} \rightarrow C_{ad} \rightarrow \Sigma CH_x \rightarrow CH_4$ of this scheme is valid.

There are many other possibilities which may cause H/D isotope effect. These possible effects will be discussed later.

5.3.1 Effect of CO Diffusion

The inverse H/D effect may possibly be caused by the different diffusivity of CO in H_2 and in D_2 ($Diff_{CO}$ in $H_2 \neq Diff_{CO}$ in D_2). The general overall rate of CH_4 can be expressed as $R_{CH_4} = kP_{H_2}^{x}P_{CO}^{y}$ with $x >$

0 and $y < 0$. If there is a diffusion effect, then the concentration gradient between the bulk and the catalyst surface will be different in either H_2 or D_2, leading to the observed H/D isotope effect. If this is the case, then adding an inert (while maintaining P_{CO} and P_{H_2} constant) will have the same effect — $Diff_{CO}$ in $H_2 \neq Diff_{CO}$ in H_2+inert. This will lead to an observation of R_{CH_4} in inert ($P_{H_2} = \ell$, $P_{CO} = m$, $P_{inert} = n$) different from R_{CH_4} ($P_{H_2} = \ell$, $P_{CO} = m$). This can be experimentally verified by comparing R_{CD_4}/R_{CH_4} with (R_{CH_4} in inert)/(R_{CH_4}) at the same reaction condition. If there is a diffusion effect, the two values should be comparable. The diffusion effect will also occur when CO is diluted with an inert.

An experiment was conducted by comparing the steady-state isotope effect

$$\frac{R\ CD_4}{R\ CH_4} \text{ vs. } \frac{R\ CH_4 \text{ in Ar}}{R\ CH_4}$$

at one particular condition. ($232^{\circ}C$, $H_2/CO = 10$, Raney nickel). The results and conditions are listed in Table 5-4.

If the isotope effect is due to the difference in mass transfer of reactant CO, then adding Ar will result in observing different steady-state reaction rate. However, as shown in Table 5-4, the mass transfer effect is not the reason for H/D isotope effect.

Table 5-4

Diffusion Effect on H/D Isotope Effect in Raney Nickel

(unit = bar)

	Pco	P_{H_2}	P_{D_2}	P_{Ar}
R CH_4	0.09	0.9	0	0
R CD_4	0.09	0	0.9	0
R CH_4 in Ar	0.09	0.9	0	1

$$\frac{R\ CD_4}{R\ CH_4} = 1.35 \qquad \frac{R\ CH_4\ in\ Ar}{R\ CH_4} = 1.05$$

5.3.2 Effect of Surface Oxygen and Carbon-Containing Species on H/D Isotope Effect

The amount of surface oxygen containing species in Raney nickel and Ni/SiO_2 is larger than that on Ni powder. This is observed by performing $^{12}CO + H_2 \rightarrow H_2$ gases delivery sequence. A large amount of H_2O was observed on Raney nickel and Ni/SiO_2. However, in Ni powder only a very small amount of H_2O is found. The amount of H_2O production represents all the oxygen containing species on the catalyst surface with metal and with support. This finding suggests that O impaired species in Ni/SiO_2 and Raney-Ni >> Ni powder. It is likely that under the steady state condition, the concentration of O impaired species in D_2 varies from that in H_2. This contributes to the $\Theta_{CD_x} > \Theta_{CH_x}$. The inverse H/D effect has been observed on Raney nickel, Ni/SiO_2. If the oxygen containing species is relatively low, then no H/D effect should be observed. This is the case for Ni powder, indicating that the nature of nickel catalyst does have an effect on H/D isotope effect.

From the H_2 adsorption study presented in Chapter 6, it is concluded that part of H or D is associated with C_β in the form of $C_\beta H_x$, $C_\beta D_x$. It is also possible that due to the thermodynamic effect, the concentration of $C_\beta H_x$ is different from $C_\beta D_x$. This is another possible source for the observation of H/D effect.

The reaction conditions may cause variations in the concentration of oxygen containing species and $C_\beta H_x$ or $C_\beta D_x$ containing species, resulting in the observation of H/D isotope effect is a function of reaction conditions.

Ozaki[61] pointed out the possiblity that the H/D isotope effect on the rate of reaction does not always arise from the RDS, but can also arise from a thermodynamic isotope effect on the concentration of an intermediate. The observed H/D isotope effect in this study may come from the nature of catalyst. In this case, the changes may arise from modifications of the metal dispersion and/or interaction with the support. The concentration of oxygen, carbon-containing species may be different in different Ni catalysts. This difference might explain why the H/D isotope effect is substantially different in different Ni catalysts.

5.4 Conclusions

1. The origin of H/D isotope effect is the coverage in reaction intermediates. The observed effect is merely a Θ effect and not a k effect.
2. The H/D isotope effect depends on the nature of the catalyst.
3. Raney nickel and Ni/SiO_2 share the same reaction mechamism. The slow step does not involve H addition. Instead, it probably involves either the C-C depolymerization or the change of C-M coordination.

6.0 H_2 ADSORPTION STUDY

6.1 Background

The aim of this investigation was to get a better understanding of the forms and concentration of hydrogen under reaction conditions. Extensive results from Raney nickel and 60 wt % Ni/SiO_2 catalysts are reported in this chapter. A few experiments done in Ni powder are also included in this chapter.

6.2 Results

In this study, various methods were used in order to measure the amount of adsorbed hydrogen on the catalyst surface. In Table 6-1, data from the study is compared to data from independent measurements by different methods.

In view of the totally different measurement methods, the consistency in our measurement with different techniques indicates that the methods applied in this study are a good way to measure the amount of adsorbed hydrogen on the catalyst surface.

Table 6-1 also indicates the inconsistency of the data in Raney nickel. Chemisorption data 3.3 ml/g versus 8.2 ml/g through transient

Table 6-1

Comparison Between Transient Measurements with Other Independent Measurements

Catalysts	Results in this study H_2 ml/g	Independent Measurement H_2 ml/g
Raney nickel	6.7[a] (350°C, P_{H_2} = 1 atm)	7.49[b]
	8.2[a] (30°C, P_{H_2} = 1 atm)	3.3[c] 6.0[i]
60 wt %Ni/SiO_2	7.2[d] (30°C, P_{H_2} = 0.3 atm)	7.04[e]
Ni powder	0.36[d] (30°C, P_{H_2} = 0.13 atm) (1.25 m^2/g)[f]	1.89[g] (m^2/g)
	1.88[a] (350°C, P_{H_2} = 1 atm)	1.74[b]
	2.23[h]	

---

a. The amount of hydrogen measured by (H_2/D_2+Ar) exchange method at P_{tot} = 1 atm in the absence of CO. The result is extrapolated from Figure 6-4.

b. TPD measurement was conducted by Miss D. Blazewick. The gas delivery sequence of the TPD is H_2 (350°C) $\xrightarrow{\text{after reduction}}$ H_2(30°C) → Ar (30°C 20 min) → Ar (350°C) at a heating rate 20°C/min.

c. H_2 chemisorption measurement was supplied by Dr. D. G. Blackmond.

d. Same as a, but H_2 and D_2 are diluted in He.

e. H_2 chemisorption measurement results at room temperature from reference (10).

f. Surface area calculation based upon the assumption H/M =1.

g. BET surface area was conducted by Exxon research laboratory.

h. Thermal desorption gas delivery sequence He (350°C) → H_2 (350°C) → H_2 (30°C) → He (30°C) → He (350°C).

i. H_2 chemisorption result obtained from Dr. R. D. Kelley with 5% Al_2O_3 in Raney nickel.

method (H_2/D_2 (trace Ar)) was observed. This can be explained by the difference in the nature of the different methods. The H_2 uptake from a typical adsorption isotherm was determined by extrapolating the H_2 uptake at P_{tot} equal to zero. The typical transient method in measuring the amount of adsorbed hydrogen in the absence of CO is shown in Figures 6-1 and 6-2. From this method, the amount of hydrogen which can be replaced by deuterium is measured. Weakly adsorbed H_2 is also included in the measurements. Since the hydrogen uptake increases with P_{H_2}, the variation of the amount of adsorbed H_2 through transient method, (D_2 + Ar + H_2), with P_{H_2} is excepted. This may explain the difference in results in transient method and in chemisorption measurements on Raney nickel.

6.2.1 The Amount of Adsorbed Hydrogen in the Absence of CO

In the absence of CO, H_{ad} measurements were conducted by D_2 (Ar trace)/H_2 exchange as a function of temperature with different nickel catalysts. The temperature dependence on the amount of adsorbed hydrogen with various catalysts is shown in Figures 6-3, 6-4 and 6-5. The amount of H_2 uptake is close to that of D_2. The in-situ thermal desorption measurements are also included in Figures 6-3 and 6-5 for comparison. As can be seen in Figures 6-3 and 6-4, the Ni/SiO_2 and Raney nickel exhibited normal behavior - the amount of adsorbed hydrogen decreased as the temperature increased. This finding is consistent with general behavior of hydrogen adsorptions -- it tends to decline as the

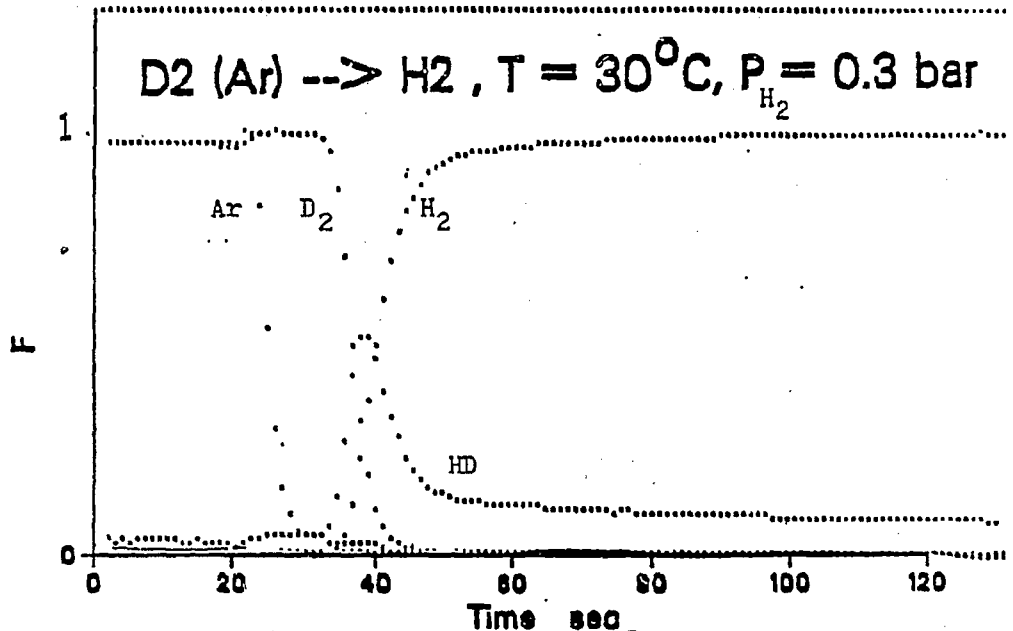

Figure 6-1 D_2 (Ar) $\rightarrow$ H_2 exchange at 30°C, P_{H_2} = 0.3 bar in 60 wt % Ni/SiO_2

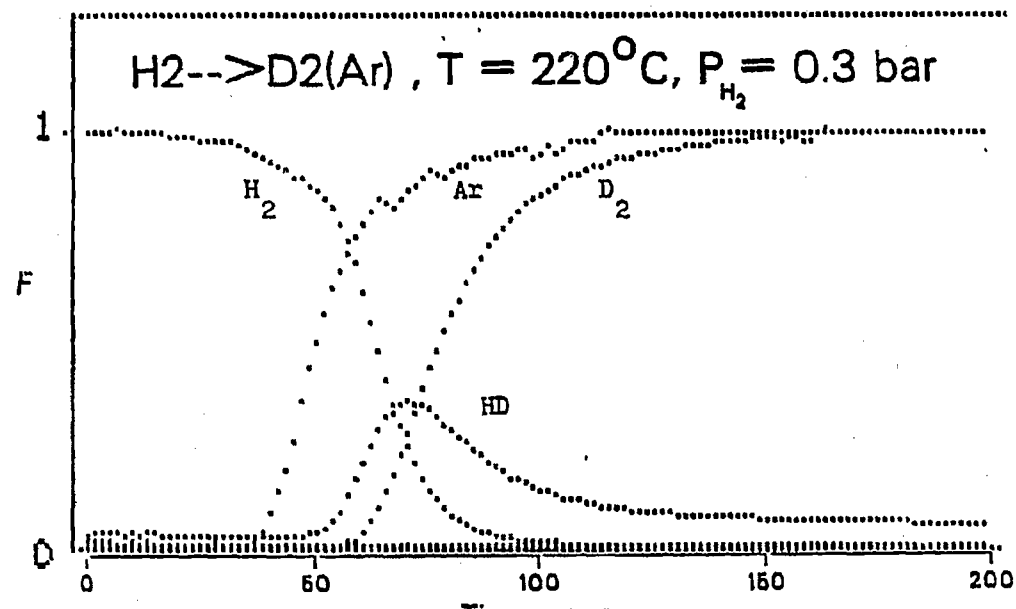

Figure 6-2 H_2 $\rightarrow$ D_2(Ar) exchange at 220°C, P_{H_2} = 0.3 bar in 60 wt % Ni/SiO_2

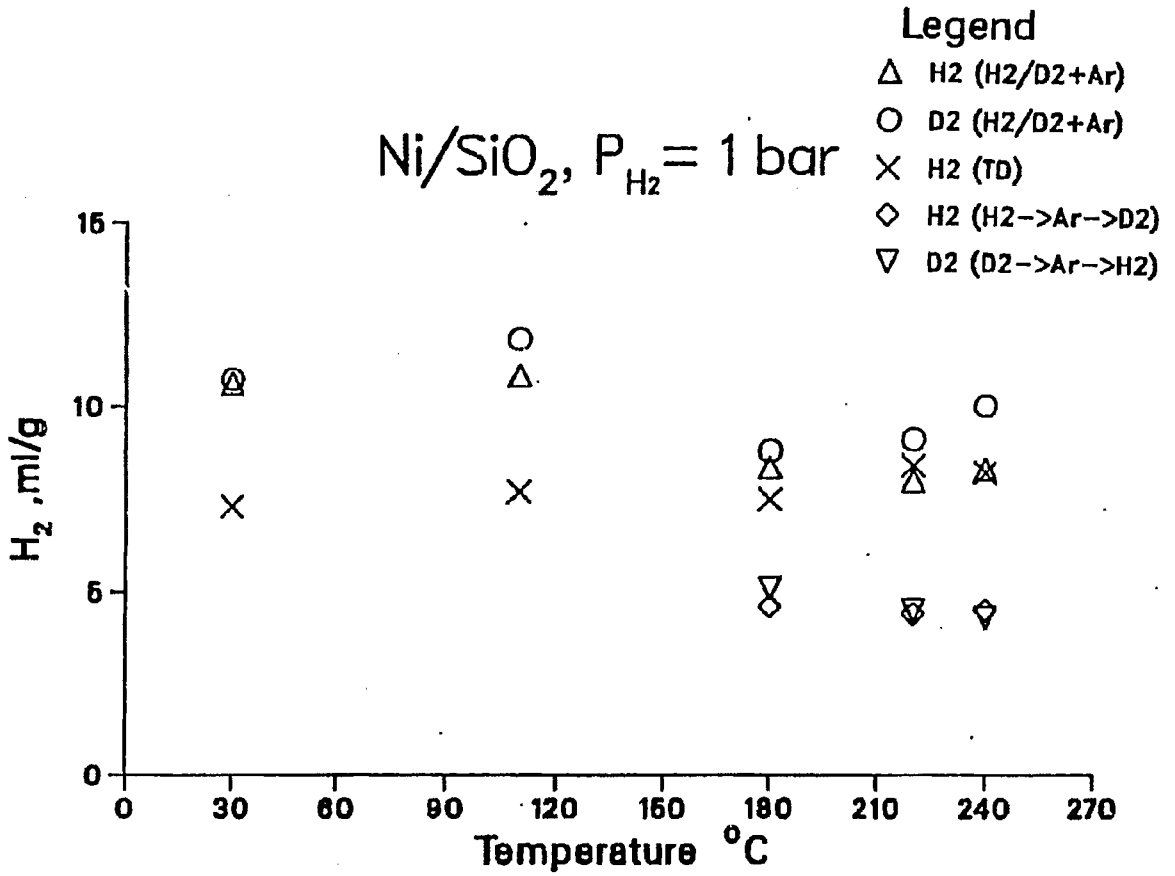

Figure 6-3 Amount of adsorbed hydrogen versus temperature (60 wt % Ni/SiO_2)

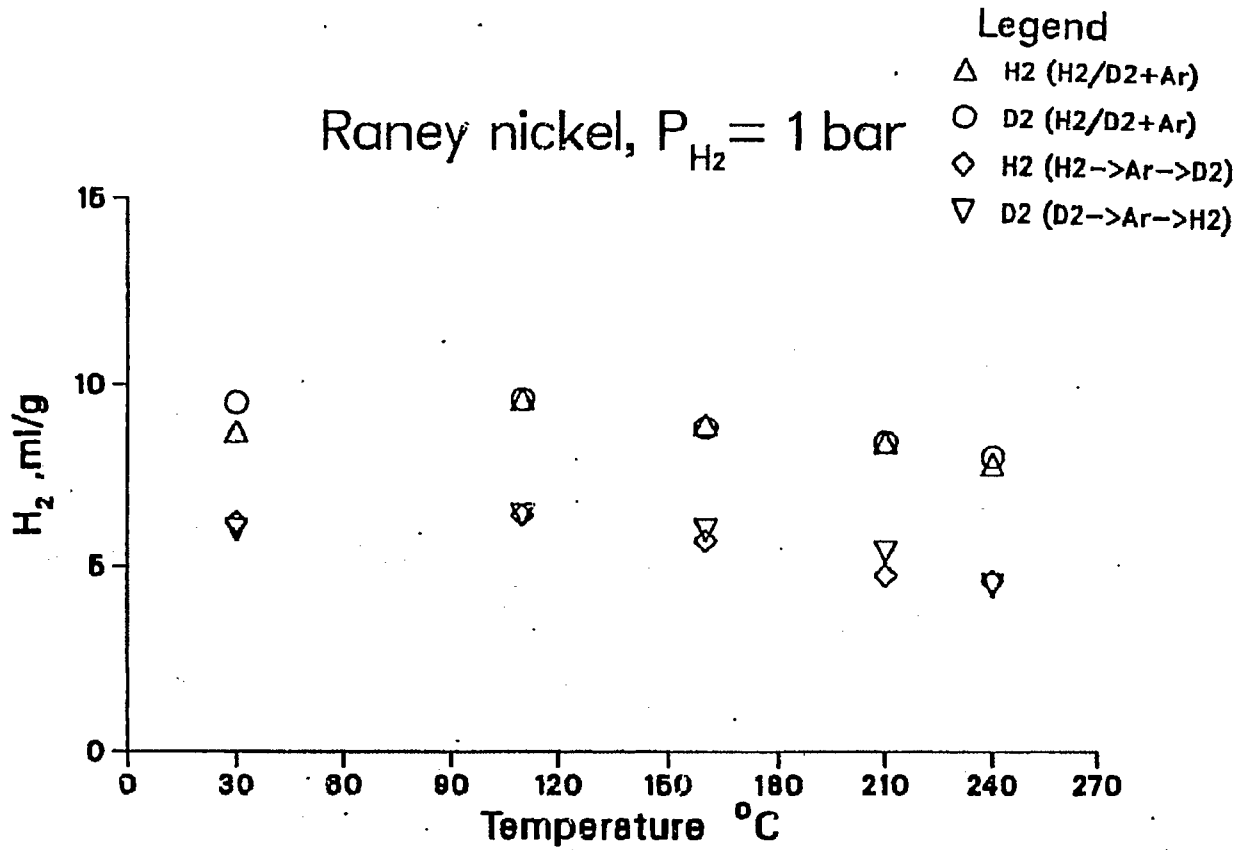

Figure 6-4 Amount of adsorbed hydrogen versus temperature (Raney nickel)

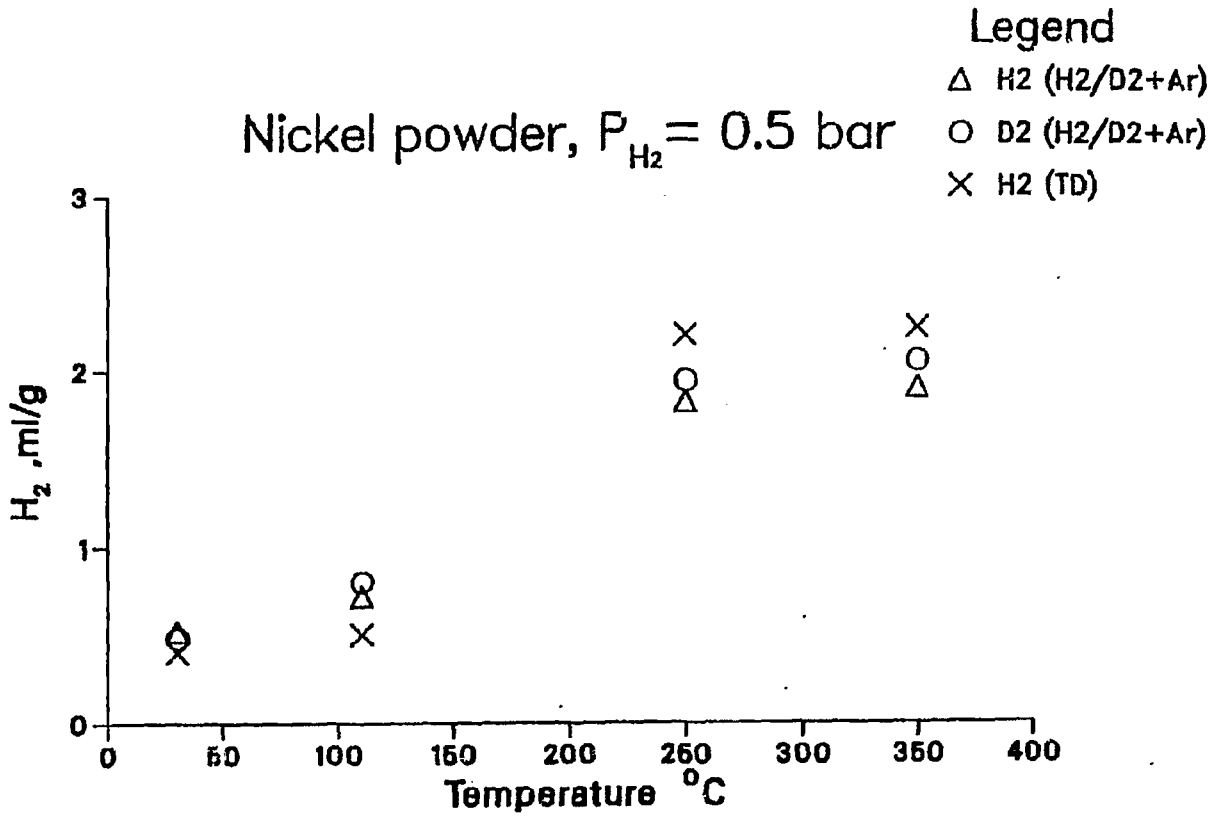

Figure 6-5 Amount of adsorbed hydrogen versus temperature (nickel powder)

temperature increases because adsorption is generally an exothermic process.[113] However, results obtained from Ni powder experiments show the opposite trend. The amount of adsorbed hydrogen increased with temperature, and then leveled off. Data obtained from thermal desorption of H_2 shown in Figures 6-3 and 6-5, shows consistent results (in view of different techniques) with the H_2/D_2 exchange measurement. This suggests that the D_2 (Ar trace)/H_2 exchange method is a reliable technique in measuring the adsorbed H_2 at the catalyst surface. The amount of adsorbed hydrogen can also be measured through the gases delivery sequence of H_2 → Ar → D_2. For the amount of adsorbed deuterium, can be measured through the gas delivery sequence D_2 → Ar → H_2 (Figure 6-6). As can be seen from Figures 6-3 and 6-4, different methods (H_2/D_2(Ar) vs. H_2 ↔ Ar ↔ D_2) give different measurement results. The measurement data from the titration method (H_2 ↔ Ar ↔ D_2) is always less than the data obtained by exchanged method (H_2/D_2+Ar). Additionally, the data obtained from titration method is around 55 to 65% of that obtained from exchange method. There are many possibile causes of the difference. The difference is probably due to the weakly adsorbed hydrogen being removed by Ar flush or hydrogen migration from the exterior of surface into the bulk of nickel. Bell and Winslow[83] also indicated recently the hydrogen migration into the bulk nickel. They also imply that the Ar flush will favor the migration process.

Although there is some variance in different methods, similarities are also observed. The amount of hydrogen adsorbed is close to that of

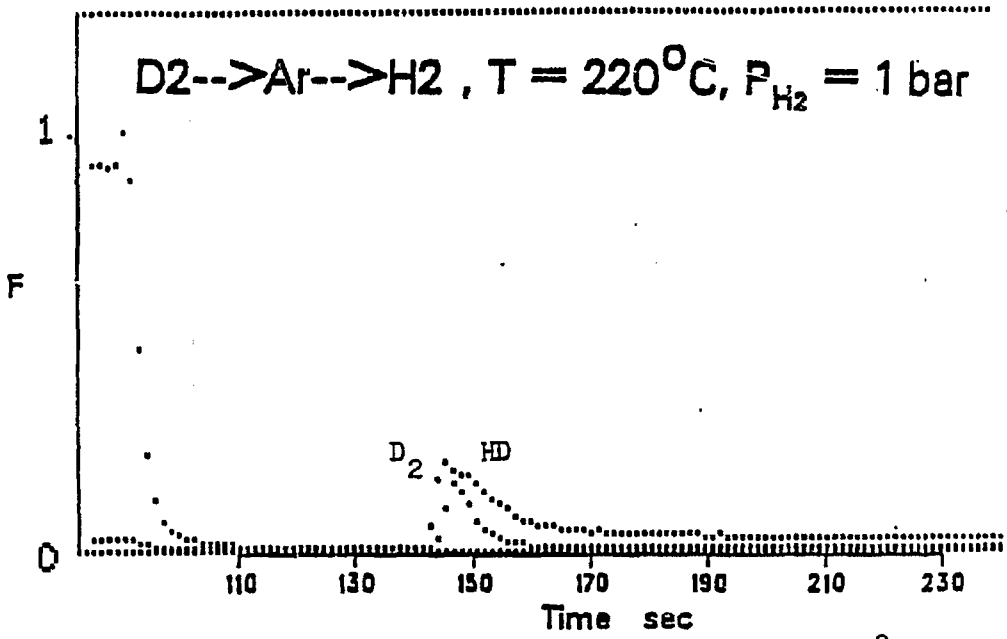

Figure 6-6 $D_2 \longrightarrow Ar \longrightarrow H_2$ on 60 wt % Ni/SiO_2 at 220 °C , P_{H_2} = 1 bar

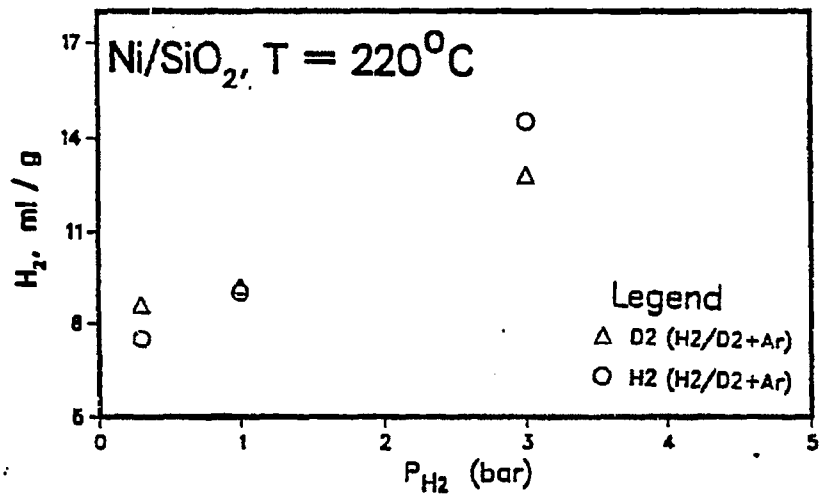

Figure 6-7 Amount of adsorbed hydrogen versus P_{H_2} (60 wt % Ni/SiO_2)

deuterium. The overall trend of H_{ad} with respect to temperature is consistent. For Raney nickel and 60 wt % Ni/SiO_2, the amount of adsorbed hydrogen decreases as the temperature increases. The opposite is observed for nickel powder. However, the different methods gave different results. In this study, the preferred procedure for measuring the amount of hydrogen adsorbed on the catalysts was the $H_2/D_2(Ar)$ exchange method as it does not interrupt the continuity of the reaction process (the titration method has to interrupt the reaction process).

The amount of adsorbed hydrogen were measured systematically by varying temperature and P_{H_2}. The data are summarized in Table 6-2. A typical result on 60 wt % Ni/SiO_2 is shown in Figure 6-7. It indicates that the amount of adsorbed H_2 increases with pressure of H_2.

As described in Chapter 2, any isotope effect due to substitution of H_2 by D_2 was assumed to be negligible.[72,84] However, it is interesting to find out how isotope effects can affect our transient measurements. If we account for the isotope effect in terms of the physical interaction with nickel surface, it can be assumed that H atoms adhere a little more strongly on the nickel surface than D atoms. If adsorbed H atoms play a role which will lead to either a tailed peak or asymmetrical peak in HD transient. A difference in the HD areas (HD from $H_2 + D_2$ and HD from $D_2 + H_2$) should also be observed. The HD formation is faster in D (preadsorbed) + H_2 system than in the H (preadsorbed) + D_2 system.

Results given in Figures 6-1 and 6-2 show that neither a tailed peak nor asymmetrical peak in HD transient was observed. Also, no

Table 6-2

Hydrogen Uptake in the Absence of CO in 60 wt % Ni/SiO_2

	$H_2/D_2(Ar)$ exchange						Thermal Desorption
	P_{H_2} = 0.3 atm		P_{H_2} = 1 atm		P_{H_2} = 3 atm		P_{H_2} = 1 atm
T	H_2	D_2(ml/g)	H_2	D_2(ml/g)	H_2	D_2(ml/g)	H_2(ml/g)
30	7.9±1.1	9.7±2.0	10.6±0.9	10.7±1.1			7.2
110	8.2±1.5	10.3±2.0	10.8±2.0	11.8±0.9			7.6
180			8.3±1.5	8.9±1.8			7.5
220	6.7±1.1	8.6±2.0	7.9±1.2	9.3±2.0	15.2±2.0	12.8±2.0	8.3
240	6.1±1.0	9.0±2.5	8.2±1.7	10.4±2.0	14.9±2	11.9±2.0	8.2

differences in the HD areas (HD from $H_2 + D_2$ and HD from $D_2 + H_2$) were observed. Based upon these two observations, it was concluded that the assumption of negligible isotope effect by substitution of H_2 to D_2 is valid.

6.2.2 The Amount of Adsorbed Hydrogen in the Presence of CO

The dependence of the amount of adsorbed hydrogen on temperature (with constant H_2/CO ratio) on various nickel catalysts is shown in Figures 6-8, 6-9 and 6-10. The overall trend for different Ni catalysts shows consistent agreement. The amount of adsorbed hydrogen at constant H_2/CO ratio increases with temperature. It can be seen that the amount of surface carbon also increases with temperature (Figures 4-8 and Table 4-4). Based upon these two observations, it is suggested that hydrogen is associated with surface carbon.

At a low temperature, 30°C, the presence of CO has a significant influence on the amount of adsorbed hydrogen. Most of the adsorbed hydrogen is replaced by CO. Only very small amount of H_{ad} is left on the surface (i.e., 0.1 monolayer of hydrogen for Ni/SiO_2, 0.15 monolayer for Raney Nickel). The full monolayer is taken as the amount of hydrogen measured by $H_2/D_2(Ar)$ exchange at the same condition, but in the absence of CO. A typical result is shown in Figure 6-11. The result indicates that D_2 and Ar decayed simultaneously and the formation of HD was much less than the formation of HD in the absence of CO (Figure 6-1). These observations suggest that most of the catalyst

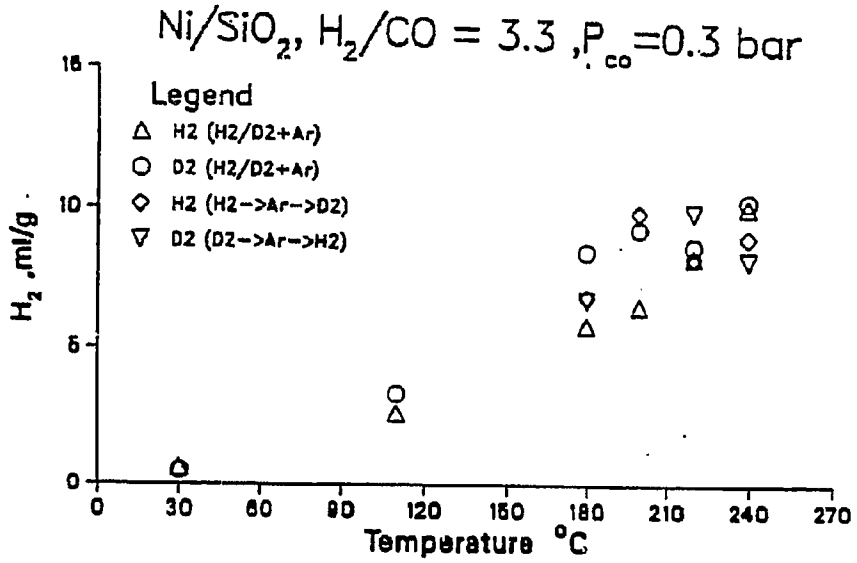

Figure 6-8 Amount of adsorbed hydrogen versus temperature (H_2/CO = 3.3, 60 wt % Ni/SiO_2)

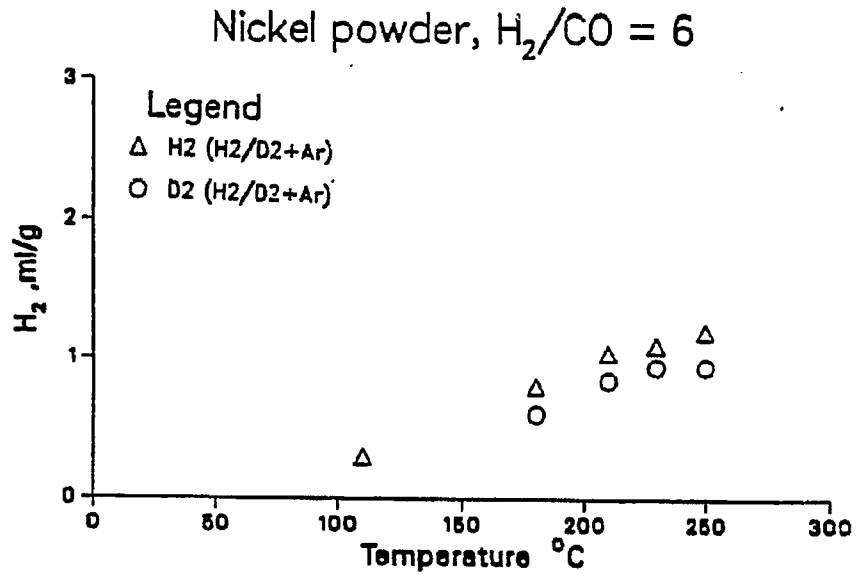

Figure 6-9 Amount of adsorbed hydrogen versus temperature (H_2/CO = 6, nickel powder)

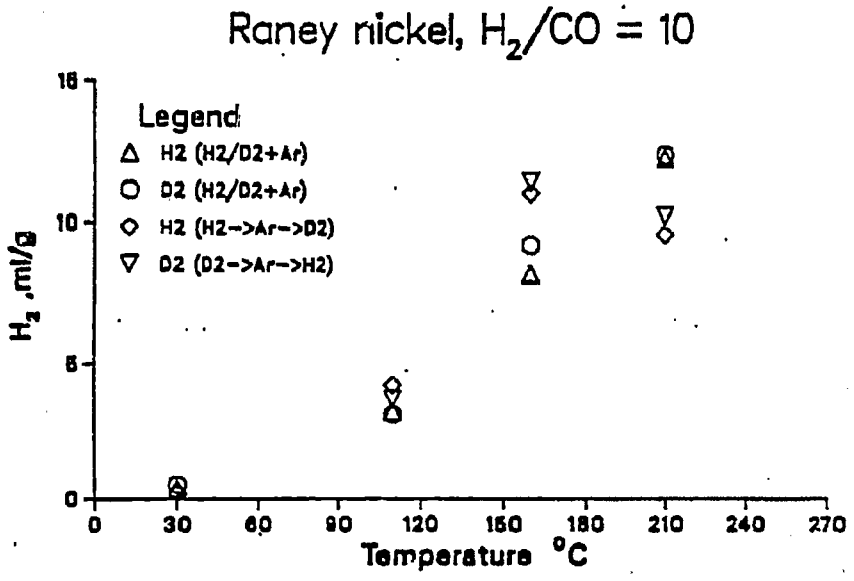

Figure 6-10 Amount of adsorbed hydrogen versus temperature
($H_2/CO = 10$, Raney nickel)

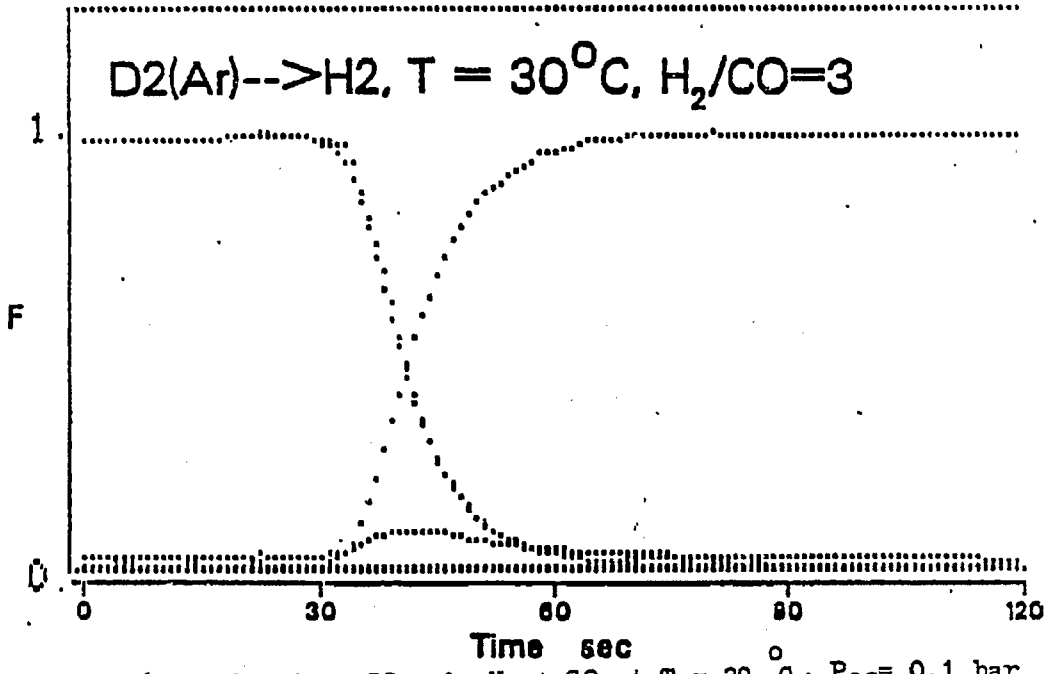

Figure 6-11 D_2 + Ar + CO ⟶ H_2 + CO at T = 30 °C, P_{CO} = 0.1 bar
($H_2/CO = 3$, 60 wt % Ni/SiO_2)

surface is covered by CO. Finding the amount of hydrogen on the catalyst surface to be small is in accord with many literature findings.(74,75,83)

As the temperature was increased to 110°C, more H_{ad} were observed, including: 0.3 monolayer Ni/SiO_2, and 0.3 ~ 0.4 monolayer for Raney nickel. It can be concluded that even at 110°C, there is some amount of hydrogen able to coexist with CO. As soon as the temperatures reached the reaction condition, more hydrogen was adsorbed on the surfaces. A typical transient result under reaction condition is shown in Figure 6-12. The amount of adsorbed hydrogen measured by titration method is also shown in Figures 6-8 and 6-10. The results from titration method and H_2/D_2 exchange method agree. The amount of adsorbed hydrogen is nearly the same as the amount of adsorbed deuterium. A typical titration method result obtained under reaction condition is shown in Figure 6-13. In the previous section, the different results between titration and exchange methods were observed in the absence of CO. In the presence of CO, there is little difference between methods. This suggests that, at $P_{H_2} \leq$ one atm and under reaction conditions, the effect of the large amount of weakly adsorbed hydrogen on the H_2/D_2 exchange measurement and hydrogen migration into bulk nickel is insignificant. The large amount of H_{ad} present under reaction conditions has also been reported by Bell et al.(38,83) Happel et al. also reported that under reaction conditions the amount of H_{ad} is close to the amount of CO_{ad}.(115)

Special experiments were conducted in Ni/SiO_2 in order to measure the amount of adsorbed hydrogen by varying the pressure of hydrogen and

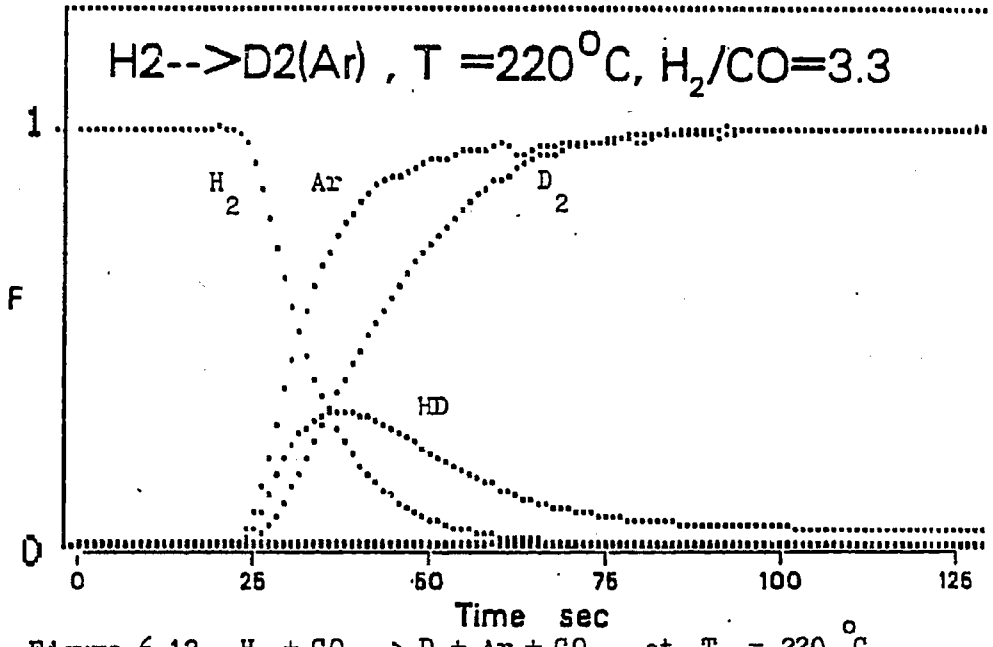

Figure 6-12 $H_2 + CO \longrightarrow D_2 + Ar + CO$ at T = 220 °C

, P_{H_2} = 1 bar with H_2/CO = 3.3 in 60 wt % Ni/SiO_2

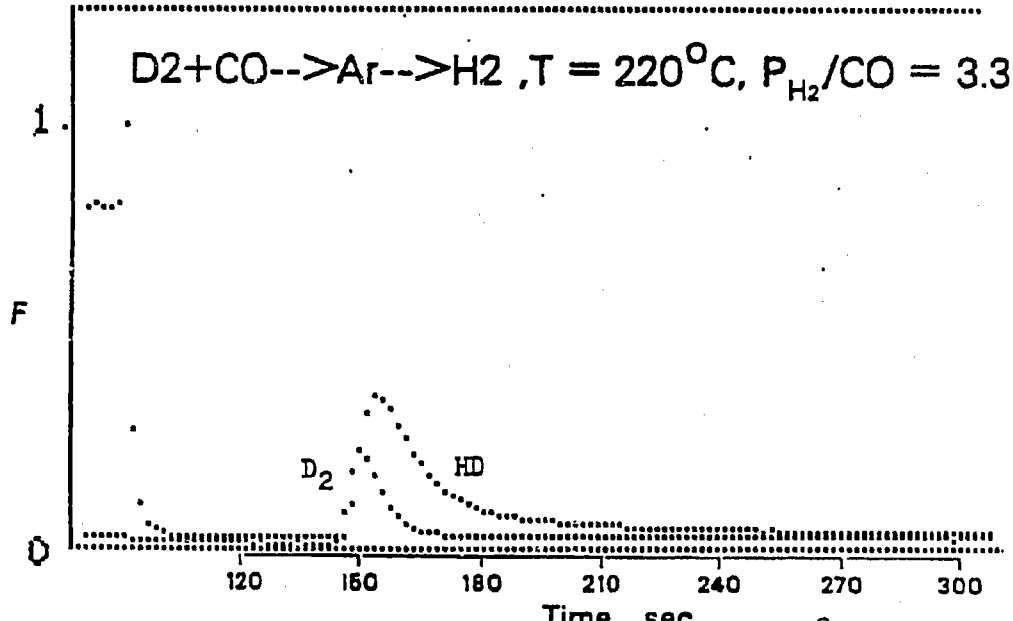

Figure 6-13 $D_2 + CO \longrightarrow Ar \longrightarrow H_2$, at T = 220 °C, P_{H_2} = 1 bar

, H_2/CO = 3.3 in 60 wt % Ni/SiO_2

carbon monoxide (independent variables). Typical results are shown in Figures 6-14 and 6-15; detailed results are summarized in Table 6-3. The results obtained were seemingly inconsistent. At constant temperature and constant pressure of CO, the amount of adsorbed hydrogen increases with the pressure of hydrogen (Figure 6-14). However, at constant temperature and constant pressure of hydogen, the amount of adsorbed hydrogen shows only a slight dependence on the pressure of CO (Figure 6-15). The amount of adsorbed hydrogen tends to incline slightly at lower pressures of CO, and levels off at higher pressures of CO. As suggested by data plotted in Figure 6-14, hydrogen and CO compete for either the same adsorption site or incomplete coverage. It was observed that the amount of adsorbed CO is highly independent of reaction conditions (Chapter 4). The amount of adsorbed CO is virtually constant as partial pressure of hydrogen varies (Figure 4-5). This finding invalidated the possibility that H_2 and CO compete for the same site. In the absence of CO the amount of adsorbed hydrogen was also observed to increase with the partial pressure of hydrogen (Figure 6-7). This suggests that at high partial pressure of hydrogen, say three bar, the measurement may suffer from large amount of physically adsorbed hydrogen; by titration method, the large amount of physically adsorbed hydrogen is eliminated. If the amount of adsorbed hydrogen measured through different methods (transient vs. titration) gives similar results, then the H_2/D_2(Ar) transient measurements are not suffering from a large amount of physically adsorbed hydrogen. Figure 6-8 shows consistencies between different measurement methods.

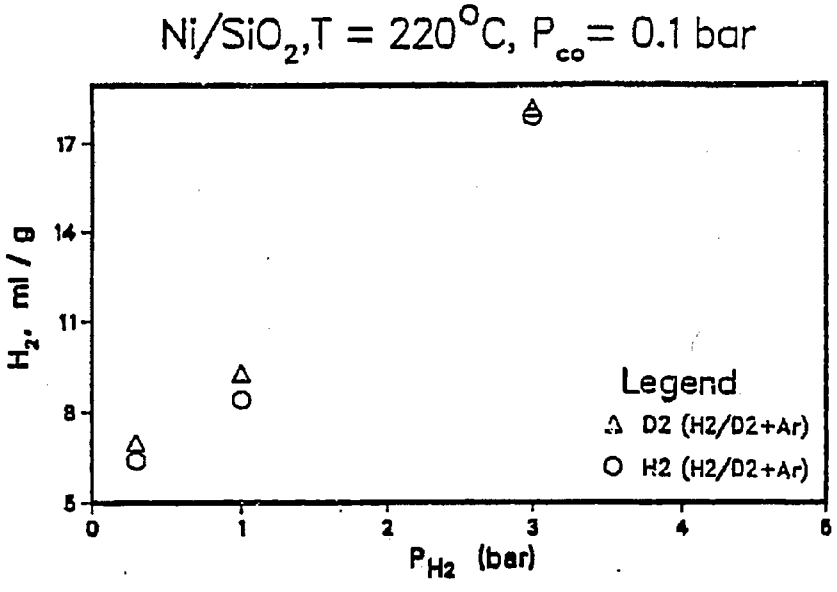

Figure 6-14 Amount of adsorbed hydrogen versus P_{H_2}
(T = 220 °C, P_{CO} = 0.1 bar, 60 wt % Ni/SiO_2)

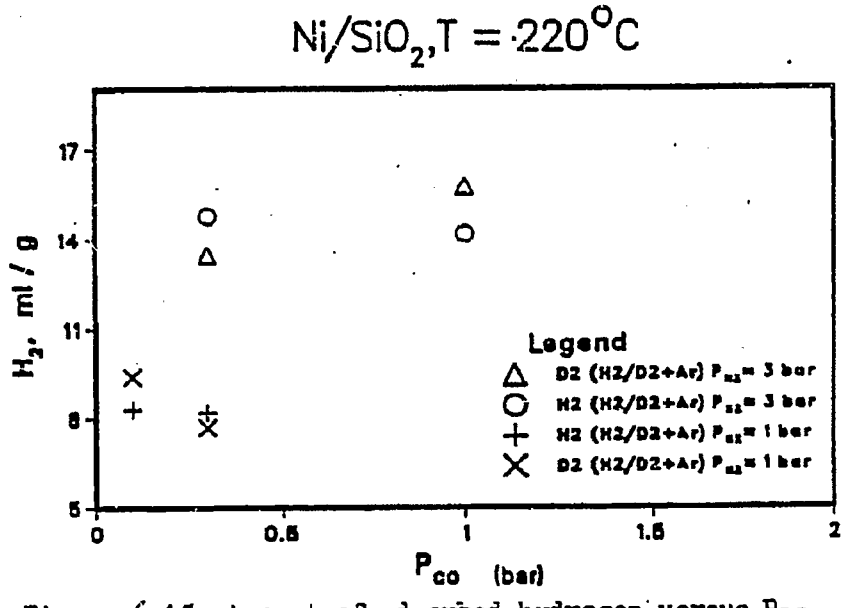

Figure 6-15 Amount of adsorbed hydrogen versus P_{CO}
(T = 220 °C, P_{H_2} = constant, 60 wt % Ni/SiO_2)

Table 6-3

The Amount of Adsorbed Hydrogen as a Function of Reaction Condition in 60 wt % Ni/SiO_2

T	P_{H_2} atm	P_{CO} atm	H_2 ml/g	D_2 ml/g
220	0.3	0.1	6.4	6.94
220	1	0.1	8.29	9.32
220	3	0.1	17.95	18.14
220	3	0.3	14.48	16.25
220	3	1	14.22	15.8
220	1	0.3	8.22	7.62
240	1	0.3	10	10.2
240	0.3	0.1	8.45	7.01
240	1	0.1	10.0	12.03
240	3	0.3	14.0	11.1
240	3	1	12.03	14.7

Therefore, at P_{H_2} equal to one bar, the catalyst surface may be free from large amount of physically adsorbed hydrogen. The results obtained from P_{H_2} equal to one bar, and varying Pco are also shown in Figure 6-15. The amount of adsorbed hydrogen is highly independent of Pco. Taken together, these findings indicate that the amount of adsorbed hydrogen is a sensitive function of pressure of hydrogen; however, at constant pressure of hydrogen it shows only slight dependence on Pco.

The amount of adsorbed hydrogen as a function of H_2/CO ratio and Pco is plotted in Figures 6-16 and 6-17 on Raney nickel. The experiments were conducted by keeping the flow rate of hydrogen constant while changing the flow rate of CO. The total pressure was maintained at one atmosphere (Figure 6-16). As seen in Figures 6-16 and 6-17, the amount of adsorbed hydrogen is highly independent of H_2/CO ratio and Pco. The findings are consistent with those presented in Figure 6-15.

From Figures 6-15, 6-16 and 6-17, one can determine that the amount of adsorbed hydrogen is highly independent of Pco or H_2/CO ratio, at constant pressure of hydrogen. This suggests that only a small portion of the adsorbed hydrogen participates in methanation, which further explains why the amount of adsorbed hydrogen is not a function of H_2/CO ratio or Pco. However, the variation of H_2/CO and Pco will affect the methanation significantly (Figure 4-18).

The sources of large amounts of hydrogen are probably largely associated with surface carbon (reactive and irreactive) and/or with nickel metal (H_2 or H_{ad}). They will be fully discussed in next section.

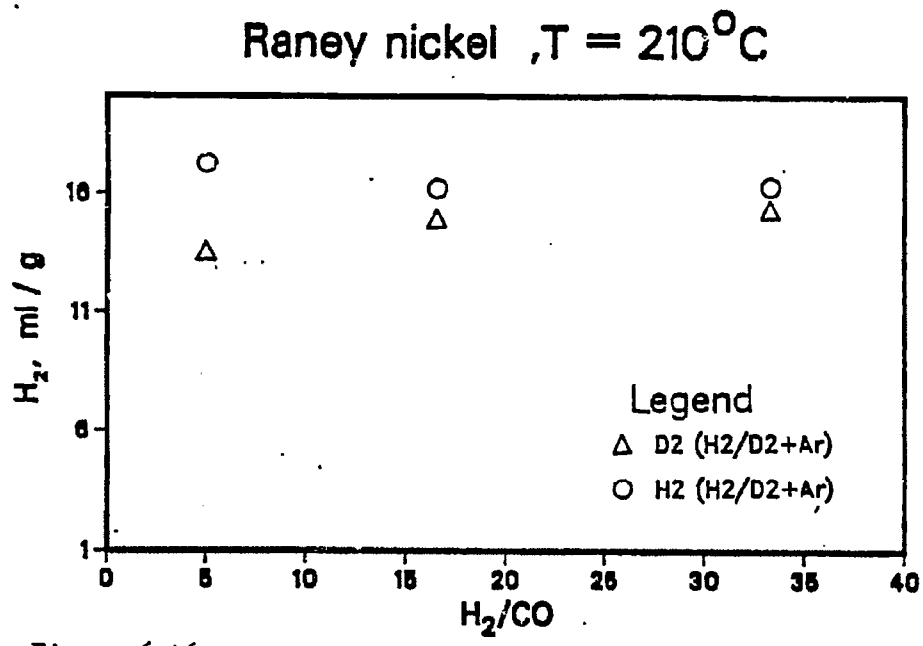

Figure 6-16 Amount of adsorbed hydrogen versus H_2/CO ratio

(Raney nickel, P_{tot} = 1 bar, T = 210 °C)

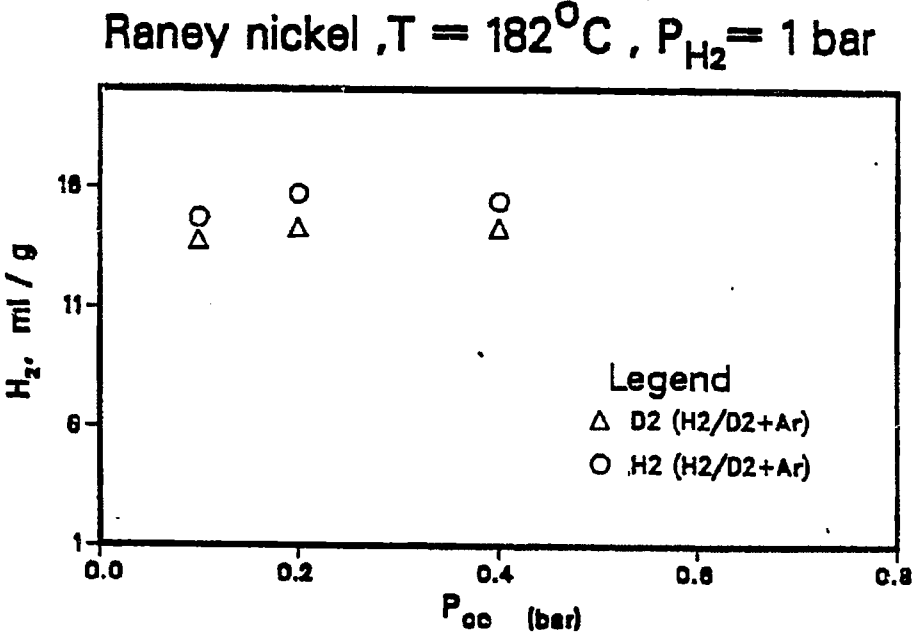

Figure 6-17 Amount of adsorbed hydrogen versus P_{CO}

(Raney nickel, T = 182 °C, P_{H_2} = 1 bar)

The transient responses can provide even more information regarding the nature of hydrogen at the catalyst surface.

At low temperature, the transient response curves without and with CO are shown in Figures 6-1 and 6-11. The area under the HD curves with the area between Ar and D_2 indicate the amount of adsorbed deuterium at the catalyst surface. As can be seen in Figure 6-1, the areas are large, which indicates that the amount of adsorbed deuterium is also large. However, as soon as CO is present on the surface, the area diminishes. This effect can be seen in the simultaneous decay of Ar and D_2 and the very small amount of HD area (Figure 6-11), both indicating the amount of adsorbed deuterium is very small.

The transient curves for a higher temperature, 110°C, are shown in Figures 6-18 and 6-19. In Figure 6-19, the coexistence of H_2 and CO, in the presence of CO, can be observed. It is worth mentioning that the shape of HD curves is relatively symmetrical for low temperatures with or without the presence of CO. Figures 6-2, 6-20 and 6-21 show the transient responses obtained in the absence of CO at different partial pressure of H_2 at temperature equal 220°C. The responses indicate that at higher pressures of H_2, more physically adsorbed hydrogen is observed. It can be seen from the transient responses. The maxima of HD curves decreases as the P_{H_2} increased. The H_2 and D_2 crossing point increased with P_{H_2}.

The transient responses obtained at reaction conditions with different P_{H_2} are shown in Figures 6-12, 6-22 and 6-23. By comparing the transient responses with and without CO, important observations are

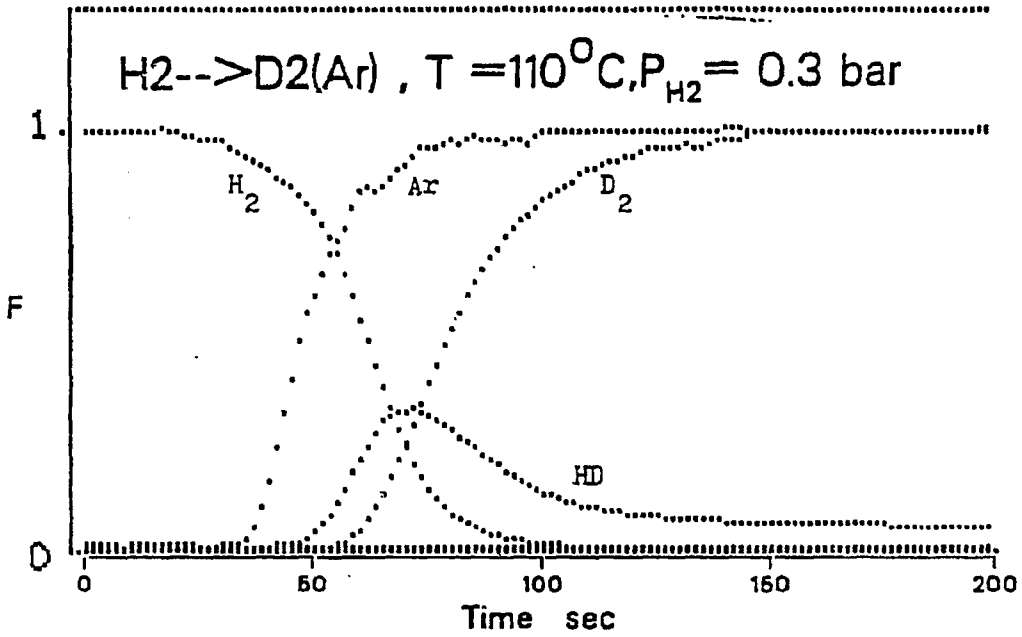

Figure 6-18 $H_2 \longrightarrow D_2(Ar)$ at 110 °C, P_{H_2} = 0.3 bar in 60 wt % Ni/SiO_2

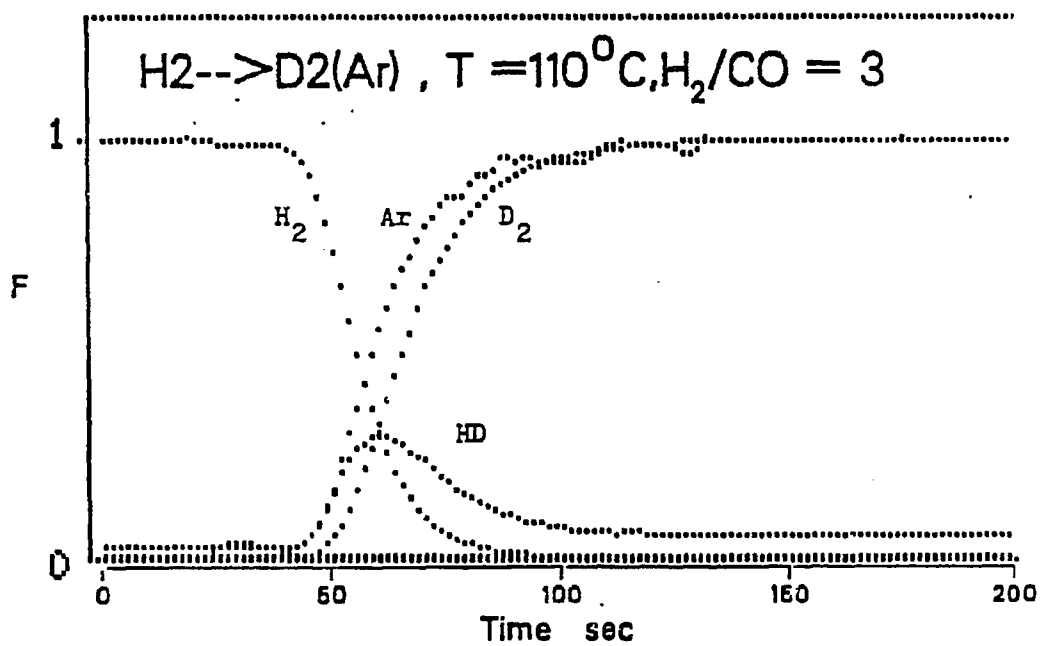

Figure 6-19 $H_2 + CO \longrightarrow D_2 + CO + Ar$ at 110 C, H_2/CO=3 in 60 wt % Ni/SiO_2 , P_{CO}= 0.1 bar

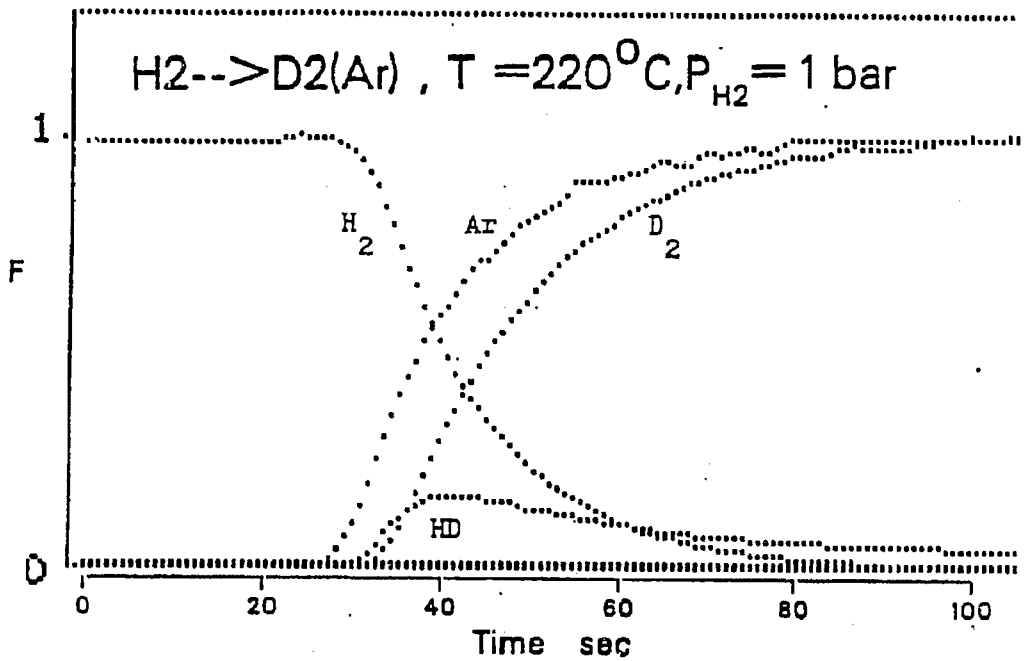

Figure 6-20 $H_2 \longrightarrow D_2 + Ar$, T = 220 °C, P_{H_2} = 1 bar in 60 wt % Ni/SiO_2

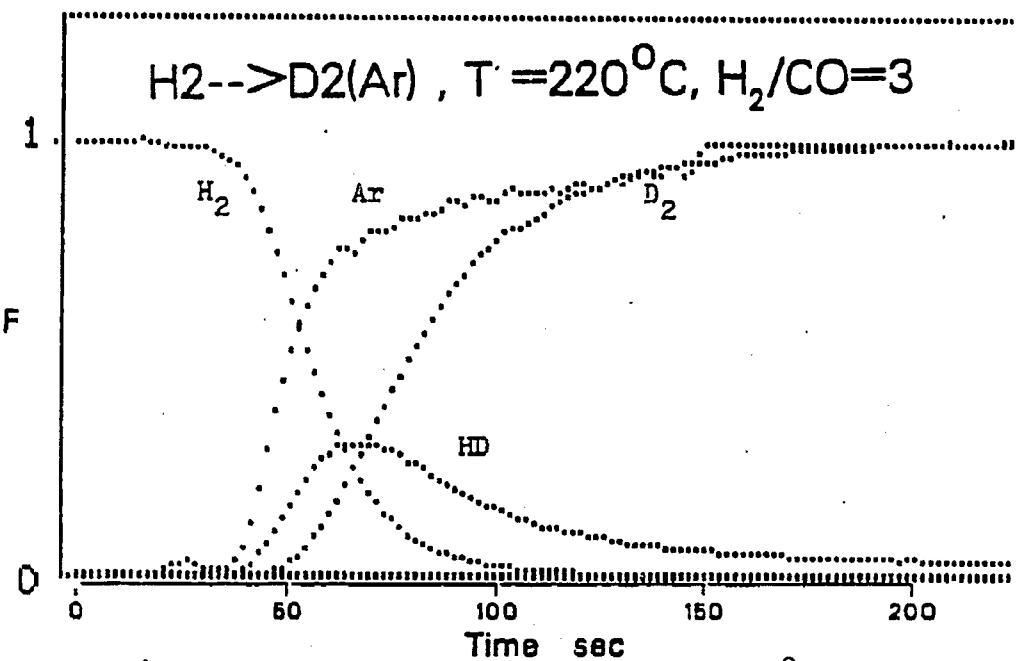

Figure 6-22 $H_2 + CO \longrightarrow D_2 + Ar + CO$, T = 220 °C, P_{H_2} = 0.3 bar, P_{CO}= 0.1 bar, 60 wt % Ni/SiO_2

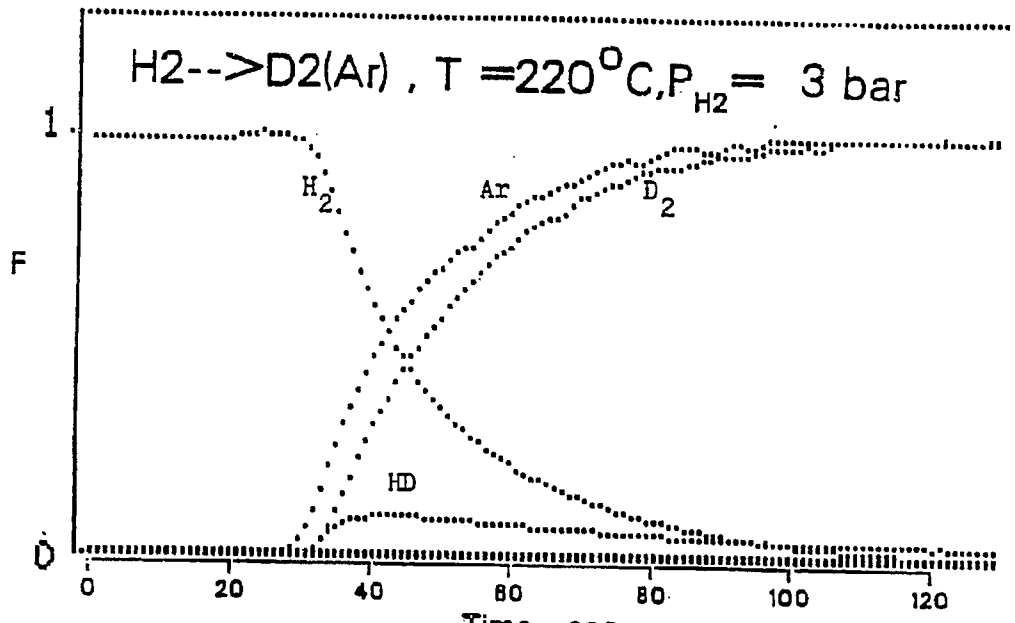

Figure 6-21 $H_2 \longrightarrow D_2 + Ar$, $T = 220^{\circ}C$, $P_{H_2} = 3$ bar in 60 wt % Ni/SiO_2

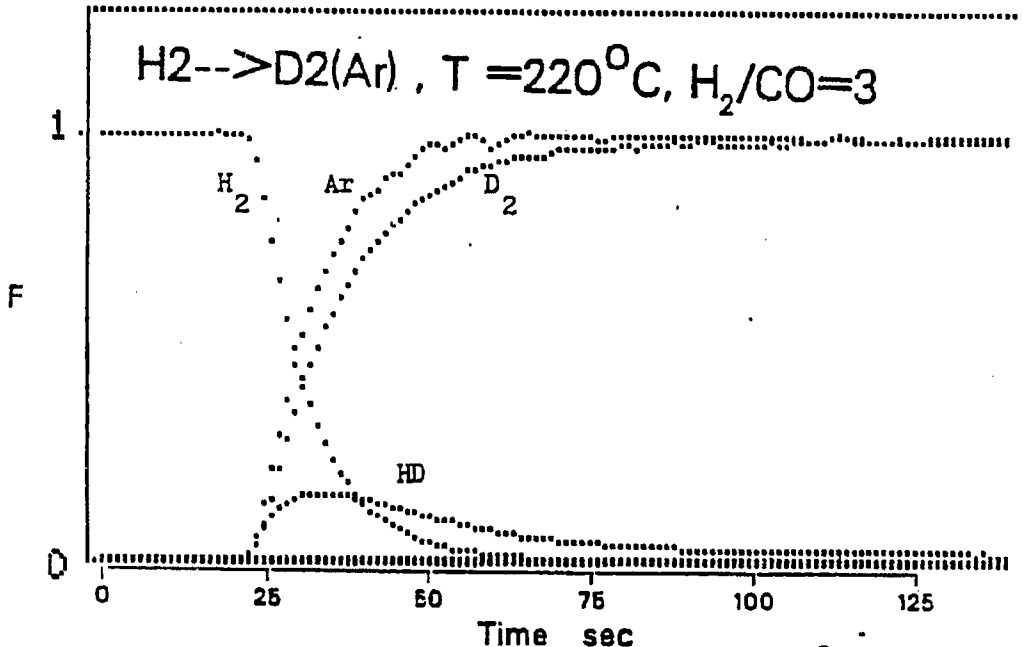

Figure 6-23 $CO + H_2 \longrightarrow CO + D_2 + Ar$, $T = 220^{\circ}C$, $P_{H_2} = 3$ bar, $P_{CO} = 1$ bar in 60 wt% Ni/SiO_2

worth mentioning. More HD formation takes place in the presence of CO than that formed in the absence of CO. This is a clear indication that, in the presence of CO, there are more adsorbed hydrogen or deuterium atoms than in the absence of CO. The adsorbed hydrogen may come from $C_\beta H_y$, CH_x, or H_{ad}. The temperature dependence on transients can also be seen by comparing the transients at different temperatures. By comparing Figure 6-24 with Figure 6-12, a significant difference is observed. Figure 6-24 is the transient obtained at 180°C. The HD area and the area between Ar and D_2 are lower than that at 220°C (Figure 6-12). The titration method also furnishes more information regarding the nature of adsorbed species. The responses for those transients are illustrated in Figure 6-6, for the condition in the absence of CO, and in Figure 6-13, under reaction conditions. In Figure 6-6, the D_2 transient is in the same magnitude as the HD transient. However, under reaction condition, significant differences are observed (Figure 6-13). The D_2 transient is much smaller than the HD transient. The shape of the D_2 peak and HD peak (Figure 6-13) are very similar to those observed when H_2 is used to displace adosrbed D-atom from the surface of nickel in the absence of any adsorbed CO or carbon (Figure 6-6). The area under the D_2 and HD curve is nearly the same (Figure 6-6), which suggests that D atom has the equal opportunity either to be D_2 or HD. However, in the presence of CO, the area between D_2 and HD show significant differences (Figure 6-13). The D_2 becomes smaller and the HD becomes larger. The ingrowth HD curve is similar to the ingrowth of methane curve (shape and location) (Figure 6-25). The additional HD

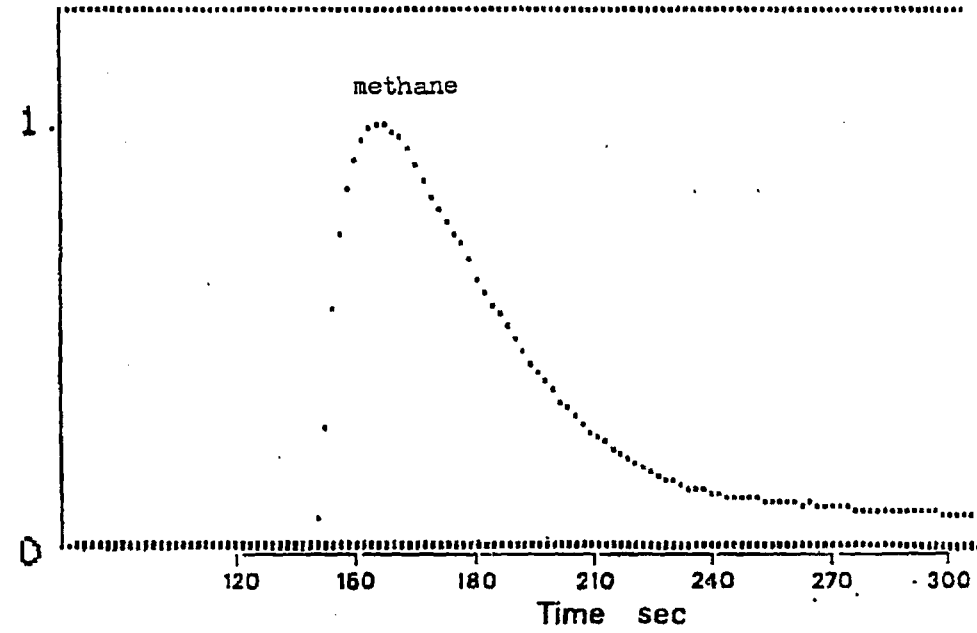

Figure 6-25 Methane ingrowth from CO + D_2 → Ar → H_2 at T = 220°C, D_2/CO = 3.3 same experiment as in Fig. 6-13

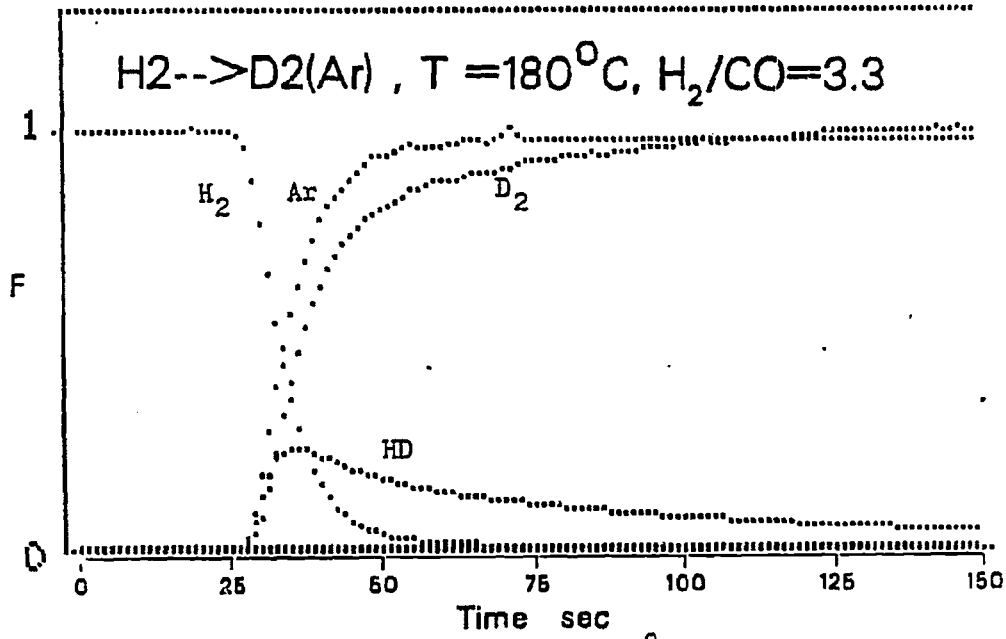

Figure 6-24 H_2 + CO → D_2 + CO + Ar, 180°C, H_2/CO = 3.3, P_{CO} = 0.3 bar, 60 wt% Ni/SiO_2

formed may associate with CH_xD_{4-x} and $C_\beta D_y$, or, to some extent, OD species. This is further evidence that the catalyst surface has a large amount of adsorbed hydrogen.

Typical transient responses obtained from Raney nickel are presented as follows. At low temperature, 30°C, the transients result in the absence of CO and presence of CO are shown in Figures 6-26 and 6-27. Again, similar behaviors are observed. At low temperature in the presence of CO most adsorbed hydrogen will be replaced by CO.

The transient result at 110°C in the absence of CO and in the presence of CO are shown in Figures 6-28 and 6-29. As seen in Figure 6-29, the adsorbed hydrogen is observable. It can be seen from the HD area and the area between Ar and D_2.

The transient result at 210°C with the of H_2/CO ratio equal to 6 is shown in Figure 6-31. Figure 6-30 shows the transient result in the absence of CO at 210°C. In view of those transients, it is indicated that in the presence of CO, more amounts of adsorbed hydrogen were observed. The HD area is larger than it would be in the absence of CO.

The titration measurements on Raney nickel are illustrated in Figures 6-32 and 6-33. In Figures 6-32 and 6-33, the D_2 transient is not in the same magnitude as the HD transient. The D_2 transient is larger than the HD transient. This observation suggests that part of D_2 transient may come from the desorption of D_2. The results indicate that the large amount of deuterium observed is originating from the D_2 transients (desorption of D_2 and/or recombination of deuterium atoms). Comparing the transients in Ni/SiO_2 (Figure 6-13) with Raney nickel

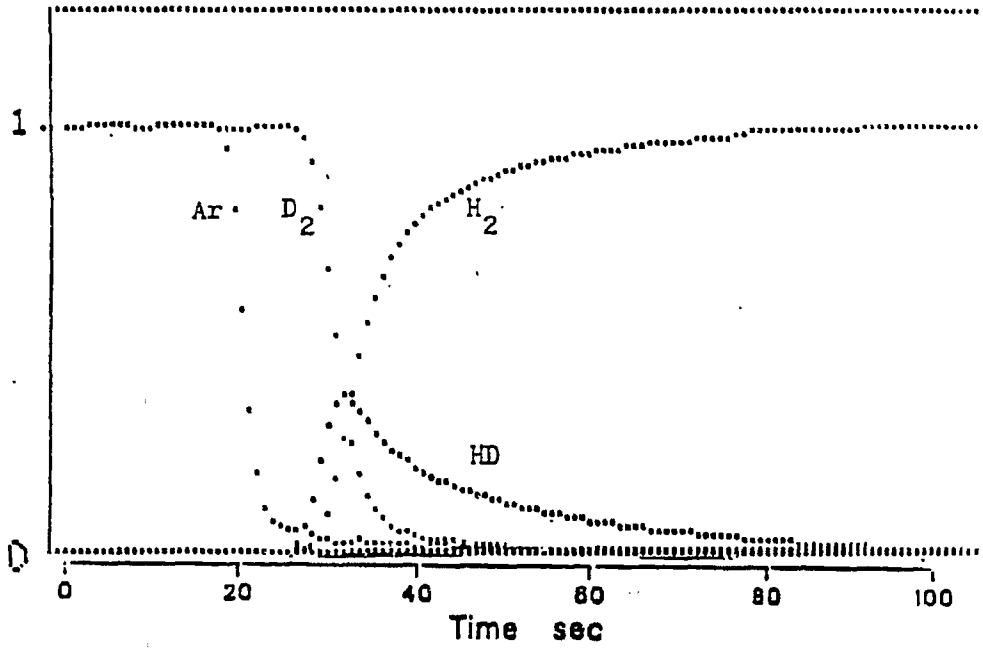

Figure 6-26 D_2+ Ar $\longrightarrow$ H_2 , 30°C, P_{H_2} = 1 bar, Raney nickel

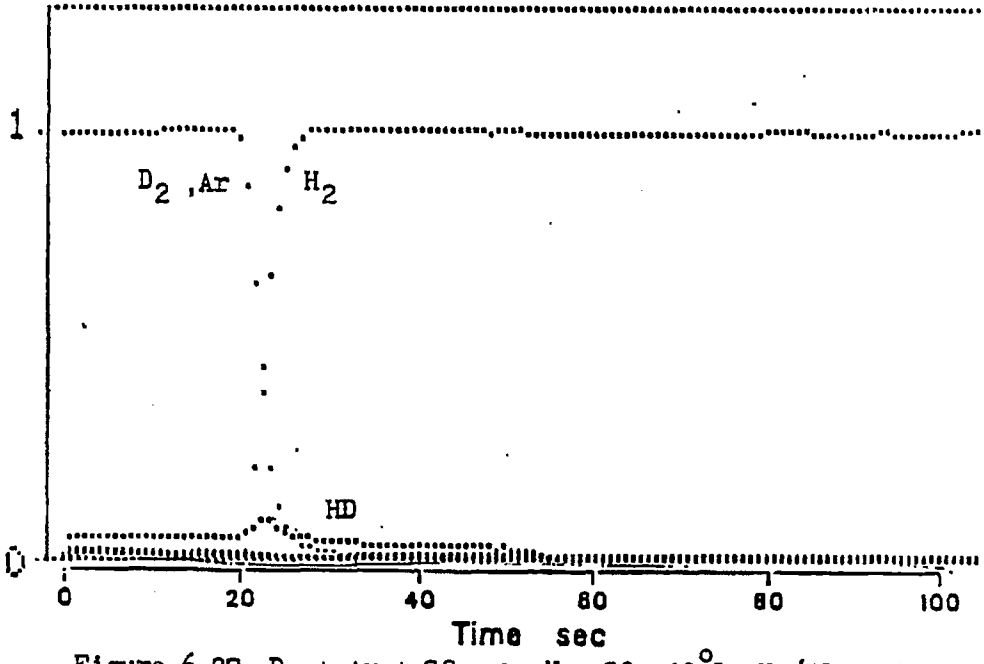

Figure 6-27 D_2 + Ar + CO $\longrightarrow$ H_2+ CO, 30°C, H_2/CO = 10, Raney nickel

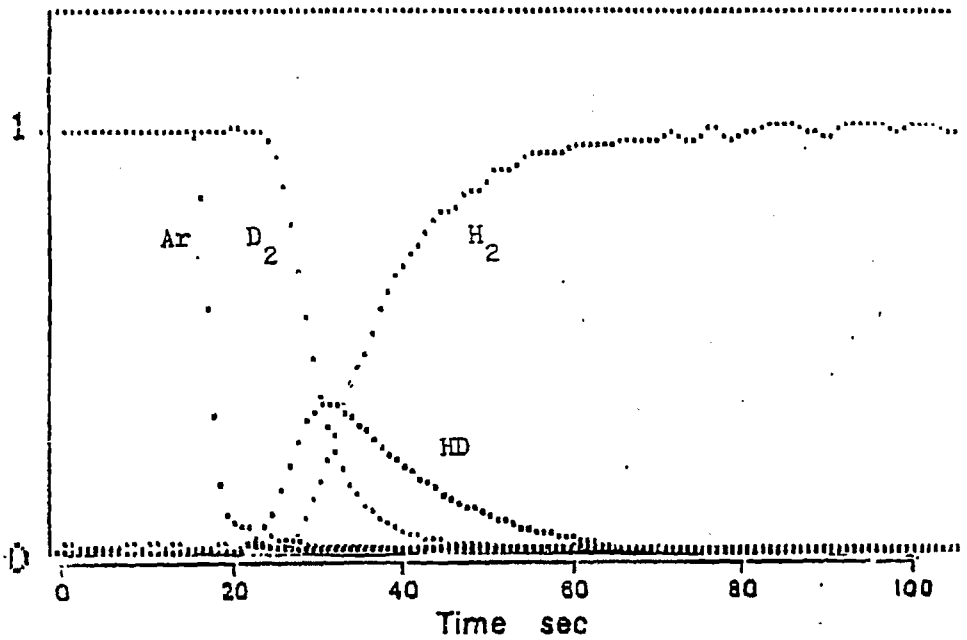

Figure 6-28 $D_2 + Ar \longrightarrow H_2$, 110°C, P_{H_2} = 1 bar, Raney nickel

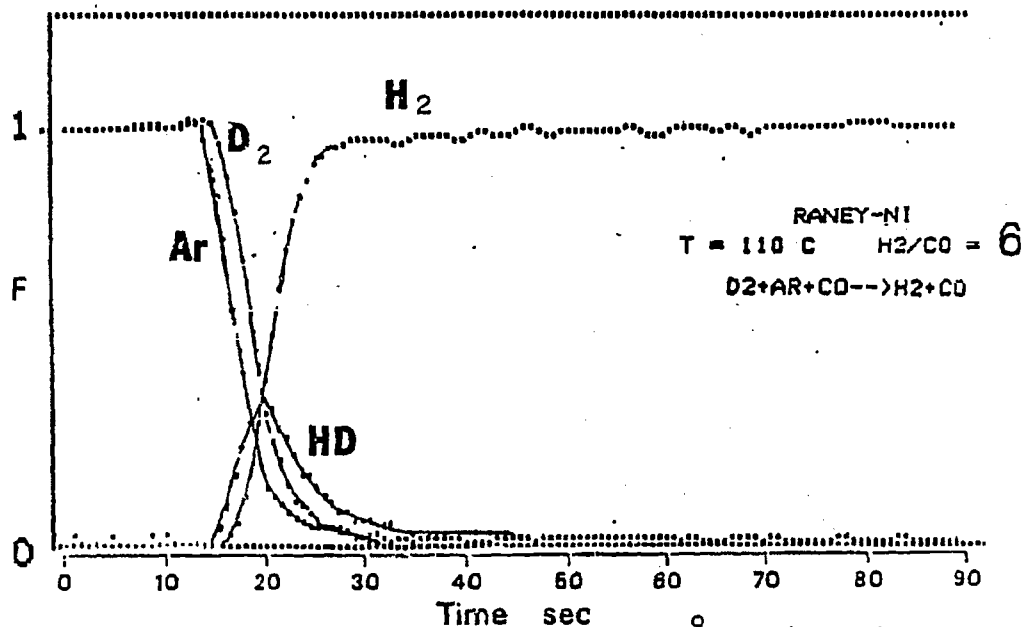

Figure 6-29 $D_2 + Ar + CO \longrightarrow H_2 + CO$, 110°C, H_2/CO = 6,

Raney nickel

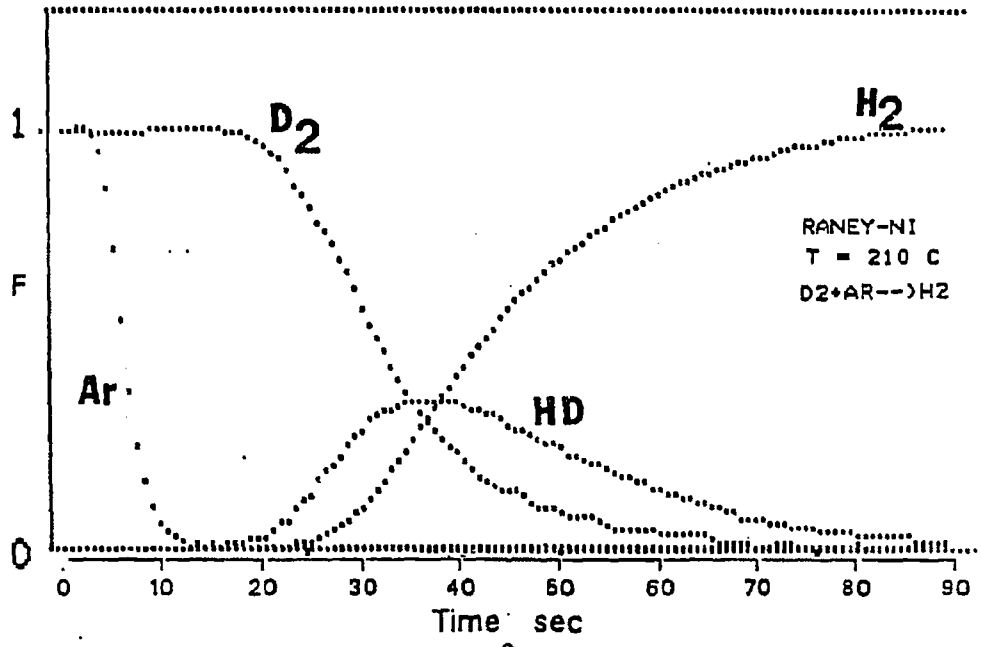

Figure 6-30 D_2 + Ar $\rightarrow$ H_2 , 210°C, P_{H_2} = 1 bar, Raney nickel

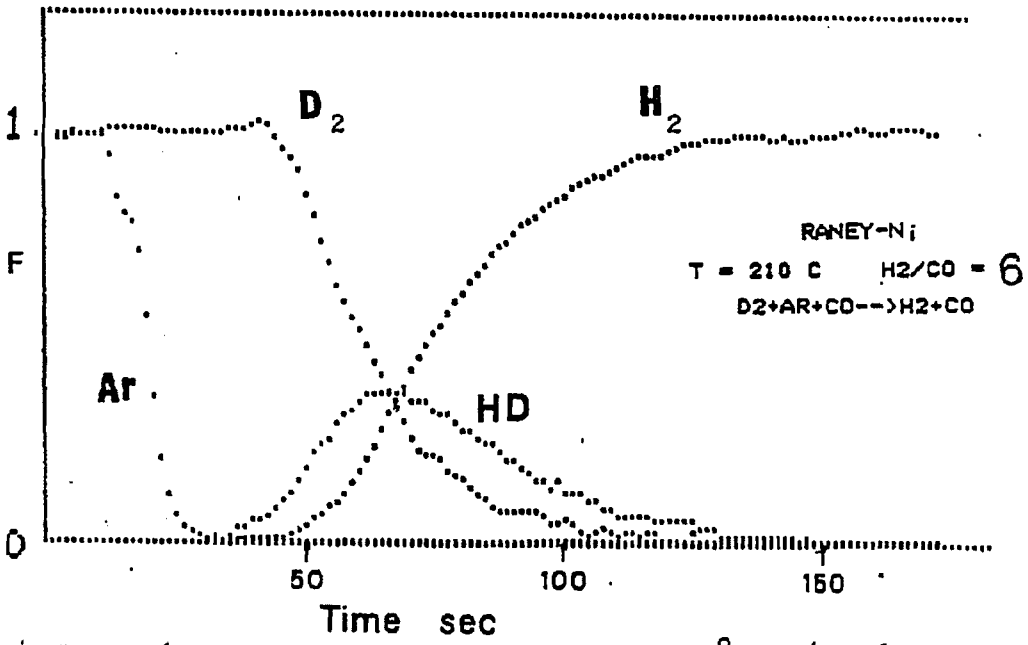

Figure 6-31 D_2 + Ar + CO $\rightarrow$ H_2+ CO, T = 210°C, H_2/CO =6, Raney nickel

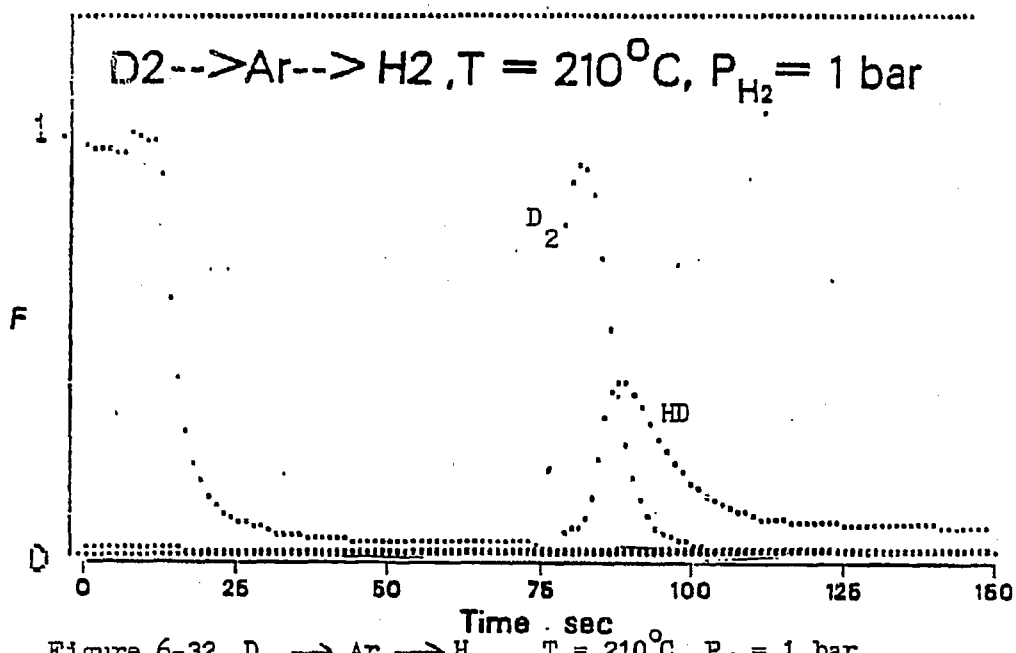

Figure 6-32 $D_2 \rightarrow Ar \rightarrow H_2$, T = 210°C, P_{H_2} = 1 bar, Raney nickel

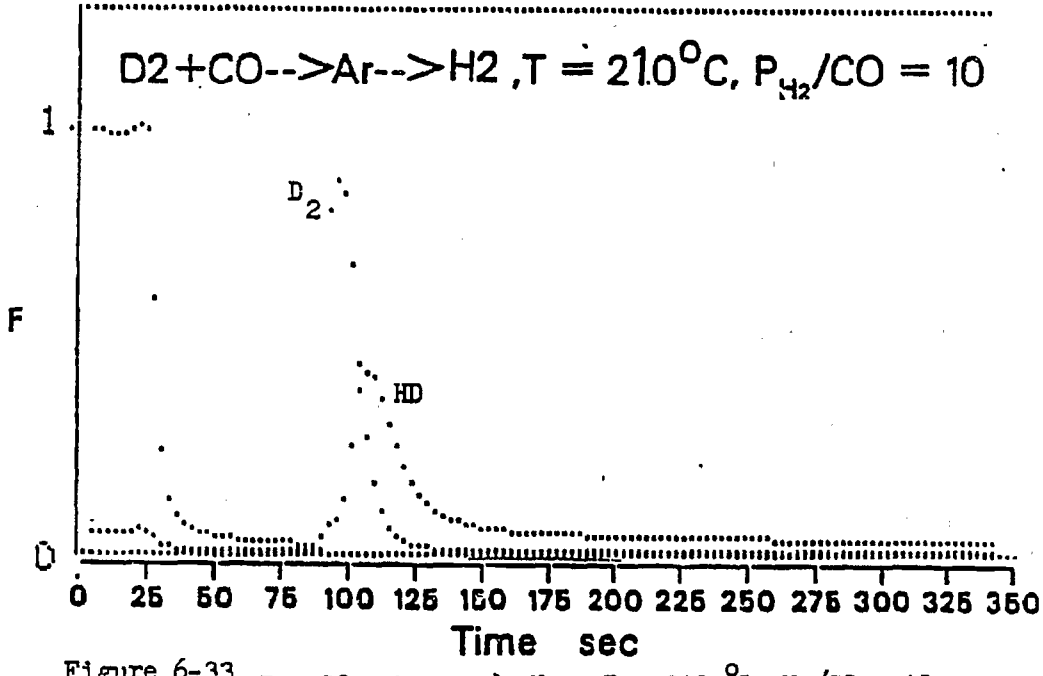

Figure 6-33 D_2+ CO $\rightarrow$ Ar $\rightarrow$ H_2 , T = 210 °C, H_2/CO = 10, Raney nickel

(Figure 6-33), a significant difference is observed. Under reaction condition, the contribution from HD to the total amount of adsorbed hydrogen is less in Raney nickel than in Ni/SiO_2. The large amount of adsorbed hydrogen is probably associated with free hydrogen atoms, adsorbed hydrogen molecules, $C_\beta H_y$, CH_x and OH. Typical transients for Ni powder with the presence and in the absence of CO are shown in Figures 6-34 and 6-35. A large amount of adsorbed hydrogen is observed under reaction condition.

6.3 Discussion

6.3.1 Stoichiometry of H/CO

It is generally accepted that the stoichiometry of H_{ad}/CO_{ad} ratio on nickel catalyst is close to one at low temperature (25^oC) static chemisorption conditions. The measurements of H_2 and CO uptake are obtained through low temperature static chemisorption (the chemisorption method of measuring hydrogen has been described in previous section). In general, H_2 adsorption follows H/M = 1.[116,117] In general dual-isotherm technique was used for CO adsorption measurements. The amount of strongly held adsorbed CO was determined by the difference of two isotherms (with a brief evacuation in between the two isotherms). The dual-isotherm technique also assumes that only weakly held CO (mainly on the support) is removed during the evacuation step (1).

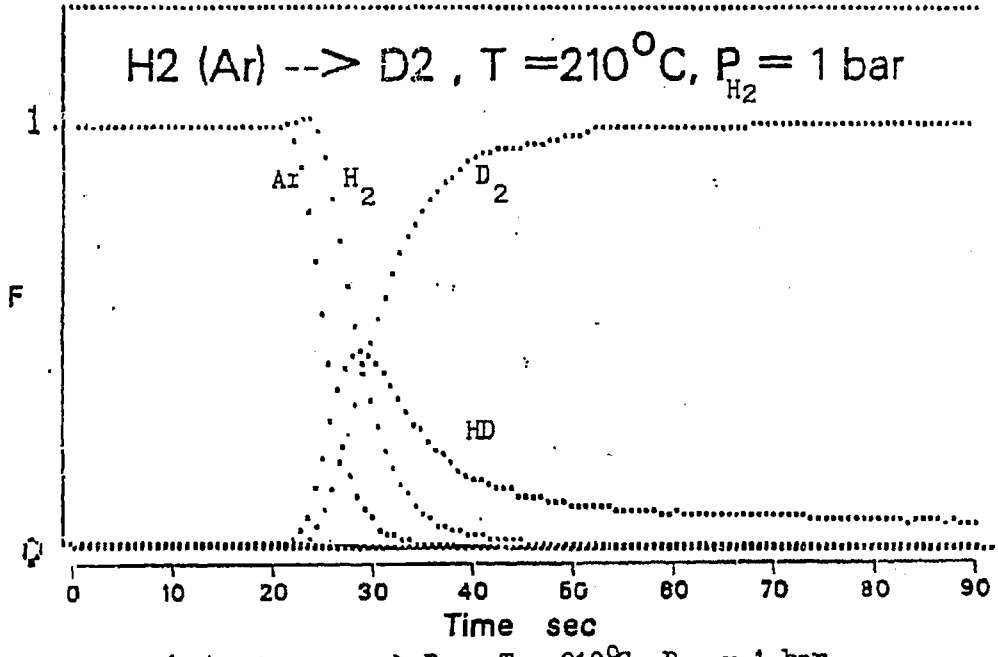

Figure 6-34 H_2 + Ar $\rightarrow$ D_2 , T = 210°C, P_{H_2} = 1 bar, nickel powder

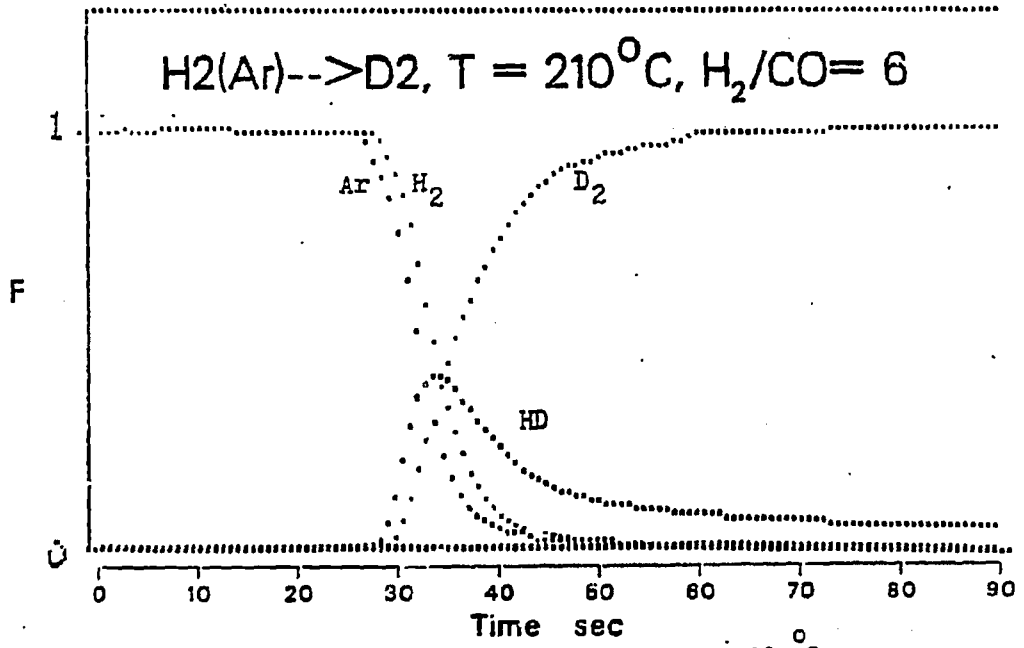

Figure 6-35 H_2 + Ar + CO $\rightarrow$ D_2 + CO, T = 210 °C, H_2/CO = 6, nickel powder

However, Fang et al.[118] showed that a significant amount of chemisorbed CO is removed from the metal.

The CO adsorption is considerably more complex, the stoichiometry of which varies with equilibration pressure, temperature, metal crystallite size, and metal loading. Formation of nickel carbonyl and substantial amounts of chemical and physical adsorption of CO on the support provide additional complications.[116] Various ranges of the stoichiometry of H/CO on nickel catalyst has been reported by Vannice[6,58,108] (range from 0.17 to 2.58) and Bartholomew and Pannel[117] (range from 0.036 to 1.84). It would be interesting to find out the stoichiometry of H/CO measured by transient measurement method in this study.

The H_2 and CO uptake measurements in this study are summarized in Table 6-4.

In view of the large variations in the H/CO stoichiometry from 1.07 to 2.54, one may ask oneself what causes the variations. It is probably due to the nature of different techniques. The transient method measures the total replaceable isotopes, including strongly and weakly adsorbed isotopes. The chemisorption method measures the strongly adsorbed species. It is therefore not surprising that different methods lead to different results. The advantages of using transient method is that the adsorbed species can be measured in-situ under reaction conditions.

Table 6-4

Stoichiometry of H/CO

Catalysts	ml/g H_2	ml/g CO	H/CO
Raney Nickel	8.2[a]	6.45[b]	2.54
60 wt % Ni/SiO_2	8.2[c]	15.21[d]	1.07
Ni powder	0.36[e]	0.406[f]	1.77

a. H_2/D_2 exchange measurements conducted at 110°C P_{tot} = 1 atm.

b. $^{12}CO/^{13}CO$ exchange measurements conducted at 110°C H_2/CO = 10 P_{tot} = 1 atm.

c. H_2/D_2 exchange measurements conducted at 110°C P_{H_2} = 0.3 atm.

d. $^{12}CO/^{13}CO$ exchange measurements conducted at 110°C Pco = 0.1 atm P_{H_2} = 3.9 atm.

e. H_2/D_2 exchange measurements conducted at P_{H_2} = 0.13 atm.

f. $^{12}CO/^{13}CO$ exchange measurements conducted at Pco = 0.13 atm P_{H_2} = 3.87 atm.

6.3.2 Equilibrium Between H_{ad} and H_2

It has been reported that the adsorbed hydrogen is in equilibrium with the gas phase H_2 on nickel catalyst.[61,71,82] Ozaki[61] and Falconer and Kester[92] indicated that adsorption of hydrogen on nickel is rapid and reversible.

Therefore, it is reasonable to assume that the adsorbed hydrogen is in equilibrium with gas phase hydrogen in the absence of CO. It is interesting to find out whether equilibrium exists between adsorbed hydrogen and gas phase hydrogen in the presence of CO.

A equilibrium index is being defined by

$$K_{in} = \frac{[I_{HD}]^2}{[I_{H_2}][I_{D_2}]} \qquad (6\text{-}1)$$

For example, the K_{in} can be determined from Figure 6-2 in the absence of CO.

I_{HD} = maximum HD intensity during H_2/D_2 exchange

I_{H_2}, I_{D_2} = H_2 and D_2 intensity corresponding to the HD intensity at the same x coordinates.

The K_{in} can also be determined in the presence of CO from Figure 6-12. The degree of equilibrium can be calculated by

$$\frac{K_{in}\ (\text{with CO})}{K_{in}\ (\text{without CO})} = D_{eq}(\%) \qquad (6\text{-}2)$$

The assumption is that in the absence of CO, the adsorbed hydrogen is in equilibrium with gas phase hydrogen.

Typical results are summarized in Table 6-5 for various nickel catalysts.

As seen in Table 6-5, at low temperature (30°C) and in the presence of CO, the adsorbed hydrogen is not in equilibrium with gas phase hydrogen. The degree of equilibrium is 0.99% for Raney nickel, and 1.88% for Ni/SiO_2. At a higher temperature (110°C), the degree of equilibrium is increasing. However, it is far from equilibrium. At 110°C with presence of CO, even though there is some amount of adsorbed hydrogen, the adsorbed hydrogen is not in equilibrium with gas phase hydrogen. Under reaction conditions, the adsorbed hydrogen is close to equilibrium with gas phase hydrogen. This conclusion is based on the degree of equilibrium shown in Table 6-5. The degree of equilibrium is in the range from 88% to 96%. The results from Table 6-5 indicated that at low temperatures (in the presence of CO) the adsorbed hydrogen is not in equlibrium with gas phase hydrogen. This is consistent with the result of Bell and Cant.[82] Under the reaction condition, the adsorbed hydrogen is close to equilibrium with gas phase hydrogen. This also is consistent with the results of Bell and coworkers.[38,81,82]

6.3.3 Effect of Nature of Nickel Catalysts

As shown in Figure 6-5, the amount of adsorbed hydrogen on Ni powder increases with temperature. This behavior is completely different from

Table 6-5

Equilibrium Between H_{ad} and H_2

Catalyst	T °C	Pco (atm)	P_{H_2} (atm)	H_2/CO	K_{in}	D_{eq}(%)
Raney-nickel	30	0	1	-	1.907	--
	30	0.09	0.91	1.0	0.019	0.99
	110	0	1	-	2.13	--
	110	0.09	0.91	10	1.44	61.0
	210	0	1	-	2.90	--
	210	0.5	0.5	1	2.80	96.0
	210	0.09	0.91	10	2.56	88.0
	210	0.03	0.97	33	2.77	95
Ni powder	110	0	1	-	1.07	--
	110	0.14	0.86	6	0.117	10.9
	210	0	1	-	1.14	--
	210	0.14	0.86	6	1.07	94
Ni/SiO_2	30	0	0.3	-	2.12	--
	30	0.1	0.3	3	0.04	1.88
	110	0	0.3	-	2.07	
	110	0.1	0.3	3	0.982	41.4
	180	0	0.3	-	2.43	--
	180	0.1	0.3	3	2.18	88.5
	220	0	0.3	-	2.17	--
	220	0.1	0.3	3	2.06	95.0

$$K_{in} = \frac{[I_{HD}]^2}{[I_{H_2}]\,[I_{D_2}]}$$

$$D_{eq} = \frac{K_{in} \text{ (in the presence of CO)}}{K_{in} \text{ (in the absence of CO)}} \times 100$$

that on Raney nickel (Figure 6-4) and 60 wt % Ni/SiO_2 (Figure 6-3). As suggested by Scott and Phillips,[120] the support induced hydroxyl group may participate in the exchange reaction with H_2 and D_2 when the temperature is increased. If this is the case, then the amount of adsorbed hydrogen, measured by H_2/D_2 transient method, should exhibit a tendency to increase with temperature. From our observations on Raney nickel (Figure 6-4) and Ni/SiO_2 (Figure 6-3), it suggested that the effect is insignificant. It cannot account for the strange behavior over Ni powder, as Ni powder has no support (i.e., no support-induced hydroxyl group). It is suspected that activated chemisorption or hydrogen migration into the bulk nickel may dominate the observed phenomena. No supporting evidence for activated chemisorption on Ni powder was found in the literature. However, independent measurements on the amount of adsorbed hydrogen showed trends consistent with the transient method measurements of this study (Table 6-1).

The observed transient responses for adsorbed hydrogen on Raney nickel and Ni/SiO_2 also exhibited a different trend. As seen for titration measurements on Ni/SiO_2, Figure 6-6, the areas under D_2 and HD are in the same magnitude. It is assumed that Ar flush can remove weakly adsorbed molecule deuterium. After Ar flush, most adsorbed deuterium is in atom form. After switching back to H_2 gas, the deuterium atom has the equal opportunity either to form HD or D_2. This is the case for Ni/SiO_2 in the absence of CO. Similar titration measurements on Raney nickel produced different results (Figure 6-32).

It is indicated that Raney nickel has a large amount of adsorbed D-M and/or adsorbed deuterium molecule. This will result in an area under D_2 larger than that under HD. On Ni/SiO_2, the titration results under reaction conditions also show different behavior from results not under reaction conditions (Figure 6-13 and Figure 6-6). The HD area is larger than D_2 area. This suggests that under reaction conditions the amount of Ni-D species decreases. A large percent of D is associated with carbon (reactive and irreactive) or surface hydroxyl groups. The titration result for Raney nickel under reaction conditions gave similar shapes and magnitudes for D_2 and HD peaks as titrations taken not under reaction conditions (Figures 6-32 and 6-33). This indicates that under reaction conditions, large amount of Ni-D and adsorbed D_2 species present on the surface coexist with some D associated with carbon (reactive and irreactive) or surface hydroxyl group.

The ultimate goal in the measurement of adsorbed hydrogen is to achieve a better understanding of the behavior of hydrogen at the catalyst surface, under reaction conditions. Up to this point, the following observations have been made:

1. In the presence of CO at low temperature, the adsorbed hydrogen is not in equilibrium with gas phase hydrogen. The adsorbed hydrogen is in equilibrium with gas phase hydrogen under reaction condition. This observation is valid for all nickel catalysts in this study.

2. The amount of adsorbed hydrogen at constant H_2/CO ratio increased with increasing reaction temperature. This phenomenon is observed for Raney nickel, nickel powder and Ni/SiO_2 catalysts.
3. The amount of adsorbed hydrogen is insensitive to the variation of H_2/CO ratio at constant total pressure (Raney nickel), or to the variation of pressure of CO at constant hydrogen pressure (Ni/SiO_2).
4. Large amounts of hydrogen coexist with close to monolayer of CO_{ad}.

Many unanswered questions and inconsistent experimental results still exist. Such as, what are the forms of adsorbed hydrogen under reaction condition? Is it associated with carbon (reactive and irreactive) and/or with oxygen (surface hydroxyl groups) and/or with Ni, etc.?

How do we explain the inconsistent experimental results (i.e., Figures 6-14 and 6-15)? Do we suffer from any complications in measuring the amount of adsorbed hydrogen?

Let us answer those questions at least to some extent.

6.3.4 Sites for Adsorbed Hydrogen

Where are the sites for adsorbed hydrogen? It has been suggested by many investigators[121-124] that the most probable bonding made is with H atoms occupying "three-fold hollow adsorption sites," i.e., the hydrogen atoms sit above holes in the cubic close-packed nickel surface at equal distance to three surface nickel atoms. Bell[81] proposed

that the hydrogen atoms are located primarily in the three- and four-fold hollows between Ru atoms under reaction condition.

6.3.5 Adsorbed Hydrogen in 60 wt % Ni/SiO_2

Bell et al.[38] proposed that the hydrogen is associated with C_β, in the forms of $C_\beta H_y$, y is between 1.8 and 2.4. Assuming that all the amount of adsorbed hydrogen measured through the transient method is associated with irreactive carbon species, it is interesting to find out the value of y in Ni/SiO_2. We obtained the value of y in $C_\beta H_y$ of 2.98 (Table 6-6). It seems to agree with Bell's observation. However, in view of the carbon irreactive value, it is the upper limit of the $\Theta_{C_{irr}}$ because we included the carbon from dissociation of CO. Actually, y will be larger than 2.98. If we assume the hydrogen is associated with total carbon on the surface, then y is 2.62. Assumptions based upon hydrogen being associated with C_β or C_{total} alone are not sufficient to explain the large value of hydrogen adsorbed on Ni/SiO_2. The remaining adsorbed hydrogen is probably associated with the three-fold sites. By comparing Figures 6-6 and 6-13, one can infer that, under reaction conditions, there is some adsorbed hydrogen associated with metal. It is probably associated with three-fold sites.

The amount of adsorbed hydrogen was observed to be not a strong function of H_2/CO ratio (i.e., at P_{H_2} maintained constant while varying P_{CO} independently, Figure 6-15) on Ni/SiO_2 catalyst. This observation suggests that the amount of H_{ad} which participates in methanation is

Table 6-6

The Concentration of Adsorbed Species in 60 wt % Ni/SiO_2

T	P_{H_2}(atm)	P_{CO}(atm)	ml/g H_2	ml/g CO	Θ_C
220	1	0	7.99[a]	-	
110	3.9	0.1	-	15[b]	
220	1	0.3	7.92[a]	9.45[b]	
220	1	0.3		0.721[c]	(0.04808)
220	1	0.3		6.03[d]	(0.402)

$$y = \frac{2 \times 7.92}{6.03 - 0.721} = 2.98 \text{ for } C_\beta H_y$$

$$y = \frac{2 \times 7.92}{6.03} = 2.62 \text{ for } CH_y \ (C_\beta H_y + CH_y)$$

a. The amount of hydrogen measured by H_2/D_2 exchange.

b. The amount of CO measured by $^{12}CO/^{13}CO$ exchange.

c. Equivalent CO translates from Θ_C reactive (measure by 12/13 exchange).

d. Equivalent CO translates from Θ_c total ($\Theta_{C_{tot}}$ measured by $H_2 + {}^{12}CO \rightarrow H_2$) (this is the upper limit of Θ_C).

small. Most adsorbed hydrogen is not participating in the reaction. This also implies that the availability of H_{ad} is not a controlling process in methanation. There is an abundance of hydrogen on the catalyst surface.

Through transient H_2/D_2 exchange methods and titration methods, the amount of adsorbed hydrogen was also observed to be close to that of deuterium (Figure 6-8). Additionally, an inverse H/D isotope effect on Ni/SiO_2 was observed (Chapter 5). When an H/D isotope effect is observed, one would expect that the amount of adsorbed hydrogen should be differ from the amount of adsorbed deuterium.

Results from the study indicate that the amount of hydrogen or deuterium participating in methanation is small compared to the total amount of hydrogen or deuterium measured. This will result in H_2 uptake being the same as D_2 uptake at a significant H/D isotope effect condition.

It has been suggested that the support-induced hydroxyl group[120,125] and D_2-H_2O-H_2 exchange reaction[82,120,126] may affect the measurement of H_2/D_2 exchange.

If this is the case, then changing reaction condition will change the concentrations of surface hydroxyl groups and H_2O. As seen in Figure 6-15, the H_2 uptake is insensitive to the change of reaction conditions. It has also been reported in the literature that the D_2-H_2O-H_2 exchange is slow on Ni catalysts.[120,126]

The possibility of the surface hydroxyl group and D_2-H_2O-H_2 exchange affecting the amount of adsorbed hydrogen measured has not be

ruled out. However, the extent of this effect in the study was considered insignificant. This possibility exists but does not play an important role in the H_2/D_2 exchange measurements. One may suspect that seeing a long tail on HD transient during the H_2/D_2 exchange under reaction condition is evidence of surface hydroxyl group and D_2-H_2O-H_2 exchange effects. We do observe some tailing in H_2/D_2 exchange; however, it does not have a significant effect on the measurement result. Besides, the tail may also come from the heterogeneity in the adsorbed species.

It is possible that all the hydrogen measured is associated with CO in the form of CH_nO. If this is the case, then a variation of the amount of adsorbed hydrogen would accompany a variation of the amount of adsorbed CO. As seen in Figure 6-8, the amount of adsorbed hydrogen increases with increasing reaction temperature. According to this hypothesis (CH_nO), the amount of adsorbed CO should increase with an increase in reaction temperature. Figure 4-4 indicates that the amount of adsorbed CO does not increase with increasing temperature. Θ_{CO} is close to a constant value. Combining these two results, the possibility of the formation of CH_nO species can be ruled out.

Inconsistent results observed are shown in Figures 6-14 and 6-15. One shows the amount of adsorbed hydrogen to increase with P_{H_2} (P_{CO} = C), the other shows the amount of adsorbed hydrogen to be virtually constant while varying the P_{CO} (P_{H_2} = C). Figure 6-14 seems to favor the effect of surface hydroxyl group and D_2-H_2O-H_2 exchange. The H_2O production also increased with P_{H_2}. However, in view of Figure 6-7, the

possibility can be ruled out. We also observed the amount of adsorbed hydrogen to increase with P_{H_2} in the absence of CO. The causes for this phenomena of H_2 uptake increasing with P_{H_2} can be either large amounts of weakly adsorbed hydrogen or H_2 spillover on unreduced nickel.

Both molecular and atomic bound hydrogen have been suggested as the state of weakly bound hydrogen.(127) Another possibility arises since, if one H atom is bound on a C_8 site, the second H atom may be found in the subsurface hole just below the C_8 site. In such a situation a hydrogen-H interaction still exists. This is called "type C H" in the literature. This results in H/metal > 1.(128) If type C hydrogen and the weakly bound hydrogen increased with P_{H_2}, this effect would have been observed (Figure 6-7).

As indicated in Chapter 4, Ni^+ and Ni^{2+} may exist on unreduced Ni/SiO_2.(222) As unreduced samples cannot chemisorb H_2, the following reactions are possible

$$H_2 + 2\ Ni^+ \rightleftharpoons 2\ Ni^0 + 2\ H^+ \qquad (6\text{-}3)$$

$$H_2 + Ni^{2+} \rightleftharpoons Ni^0 + 2\ H^+ \qquad (6\text{-}4)$$

One may speculate the presence of Ni^+ and Ni^{2+} on the Ni^0 metallic particle, in some instances, would increase the hydrogen uptake as a result of the reduction of these Ni^+ and Ni^{2+}.(112,129)

High P_{H_2} may also favor the hydrogen spillover. This would result in the amount of adsorbed hydrogen increasing with P_{H_2}.

6.3.6 Adsorbed Hydrogen in Raney Nickel

If we assume all the adsorbed hydrogen is associated with $C_{total}H_y$ or $C_\beta H_y$, then the y values are 2.32 and 2.71 respectively (Table 6-7). These results seem reasonable compared with Bell's result, however the y value will actually be higher because the total carbon value reported is the upper limit. It is not sufficient to explain the large amount of adsorbed hydrogen on Raney nickel based upon hydrogen associated with C_β or C_{total}. The rest of the hydrogen is probably associated with three fold sites.

Figures 6-16 and 6-17 indicate that the amount of adsorbed hydrogen is not a sensitive function of reaction condition. Results shown in Figure 6-10 indicate that the amount of adsorbed hydrogen is close to that of deuterium. We also observed an inverse H/D isotope effect (Chapter 5). The same conclusion is obtained as on Ni/SiO_2. The amount of hydrogen or deuterium participating in methanation is small compared to the total amount of hydrogen or deuterium at the catalyst surface.

The availability of H_{ad} may not be a controlling process in methanation. Raney nickel also exhibits a similar behavior (Figure 6-17), as does Ni/SiO_2 (Figure 6-15). The same conclusion regarding the insignificance of surface hydroxyl group and D_2-H_2O-H_2 exchange effects is obtained. It is also concluded that the large amount of hydrogen is not associated with CO in a form of CH_nO (Figure 6-16). This is based upon the same discussion as in Ni/SiO_2.

Table 6-7

The Concentration of Adsorbed Species in Raney Nickel

T	H_2/CO	ml/g H_2	ml/g CO	Θ_C
210	∞	8.5[a]		
110	10	-	6.45[b]	
210	6	11.47[a]	5.5[b]	
210	6			
210	6		9.868[c]	1.53
210	6		1.419[d]	0.22

$C_\beta H_y$

$$y = \frac{11.47 \times 2}{9.868 - 1.419} = 2.7$$

$C_{tot}H_y$

$$y = \frac{11.47 \times 2}{9.868} = 2.32$$

a. The amount of hydrogen measured by H_2/D_2 exchange at P_{tot} = 1 atm.

b. The amount of CO measured by $^{12}CO/^{13}CO$ exchange at P_{tot} = 1 atm.

c. Equivalent CO translates from C reactive (measured by $^{12}CO/^{13}CO$ exchange).

d. Equivalent CO translates from $\Theta_{C_{tot}}$ ($\Theta_{C_{tot}}$ measured by H_2 + ^{12}CO + H_2. This is upper limit for the total carbon on the surface.

It has been reported in the literature that a large volume of hydrogen evolved when Raney nickel was heated was formerly considered as evidence for a hydride[130] or nickel dissolved hydrogen [131] structure. Anderson et al.[89] indicate that this may be explained on the basis of the reaction between residual aluminum and H_2O bound as alumina trihydrate.

$$Al + 3\ H_2O \rightarrow Al(OH)_3 + 1.5\ H_2 \qquad (6\text{-}5)$$

If this is the case, then by varying the concentration of H_2O may have significant effect on the amount of adsorbed hydrogen. As shown in Figure 6-17, the amount of adsorbed hydrogen is highly independent of H_2/CO ratio (H_2O concentration will vary with H_2/CO ratio). Even though this reaction does occur under measurements in this study, however, the effect may not be very important.

Further conclusions regarding the detailed behavior of the hydrogen on Ni powder cannot be reached due to the limited amount of experimental data obtained under reaction conditions.

6.4 Conclusions

From the study of the amount of adsorbed hydrogen, various important results are summarized as follows:

1. At room temperature, in the presence of CO, almost all adsorbed hydrogen at the catalyst surface is replaced by CO. The adsorbed hydrogen is not in equilibrium with gas phase hydrogen.
2. At a higher temperature ($110^{o}C$) the CO co-exists with less than 0.3 monolayer of hydrogen (taking the amount of hydrogen measured at $110^{o}C$ in the absence of CO as one monolayer). The adsorbed hydrogen is not in equilibrium with the gas phase hydrogen.
3. The amount of adsorbed hydrogen at constant H_2/CO ratio is increased with the temperature. The adsorbed hydrogen is close to equilibrium with the gas phase hydrogen at $210^{o}C$. The coexistence of large amounts of hydrogen with close to monolayer of CO under reaction condition is observed.
4. The large amount of hydrogen observed under reaction condition is probably associated with two sources-with the surface carbon as $C_{\beta}H_{y}$ and CH_{x}, and in an atomic and/or molecular form, with nickel.
5. The availability of hydrogen for methanation may not be a limiting process. There is an abundance of hydrogen at the catalyst surface under reaction condition.
6. The transient method is a good method in measuring the amount of adsorbed hydrogen under reaction condition.

7.0 SUMMARY

This study was aimed at establishing a better understanding of the mechanism of methanation on nickel catalysts. The proposed mechanism involved both adsorbed hydrogen atoms and CO being in equilibrium with gas phase hydrogen and CO. The dissociation of CO is a fast and irreversible process. The reaction of surface carbon proceeds through a slow step (change in the carbon metal coordination or carbon-carbon depolymerization) and then reacts very rapidly via a reversible sequence of steps to form a CH_x (x = 1-3) group. The $CH_{3_{ad}}$ species further reacts with H_{ad} to form $CH_{4(g)}$.

In the catalyst aging study on Raney nickel the formation of methane via two parallel pathways was observed. The origin of catalyst aging in this particular case is in essence not a process of site blocking, but rather a slow "deterioration" of the Raney nickel itself, causing pronounced kinetic heterogeneity.

The observed low value of fractional coverage of reaction intermediates is not due to a carbidic adlayer which blocks a large fraction of the surface.

Small coverages in C_{irr} and oxygen appearing to inhibit the CO dissociation, thereby limiting the steady-state production of carbidic reaction intermediates.

The coverage of reaction intermediates (θ_C) and its reactivities (k_2) are significantly more structure/catalyst sensitive than what is indicated by their algebraic product:

$$K_2\ \Theta_C = TOF_{CH_4}$$

The results from the study of H/D isotope effect indicate that the origin of H/D isotope effect is a thermodynamic isotope effect (the coverage of reaction intermediates effect). The H/D isotope effect is sensitive to the nature of the nickel catalysts. A slow step not involving hydrogen in methanation was confirmed in the study of H/D isotope effect.

The amount of adsorbed CO is not sensitive to the reaction condition. A large amount of hydrogen coexists with close to a monolayer of CO found under reaction condition. The adsorbed hydrogen is in equilibrium with gas phase hydrogen under reaction condition. The large amount of hydrogen observed under reaction condition is associated with surface carbon ($C_\beta H_y$ and CH_x) and associated with nickel metal (in atomic and/or in molecular form).

APPENDIX A

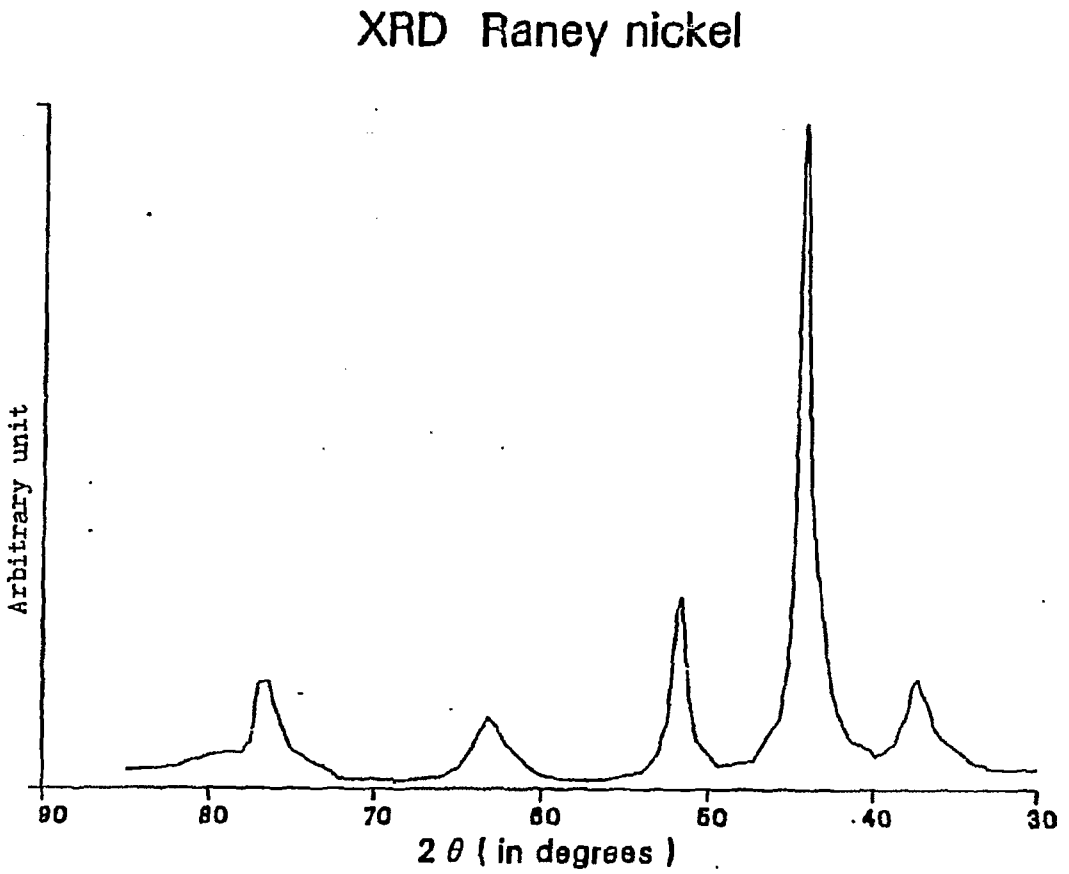

Figure A-1 XRD spectrum for Raney nickel

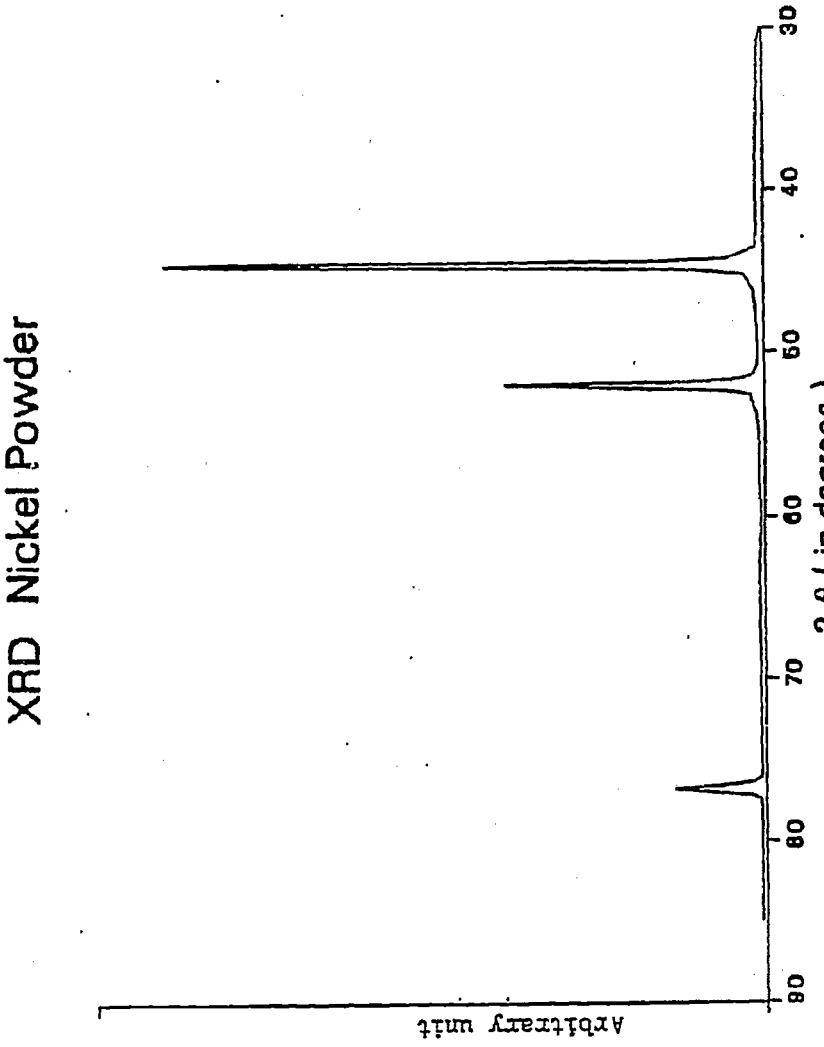

Figure A-2 XRD spectrum for nickel powder

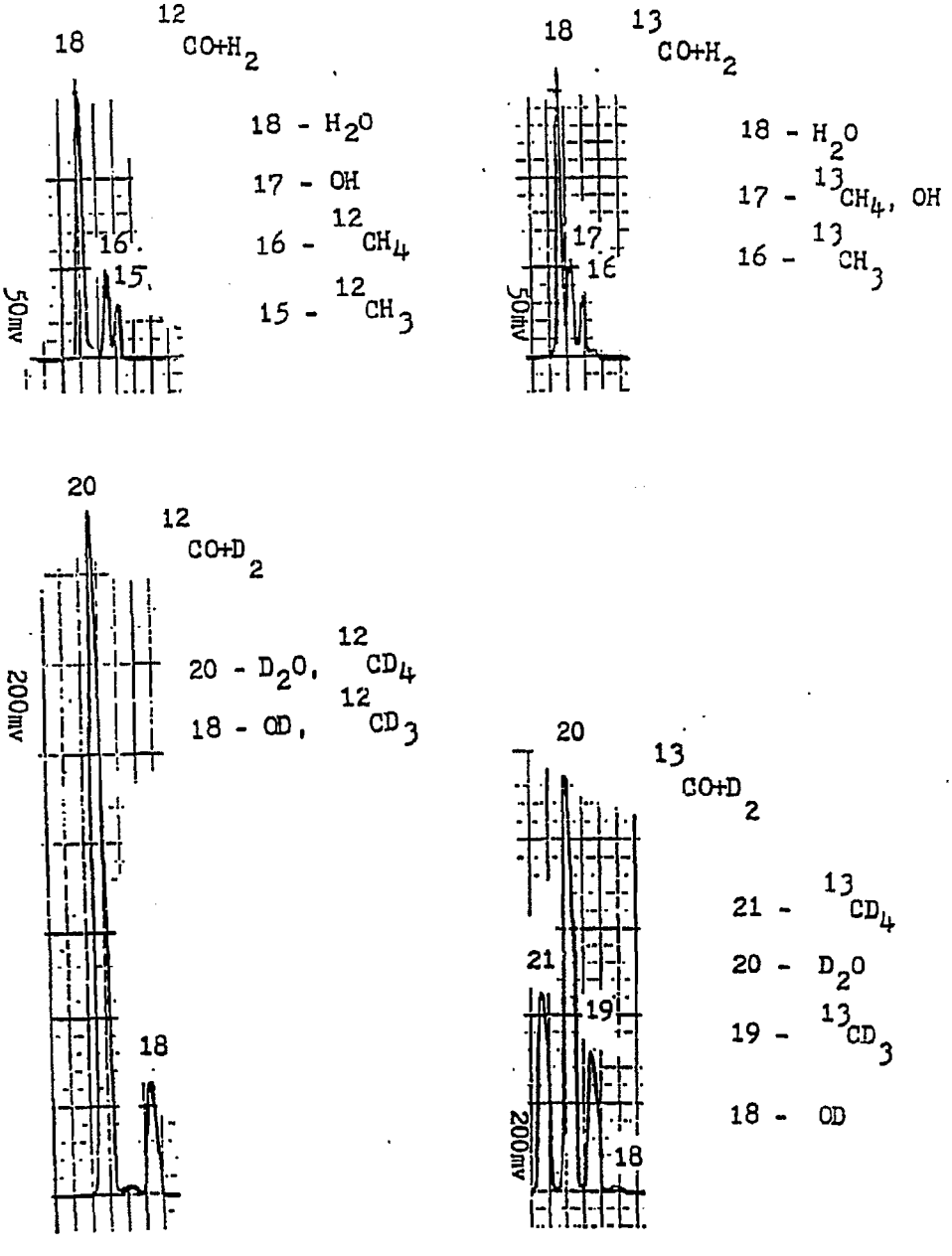

Figure A- 3 Fragmentation patterns for CH_4,CD_4,H_2O and D_2O

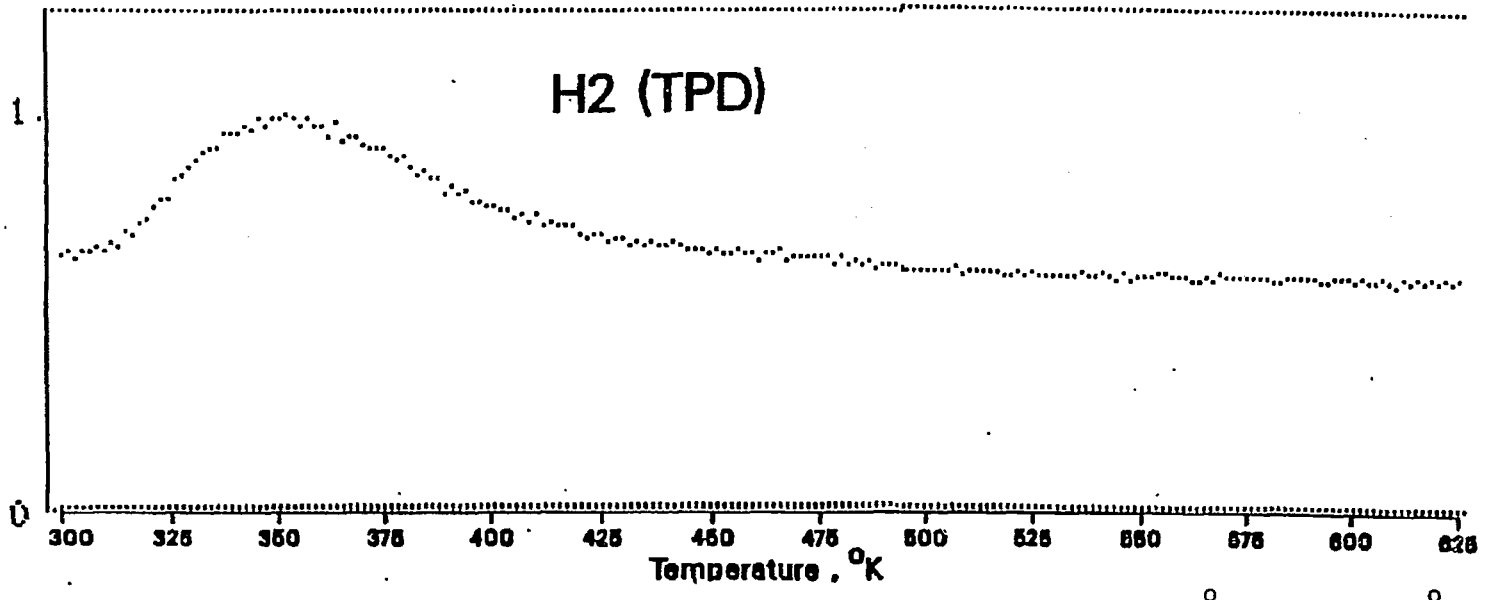

Figure A-4 Hydrogen thermal desorption result. Gas delivery sequence H_2 (383 °K) → H_2 (303 °K) → He (303 °K, 0.5 hr) → He (623°K) at 10°K/min, 60 wt % Ni/SiO_2

APPENDIX A

The TPD spectrum in 60 wt % Ni/SiO_2 shows a single major peak with peak maximum temperature 80°C (Figure A-4). The single desorption peak agrees with literature data.[132,133] The peak maximum temperature 80°C is lower than the result reported by Bartholomew and Weatherbee,[132] who reported the peak maximum temperature in the range of 135 to 145°C over different weight percentage Ni on silica catalysts. The difference in the peak maximum temperature is probably due to different temperature ramping rate, different adsorption temperature and a different carrier gas.

APPENDIX B

APPENDIX B

```
1   HOME
5   REM        DAAG4 6/18/85
6   DIM VI(10,120),T(9),Z$(4)
10   DIM MI(10),PI(10),VO(10)
11   DIM TR%(120),MG(10),GK(10)
20   DIM QI%(10,120),SI%(10),PI%(10)
40   REM  MI IS MASS NUMBER
80   REM  VO IS VOLTAGE OUTPUT FROM ISAAC D/A
100  PRINT
111   INPUT " MUL H.V ? ";T(3)
112   INPUT "SWITCH TYPE ?";Z$(1)
113   INPUT "DATE ?";Z$(2)
114   INPUT "PAUSE BETWEEN CYCLES( 0-16SEC)?)";T(9)
116   INPUT "WHAT H2/CO RATIO ?";T(5)
118   INPUT "WHAT FILE NAME ?";FILE$
119   INPUT "WANT TO INPUT MASS RA NGE(Y/N)?";RE$
120   IF RE$ = "Y" THEN  GOTO 150
130   IF RE$ = "N" THEN  GOTO 355
140   GOTO 119
150 NO = 0
160   PRINT
170 NO = NO + 1
180   PRINT "WHAT MASS NUMBER?"
190   PRINT "[";NO;"]": INPUT " > ";MI(NO)
200   PRINT
210   PRINT "WHAT SENSIVITY (L=0, M=1,H=2)?"
215   PRINT "[";NO;"]": INPUT " )";GK(NO)
217   IF GK(NO) = 0 THEN SI%(NO) = 4095
219   IF GK(NO) = 1 THEN SI%(NO) = 4095
220   IF GK(NO) = 2 THEN SI%(NO) = 2048
221   PRINT
222   IF NO >  = 10 THEN  GOTO 270
230   INPUT "INPUT ANOTHER MASS NUMBER(Y/N)?";RF$
240   IF RF$ = "Y" THEN  GOTO 160
250   IF RF$ = "N" THEN  GOTO 270
260   GOTO 230
270   PRINT
280   INPUT "TOTAL NUMBERS OF CYCLES(MAX 120)?)";CY
300   PRINT
```

```
304  INPUT "ION GAUGE P *E-6 Torr ?";T(1)
308  INPUT "MASS ELE ENERGY EV ?";T(2)
315  INPUT "WHAT TEMPERATURE ?";T(4)
316  INPUT "WHAT D2/CO RATIO ?";T(6)
330  INPUT "WHAT CO FLOW RATE (N. L./H) ?";T(7)
340  INPUT "CATALYST TYPE ?";Z$(3)
345  INPUT "CATALYST WEIGHT (g) ? ";T(8)
350  INPUT " OTHERS ?";Z$(4)
355 TS = T(9)
360  FOR I = 1 TO NO
365 MG(I) = MI(I) - 0.08 + 0.0049 * MI(I)
366  - 0.00011 * MI(I) * MI(I)
370 VO(I) =  - MG(I) * 0.1008
372 PI(I) = (4.992 - MG(I) * 0.1008) * 409.6
374 PI%(I) = PI(I)
375 PZ = PI(I) - PI%(I)
376  IF PZ <  = 0.5 GOTO 385
377 PI%(I) = PI%(I) + 1
385  PRINT "[";I;"] MG=";MG(I);
386 " MI=";MI(I);" SI=";GK(I)
390  NEXT I
420  PRINT "(PRESS THE RETURN KEY TO START)"
430  INPUT " ";A$
440  IF A$ > " " GOTO 420
460  FOR J = 1 TO CY
470  & CLRTIMER
474  & PAUSE = TS
480  FOR I = 1 TO NO
490 P = PI%(I)
520 S = SI%(I)
522  IF GK(I) > 0 THEN  GOTO 525
523  & AOUT,(DV) = 2048,(C#) = 2
524  GOTO 530
525  & AOUT,(DV) = 4095,(C#) = 2
530  & AOUT,(DV) = S,(C#) = 3
550  & AOUT,(DV) = P,(C#) = 0
551  & PAUSE = 0.01
552  & PAUSE = 0.01
553  & PAUSE = 0.01
554  & PAUSE = 0.01
555  & PAUSE = 0.01
556  & PAUSE = 0.01
560  & AIN,(TV) = Q,(C#) = 5
570 QI%(I,J) = Q
580  NEXT I
590  & TIMERIN,(TV) = T
600 TR%(J) = T
```

```
620  NEXT J
625  & AOUT,(DV) = 4095,(C#) = 2
626  & AOUT,(DV) = 4095,(C#) = 3
630 D$ =  CHR$ (4): REM   CTRL D
635  PRINT " SAVE DATA "
636  & BUZZ ON
637  & PAUSE = 2
638  & BUZZ STOP
640  FOR J = 1 TO CY
645 TR%(I) = TR%(I) + 20
650  FOR I = 1 TO NO
655 VI(I,J) = QI%(I,J) / 409.6 - 4.978
658  NEXT I
660  NEXT J
680  PRINT D$;"MON C,I,O"
690  PRINT D$;"OPEN ";FILE$
700  PRINT D$;"DELETE ";FILE$
710  PRINT D$;"OPEN ";FILE$
720  PRINT D$;"WRITE ";FILE$
730  PRINT NO
731  PRINT CY
732  FOR I = 1 TO 9
734  PRINT T(I)
736  NEXT I
738  FOR I = 1 TO 4
740  PRINT Z$(I)
742  NEXT I
750  FOR I = 1 TO NO
760 : PRINT MI(I)
767  PRINT GK(I)
770  NEXT I
780  FOR J = 1 TO CY
810 : PRINT TR%(J)
820  FOR I = 1 TO NO
830 : PRINT VI(I,J)
840  NEXT I
850  NEXT J
855  & ERRPTCH
856  ONERR  GOTO 4000
860  PRINT D$;"CLOSE";FILE$
870  & BUZZ ON
880  & PAUSE = 6
900  & BUZZ STOP
```

```
910  PRINT
915  & AOUT,(DV) = 4095,(C#) = 2
916  & AOUT,(DV) = 4095,(C#) = 3
920  INPUT "WANT TO RUN ANOTHER SCAN(Y/N)?";RD$
930  IF RD$ = "Y" THEN  GOTO 100
940  IF RD$ = "N" THEN  GOTO 3000
950  GOTO 920
3000  TEXT : PRINT
3010  PRINT "OK, I WILL STOP NOW!"
3015  & AOUT,(DV) = 4095,(C#) = 2
3016  & AOUT,(DV) = 4095,(C#) = 3
3020  END
4000  & BUZZ ON
4002  & PAUSE = 10
4003  & BUZZ STOP
4009  INPUT "WANT WRONG, NEW FILE MAME ?";FILE$
4010  GOTO 680
```

```
5  REM   DASP4 6/13/85
10  DIM MI(10),VI(10,120),NR(10,120),VO(10)
12  DIM T(9),Z$(5),GK(10),SI%(10)
15  DIM MG(10),AV(10,2),TR%(120),DA(240),DB(240)
660  INPUT "WHAT FILE NAME?";FILE$
665 D$ =  CHR$ (4): REM  CHR$(4) IS CRTL-D
667  PRINT D$;"MON C,I,O"
670  PRINT D$;"OPEN ";FILE$;" ,D1"
680  PRINT D$;"READ ";FILE$
690  INPUT NO
691  INPUT CY
693  FOR I = 1 TO 9
694  INPUT T(I)
695  NEXT I
696  FOR I = 1 TO 4
697  INPUT Z$(I)
698  NEXT I
705  FOR I = 1 TO NO
710  INPUT MI(I)
717  INPUT GK(I)
720  NEXT I
730  FOR J = 1 TO CY
740  INPUT TR%(J)
750  FOR I = 1 TO NO
765  INPUT VI(I,J)
770  NEXT I
780  NEXT J
790  PRINT D$;"CLOSE ";FILE$
800 Z$(5) = FILE$
972  INPUT "WANT TO PRINT DATA NOW(Y/N)?";RH$
980  IF RH$ = "Y" THEN  GOTO 1010
990  IF RH$ = "N" THEN  GOTO 1225
1000  GOTO 972
1010  GOSUB 9000
1040  INPUT "WHICH MASS NUMBER?";MA
1050  TEXT
1058  GOSUB 9430
1060  PRINT "[";MA;"] ";MI(MA)
1080  PRINT "CYCLE","TIME(SEC)";"    ANA.VOLT"
1100  FOR J = 1 TO CY
1110  PRINT J,TR%(J) / 1000,"",VI(MA,J)
1120  NEXT J
1210  GOTO 972
1225  INPUT "WANT TO PLOT NOW(Y/N)?";RP$
```

```
1230  IF RP$ = "Y" THEN  GOTO 1250
1240  IF RP$ = "N" THEN  GOTO 1920
1250  GOSUB 9255
1265  INPUT "WHICH PEAK?";NP
1320 MAX = 0
1330  FOR J = 1 TO CY
1340  IF VI(NP,J) > MAX THEN MAX = VI(NP,J)
1350  NEXT J
1420 MP = MI(NP)
1430  FOR J = 0 TO (CY * 2) STEP 2
1436 AA = VI(NP,J / 2)
1440  IF AA < 0 THEN AA = 0
1442 DA(J) = AA * 100 / MAX
1450  NEXT J
1460  INPUT "A SECOND PEAK (Y/N)?";RN$
1470  IF RN$ = "Y" THEN  GOTO 1500
1480  IF RN$ = "N" THEN  GOTO 1680
1500  INPUT "WHICH PEAK?";NR
1550 MBX = 0
1560  FOR J = 1 TO CY
1570  IF VI(NR,J) > MBX THEN MBX = VI(NR,J)
1580  NEXT J
1640 MR = MI(NR)
1650  FOR J = 0 TO (CY * 2) STEP 2
1656 CC = VI(NR,J / 2)
1658  IF CC < 0 THEN CC = 0
1660 DB(J) = CC * 100 / MBX
1670  NEXT J
1680  GOSUB 8000
1871  ONERR  GOTO 1225
1872  PRINT "1- ";MP,MAX"VOLTS"
1874  PRINT "2- ";MR,MBX"VOLTS"
1880  GOTO 972
1920  TEXT
1930  INPUT "WANT TO NORMALIZE DATA PTS.(Y/N)?";RA$
1940  IF RA$ = "Y" THEN  GOTO 1960
1950  IF RA$ = "N" THEN  GOTO 3170
1960  GOSUB 9000
1990  INPUT "WHICH  MASS NUMBER?";MB
2000  PRINT "DETERMINE L VALUE"
2110  INPUT "FROM WHICH POINT NL?";NL
2130  INPUT "TO WHICH POINT LR?";LR
2140 LA = 0
2150  FOR J = NL TO LR
2160 NR(MB,J) = VI(MB,J)
```

```
2170 LA = LA + NR(MB,J)
2180  NEXT J
2190 L = LA / (LR - NL + 1)
2200 AV(MB,1) = L
2210  PRINT "DETERMINE R VALVE"
2225  INPUT "FROM WHICH POINT RL?";RL
2228  INPUT "TO WHICH POINT RR?";RR
2230 RS = 0
2240  FOR J = RL TO RR
2250 NR(MB,J) = VI(MB,J)
2260 RS = RS + NR(MB,J)
2270  NEXT J
2280 R = RS / (RR - RL + 1)
2290 AV(MB,2) = R
2300  INPUT "CURVE IS UP OR DOWN(U/D)?";ZY$
2310  IF ZY$ = "U" THEN  GOTO 2370
2320  IF ZY$ = "D" THEN  GOTO 2330
2325  GOTO 2300
2330  FOR J = 1 TO CY
2340 WZ = (VI(MB,J) - R) / (L - R)
2342  IF WZ < 0 THEN WZ = 0
2344 NR(MB,J) = WZ
2350  NEXT J
2360  GOTO 2430
2370  FOR J = 1 TO CY
2380 QZ = (VI(MB,J) - L) / (R - L)
2390  IF QZ < 0 THEN QZ = 0
2400 NR(MB,J) = QZ
2410 VI(MB,J) = QZ
2420  NEXT J
2430  INPUT "WANT TO MODIFY DATA (N/O/L)?";IA$
2431  IF IA$ = "N" THEN  GOTO 2500
2432  IF IA$ = "O" THEN  GOTO 2442
2436  IF IA$ = "L" THEN  GOTO 2480
2442  INPUT "FROM WHICH POINT MJ?";MJ
2444  INPUT "TO WHICH POINT MU?";MU
2446  FOR J = MJ TO MU
2448 ZK = NR(MB,J)
2450  IF (ZK - 1) >  = 0 THEN  GOTO 2460
2452 NR(MB,J) = 1 - ((1 - ZK) / 20)
2453 VI(MB,J) = NR(MB,J)
2454  GOTO 2470
2460 NR(MB,J) = 1 + ((ZK - 1) / 20)
2462 VI(MB,J) = NR(MB,J)
2470  NEXT J
```

```
2472  GOTO 2430
2480  INPUT "FROM WHICH POINR IW ? ";IW
2482  INPUT "TO WHICH POINT IX?";IX
2483 IZ = IX + 1
2484 IA = IZ + 1
2485 VE = (VI(MB,IZ) + VI(MB,IA)) / 2
2494  FOR J = IW TO IX
2496 NR(MB,J) = VE
2497 VI(MB,J) = VE
2498  NEXT J
2500  GOTO 1930
2530  INPUT "WANT TO CALCULATE AREA(Y/N)?";AZ$
2535  IF AZ$ = "Y" THEN  GOTO 2550
2540  IF AZ$ = "N" THEN  GOTO 4230
2550  PRINT
2551  PR# 1
2552  GOSUB 9430
2553  PRINT "AREA TYPE 1 : AREA B ETWEEN TWO CURVES"
2554  PRINT "AREA TYPE 2 : AREA A
2555  AND BELOWMAXIMUM
2566  PRINT "L MASS"," ","R MASS"","L","","R",

2567 "TYPE","  AREA(SEC)"
2568  PR# 0
2569  INPUT "AREA TYPE ?";BZ
2570  IF BZ = 1 THEN  GOTO 2590
2580  IF BZ = 2 THEN  GOTO 2900
2590  GOSUB 9000
2620  INPUT "WHICH MASS NUMBER FOR THE LEFT CURVE?";ML
2630  INPUT "WHICH MASS NUMBER FOR THE RIGHT CURVE?";MR
2635  INPUT " AREA FROM 1 TO WHICH POINT JR ?";JR
2640 W1 = 0
2650  FOR J = 1 TO JR
2660 W1 = W1 + (NR(MR,J) - NR(ML,J))
2670  NEXT J
2680 W1 = W1 * TR%(14) / 1000
2770  PR# 1
2771  PRINT
2772  PRINT MI(ML),MI(MR),"  ",AV(MR,1)," ",
2773 AV(MR,2),",BG,"",W1
2800  PR# 0
2820  INPUT "WANT ANOTHER AREA(Y/N)?";C2$
2830  IF C2$ = "Y" THEN  GOTO 2569
2840  IF C2$ = "N" THEN  GOTO 3170
2900  GOSUB 9000
2930  INPUT "WHICH MASS NUMBER FOR LEFT CURVE?";ZL
2940  INPUT "WHICH MASS NUMBER FOR RIGHT CURVE?";ZR
```

```
2945  INPUT "AREA FROM 1 TO WHICH POINT DR?";DR
2952 Z3 = 0
2960  FOR J = 1 TO DR
2965 ZD = (1 - NR(ZL,J) - NR(ZR,J))
2975 Z3 = Z3 + ZD
2980  NEXT J
2990 Z4 = Z3 * TR%(14) / 1000
3081  PRINT
3082  PR# 1
3084  PRINT MI(ZL),MI(ZR),"    ",AV(ZR,1),"   ",
3085 AV(ZR,2),"   ",BZ,"   ",Z4
3086  PR# 0
3090  GOTO 2820
3170  INPUT "WANT TO SMOOTH DATA PTS.(Y/N)?";FZ$
3175  IF FZ$ = "Y" THEN  GOTO 3200
3180  IF FZ$ = "N" THEN  GOTO 2530
3200  GOSUB 9000
3230  INPUT "WHICH MASS NUMBER?";ME
3232  INPUT "ORDERS OF SMOOTHING?";OS
3234 MO = ME:OT = OS
3240  GOSUB 9255
3260  GOSUB 9300
3300  FOR J = 0 TO (CY * 2) STEP 2
3310 EX = VI(ME,J / 2)
3315  IF EX < 0 THEN EX = 0
3320 DA(J) = EX * 100
3325  NEXT J
3330  INPUT "A SECOND PEAK(Y/N)?";LZ$
3340  IF LZ$ = "Y" THEN  GOTO 3360
3350  IF LZ$ = "N" THEN  GOTO 3530
3360  INPUT "WHICH PEAK?";MF
3370  INPUT "ORDERS OF SMOOTHING?";OV
3380 MO = MF:OT = OV
3390  GOSUB 9300
3400  FOR J = 0 TO (CY * 2) STEP 2
3405 FX = VI(MF,J / 2)
3410  IF FX < 0 THEN FX = 0
3415 DB(J) = FX * 100
3420  NEXT J
3530  GOSUB 8000
3710  PRINT "MASS-";MI(ME)
3712  PRINT "MASS-";MI(MF)
3720  INPUT "PLOT ON PRINTER(Y/N)?";GZ$
3730  IF GZ$ = "Y" THEN  GOTO 3750
3740  IF GZ$ = "N" THEN  GOTO 3790
```

```
3750  GOSUB 8880
3762  PR# 1
3770  PRINT "MASS-";MI(ME)
3772  PRINT "MASS-";MI(MF)
3789  GOSUB 9430
3790  PR# 0
3791  TEXT
3800  GOTO 3170
4230  INPUT "WANT TO READ OR SAVE FILE(R/S/P/N)?";RM$
4240  IF RM$ = "N" THEN  GOTO 5020
4250  IF RM$ = "R" THEN  GOTO 660
4255  IF RM$ = "P" THEN  GOTO 972
4258  IF RM$ = "S" THEN  GOTO 4400
4260  ONERR  GOTO 1225
4400  INPUT "WANT NEW FILE NAME ?";NF$
4460  PRINT D$;"OPEN ";NF$;" ,D2"
4470  PRINT D$;"WRITE ";NF$
4480  PRINT NO
4490  PRINT CY
4500  FOR I = 1 TO 9
4510  PRINT T(I)
4520  NEXT I
4530  FOR I = 1 TO 5
4540  PRINT Z$(I)
4550  NEXT
4560  FOR I = 1 TO NO
4570  PRINT MI(I)
4580  PRINT GK(I)
4590  NEXT I
4600  FOR J = 1 TO CY
4610  PRINT TR%(J)
4620  FOR I = 1 TO NO
4630  PRINT VI(I,J)
4640  NEXT I
4650  NEXT J
4660  PRINT D$;"CLOSE";NF$
4670  GOTO 4230
5020  END
8000  HGR
8010 PLT =  PEEK (966) +  PEEK (967) * 256
8020  POKE PLT,0
8030  & SCROLLSET
8040  & OUTLINE
8050  HPLOT 8,40 TO 12,40
8060  & LABEL = "1" AT 6,38
```

```
8070  & LABEL = "0" AT 6,141
8080  & LABEL = "   TIME      ,(SEC)" AT 50,155
8090  & PLTFMT = 1,1
8100  FOR N = 1 TO (CY * 2)
8110  & NXTPLT = DA(N)
8120  & NXTPLT = DB(N)
8130  NEXT N
8160  RETURN
8880 I$ =  CHR$ (9)
8890 D$ =  CHR$ (4)
8900  PRINT D$"PR#1": PRINT I$"2H"
8905  PRINT D$"PR#0"
8910  RETURN
9000  FOR I = 1 TO NO
9020  PRINT "[";I;"] ";MI(I)
9030  NEXT I
9040  RETURN
9255  FOR I = 0 TO 240
9256 DA(I) = 0
9257 DB(I) = 0
9258  NEXT I
9260  RETURN
9300  IF OT > 0 THEN  GOTO 9305
9301  FOR J = 1 TO CY
9302 VI(MO,J) = NR(MO,J)
9303  NEXT J
9304  GOTO 9420
9305  FOR J = 2 TO CY - 1
9310 VI(MO,J) = (NR(MO,J - 1) + 2 * NR(MO,J)
9320  + NR(MO,J + 1)) / 4
9330 OT = OT - 1
9340  IF OT <  = 0 THEN  GOTO 9400
9350  FOR J = 2 TO CY - 1
9360 NR(MO,J) = VI(MO,J)
9370  NEXT J
9380  GOTO 9305
9400 VI(MO,1) = VI(MO,2)
9410 VI(MO,CY) = VI(MO,CY - 1)
9420  RETURN
9430  PRINT FILE$;" DATA = ";Z$(3);" WEIGHT = ";T(8);" gram"
9450  PRINT "T=";T(4);" C";"     H 2/CO=";T(5);" D2/CO=";
9451 T(6);" CO FLOW= ";T(7);" N.L/H";
9452  PRINT
9460  PRINT "SWITCH TYPE=";Z$(1);"     DATE = ";Z$(2);
9466 " TIME DIF= ";TR%(119) / 1000
9470  RETURN
```

BIBLIOGRAPHY

1. Muetterties, E.L., and Stein, J., "Mechanistic Features of Catalytic Carbon Monoxide Hydrogenation Reactions," Chemical Reviews, Vol. 79 (December 1979), pp. 479-490.

2. Dalla Betta, R.A., and Shelef, M., "Heterogeneous Methanation: Absence of H_2-D_2 Kinetic Isotope Effect on Ni, Ru, and Pt," Journal of Catalysis, Vol. 49 (1977), pp. 383-385.

3. Ho, S.V., and Harriott, P., "The Kinetics of Methanation on Nickel Catalysts," Journal of Catalysis, Vol. 64 (1980), pp. 272-283.

4. Fitzharris, W.D., Katzer, J.R., and Manogue, W.H., "Sulfur Deactivation of Nickel Methanation Catalysts," Journal of Catalysis, Vol. 76 (1982), pp. 369-384.

5. Pearce, R. and Patterson, W.R., ed., Catalysis and Chemical Processes, "Carbon-Carbon Formation, I: Carbonylation, by D. T. Thompson," (New York: John Wiley and Sons, New York, 1981).

6. Vannice, M.A., "The Catalytic Synthesis of Hydrocarbons from H_2/CO Mixtures Over Group VIII Metals, II: The Kinetics of Methanation Reaction Over Supported Metals," Journal of Catalysis, Vol. 37 (1975), pp. 462-473.

7. Mori, T., Masuda, H., Imai, I., Miyamoto, A., Baba S., and Murakami, Y., "Kinetics, Isotope Effects, and Mechanism for the Hydrogenation of Carbon Monoxide on Supported Nickel Catalysts," Journal of Physical Chemistry, Vol. 86 (1982), pp. 2753-2760.

8. Biloen, P. and Sachtler, W.M.H., "Mechanism of Hydrocarbon Synthesis over Fischer-Tropsch Catalysts," Advance in Catalysis, Vol. 30 (1981) pp. 165-216.

9. van Nisselrodij, P.F.M.T., Luttikholt, J.A.M., van Meerten, R.Z.C., Croon M.H.J.M., and Coenen, J.W.E., "Hydrogen/Deuterium Kinetic Isotope Effect in the Methanation of Carbon Monoxide on a Nickel-Silica Catalyst," Applied Catalysis, Vol. 6 (1983), pp. 271-281.

10. Otarod, M., Ozawa, S., Yin, F., Chew, M., Cheh H.Y., and Happel, J., "Multiple Isotope Tracing of Methanation Over Nickel Catalyst III: Completion of ^{13}C and D Tracing," Journal of Catalysis, Vol. 84 (1983), pp. 156-169.

11. Klose, J. and Baerns, M., "Kinetics of the Methanation of Carbon Monoxide on an Alumina-Supported Nickel Catalyst," Journal of Catalysis, Vol. 85 (1984), pp. 105-116.

12. Hayes, R.E., Thomas, W.J., and Hayes, K.E., "Surface Intermediates in the Nickel Catalysed Methanation of Carbon Monoxide as Revealed by Computer Enhanced Spectroscopy," Applied Catalysis, Vol. 6 (1983), pp. 53-59.

13. King, D.A., and Woodruff, D.P., ed., The Chemical Physics of Solid Surfaces and Heterogeneous Catalysis, "The Methanation Reaction by R. D. Kelley and D. W. Goodman," (Amsterdam-Oxford-New York, Elsevier Sci. Pub. Co., (1982)) pp. 427-454.

14. Underwood, R.P., and Bennett, C.O., "The CO/H_2 Reaction Over Nickel-Alumina Studied by the Transient Method," Journal of Catalysis, Vol. 86 (1984), pp. 245-253.

15. Stockwell, D.M., Isotopic Tracing of Methanation Over Nickel, (M.S. Thesis, University of Connecticut, 1984).

16. Raupp, G.B. and Dumesic, J.A., "Effects of Titania on the Coadsorption of H_2 and CO on Nickel Surfaces: Consequences for Understanding Methanation Over Titania-Supported Nickel Catalysts," Journal of Catalysis, Vol. 96 (1985), pp. 597-612.

17. Hadjigeorghiou, G.A., and Richardson, J.T., "Fischer-Tropsch Selectivity of Ni/Al_2O_3 Catalysis," Applied Catalysis, Vol. 21 (1986), pp. 11-35.

18. Ponec, V., "Some Aspects of the Mechanism of Methanation and Fischer-Tropsch Synthesis," Catalysis Reviews - Science and Engineering, Vol. 18 (1978), pp. 151-171.

19. Sormorjai, G.A., "The Catalytic Hydrogenation of Carbon Monoxide. The Formation of C_1 Hydrocarbons," Catalysis Reviews - Science and Engineering, Vol. 23 (1981), pp. 189-202.

20. Mills, G.A., and Steffgen, F.W., "Catalytic Methanation," Catalysis Reviews, Vol. 8 (1973), pp. 159-210.

21. Vannice, M.A., "The Catalytic Synthesis of Hydrocarbons from Carbon Monoxide and Hydrogen," Catalysis Reviews - Science and Engineering, Vol. 14 (1976), pp. 153-191.

22. Bell, A.T., "Catalytic Synthesis of Hydrocarbons over Group VIII Metals. A Discussion of the Reaction Mechanism," Catalysis Reviews - Science and Engineering, Vol. 23 (1981), pp. 203-232.

23. Bond, G.C., and Webb, G., ed., Catalysis, "Fischer-Tropsch Synthesis and Related Reactions, by V. Ponec," Vol. 5 (1982) pp. 48-80. (The Royal Society of Chemistry, Burlington House, London 1982).

24. Dowden, D.A., and Kemball, C., ed., Catalysis Science and Technology, Vol. 2, "The Heterogeneously Catalysed Hydrogenation of Carbon Monoxide by P. J. Denny and P. A. Whan," The Chemical Society, Burlington House, London (1978), pp. 46-86.

25. Biloen, P., Helle, J.N., van den Berg F.G.A., and Sachtler, W.M.H., "On the Activity of Fischer-Tropsch and Methanation Catalysts: A Study Utilizing Isotopic Transients," Journal of Catalysis, Vol. 81 (1983), pp. 450-463.

26. Biloen, P., Helle, J.N., and Sachtler, W.M.H., "Incorporation of Surfact Carbon into Hydrocarbons During Fischer-Tropsch Synthesis: Mechanistic Implications," Journal of Catalysis, Vol. 58 (1979), pp. 95-107.

27. Happel, J., Suzuki, I., Kokayell, P. and Fthenakis, V., "Multiple Isotope Tracing of Methanation over Nickel Catalyst," Journal of Catalysis, Vol. 65 (1980), pp. 59-77.

28. Happel, J., Cheh, H.Y., Otarod, M., Ozawa, S., Severdia, A.J., Yoshida, T., and Fthenakis, V., "Multiple Isotope Tracing of Methanation Over Nickel Catalysts, II: Deuterometrane Tracing," Journal of Catalysis, Vol. 75 (1982), pp. 314-328.

29. Biloen, P., "Transient Kinetic Methods," Journal of Molecular Catalysis, Vol. 21 (1983), pp. 17-24.

30. Yang, C.-H., Soong, Y., and Biloen, P., "Abundancy and Reactivity of Surface Intermediates in Methanation, Determined with Transient Kinetic Method," Proceeding, 8th International Congress on Catalysis, Berlin, 2-6 July 1984, Vol. II, pp. 3-14.

31. Yang, C.-H., Soong, Y., and Biloen, P., "A Comparison of Nickel- and Platinum-Catalyzed Methanation, Utilizing Transient-Kinetic Methods," Journal of Catalysis, Vol. 94 (1985), pp. 306-309.

32. Soong, Y., Krishna, K., and Biloen, P., "Catalyst Aging Studied with Isotopic Transients: Methanation Over Raney Nickel," Journal of Catalysis, Vol. 97 (1986), pp. 330-343.

33. Kobayashi, M. and Kobayashi, H., "Transient Response Method in Heterogeneous Catalysis," Catalysis Reviews - Science and Engineering, Vol. 10 (1974), pp. 139-176.

34. Bennett, C.O., "The Transient Method and Elementary Steps in Heterogeneous Catalysis," Catalysis Reviews - Science and Engineering, Vol. 13 (1976), pp. 121-148.

35. McCarty, J.G. and Wise, H., "Hydrogenation of Surface Carbon on Alumina-Supported Nickel," Journal of Catalysis, Vol. 57 (1979), pp. 406-416.

36. Goodman, D.W., Kelley, R.D., Madey, T.E., and White, J.M., "Measurement of Carbide Buildup and Removal Kinetics on Ni(100)," Journal of Catalysis, Vol. 64 (1980), pp. 479-481.

37. Bartholomew, C.H., "Carbon Deposition in Steam Reforming and Methanation," Catalysis Reviews - Science and Engineering, Vol. 24 (1982), pp. 67-112.

38. Winslow, P., and Bell, T.A., "Studies of the Surface Coverage of Unsupported Ruthenium by Carbon- and Hydrogen-Containing Adspecies During CO Hydrogenation," Journal of Catalysis, Vol. 91 (1985), pp. 142-154.

39. Dalmon, J.A., and Martin, G.A., "The Kinetics and Mechanism of Carbon Monoxide Methanation Over Silica-Supported Nickel Catalysts," Journal of Catalysis, Vol. 84 (1985), pp. 45-54.

40. Zhang, X., and Biloen, P., "A Transient Kinetic Observation of Chain Growth in the Fischer-Tropsch Synthesis," Journal of Catalysis, Vol. 98 (1986), pp. 468-476.

41. Winslow, P., and Bell, A.T., "Application of Transient Response Techniques for Quantitative Determination of Adsorbed Carbon Monoxide and Carbon Present on the Surface of Ruthenium Catalyst During Fischer-Tropsch Synthesis," Journal of Catalysis, Vol. 86 (1984), pp. 158-172.

42. Dautzenberg, F.M., Helle, J.N., van Santen, R.A., and Verbeek, H, "Pulse-Technique Analysis of the Kinetics of the Fischer-Tropsch Reaction," Journal of Catalysis, Vol. 50 (1977), pp. 8-14.

43. Dalla Betta, R.A., Piken, A.G., and Shelef, M., "Heterogeneous Methanation: Steady-State Rate of CO Hydrogenation on Supported Ruthenium, Nickel and Rhenium," Journal of Catalysis, Vol. 40 (1975), pp. 173-183.

45. van der Burg, A., Doornbos, J., Kos, N.J., Ultee, N.J., and Ponec, V., "Selectivity of Ni-Cu and Pt-Au Alloy in Reactions of Butanol and Realted Compounds,"Journal of Catalysis, Vol. 54 (1978), pp. 243-253.

46. Trim, D.L., Design of Industrial Catalysis, (New York: Elsevier Scientific Publishing Company, 1980).

47. Boudart, M., and Djega-Mariadassou, G., Kinetics of Heterogeneous Catalytic Reactions, (Princeton University Press, 1984).

48. Boudart, M., "Heterogeneous Catalysis by Metals," Journal of Molecular Catalysis, Vol. 30 (1985), pp. 27-38.

49. Boudart, M., "Carbon Monoxide Oxidation and Related Reactions on A High Divided Nickel Oxide,"Advanced Catalysis, Vol. 20 (1969), pp. 153-166.

50. Gomer, R., ed., Interactions on Metal Surfaces, Topics in Applied Physics, "Concepts in Heterogeneous Catalysis, by M. Boudart," (Springer-Verlag, Berlin, 1975), pp. 275-298.

51. Boudart, M., "Effect of Surface Structure on Catalytic Activity," Proceedings of the Sixth International Congress on Catalysis, Vol. 1, (1977), pp. 1-9.

52. Katzer, J., and Manogue, W.H., "On Subdivision of the Classification of Demanding Reactions," Journal of Catalysi, Vol. 32 (1974), pp. 166-169.

53. Ostermaier, J.J., Katzer, J.R., and Manoque, W.M., "Platinum Catalyst Deactivation in Low-Temperature Ammonia oxidation Reactions I. Oxidation of Ammonia by Molecular Oxygen," Journal of Catalysis, Vol. 41 (1976), pp. 277-292.

54. Preprints of Division of Petroleum Chemistry, American Chemical Society, Vol. 31, No. 1 (1986). "Alcohols Synthesis from Carbon Oxides and Hydrogen on Palladium and Rhodium Ctalysts. Study of Active Species, by Kiennemann, A., J. P. Hindermann, R. Breault and H. Idriss," p. 46.

55. Van Meerten, R.Z.C., Beaumont, A.H.G.M., Van Nisselrooij, P.F.M.T., and Coenen, J.W.E., "Structure Sensitivity and Crystallite Size Change of Nickel During Methanation of CO/H_2 on Nickel-Silica Catalysts," Surface Science, Vol. 135 (1983), pp. 565-579.

56. Van Hardeveld,R. and Hartog, F., "The Statistics of Surface Atoms and Surface Sites on Metal Crystals," Surface Science, Vol. 15 (1969), pp. 189-230.

57. Bartholomew, C.H., Pannell, R.B., and Butler, J.L., "Support and Crystallite Size Effects in CO Hydrogenation on Nickel," Journal of Catalysis, Vol. 65 (1980), pp. 335-347.

58. Vannice, M.A., "The Catalytic Synthesis of Hydrocarbons from H_2/CO Mixtures Over the Group VIII Metals. IV: The Kinetic Behavior of CO Hydrogenation Over Ni Catalysts," Journal of Catalysis, Vol. 44 (1976), pp. 152-162.

59. van Meerten, R.Z.C., Vollenbrook, J.G., de Croon, M.H.J.M., van Nisselrooj, P.F.M.T., and Coenen, J.W.E., "The Kinetics and Mechanism of the Methanation of Carbon Oxide on a Nickel-Silica Catalyst," Applied Catalysis, Vol. 3 (1982), pp. 29-36.

60. Boudart, M., Kinetics of Chemical Processes, Prentice-Hall, New York, 1968.)

61. Ozaki, A., Isotopic Studies of Heterogeneous Catalysis, (Kodansha Ltd. Academic Press, Tokyo 1976.)

62. Rock, P.A., Isotopes and Chemical Principles, (American Chemical Society, Washington, DC 1975).

63. Funcan, J.F., and Cook, G.B., Isotopes in Chemistry, (Clarendon Press, Oxford 1968).

64. Laidler, K.J., Chemical Kinetics, (McGraw-Hill, New York 1965).

65. Collins, C.J., Boorman, N.S., Isotope Effects in Chemical Reactions, (Van Nostrand Reinhold Company, New York 1970).

66. Glasstone, S., Laidler, K., and Eyring, H., The Theory of Rate Processes, (McGraw-Hill, New York, 1941).

67. Polizzotti, R.S., and Schwarz, J.A., "Hydrogenation of CO to Methane: Kinetic Studies on Polycrystalline," Journal of Catalysis, Vol. 77 (1982), pp. 1-15.

68. Kellner, C.S., and Bell, A.T., "Evidence for H_2/D_2 Isotope Effects on Fischer-Tropsch Synthesis Over Supported Ruthenium Catalysts," Journal of Catalysis, Vol. 67 (1981), pp. 175-185.

69. Wilson, T.P., "Comments on Heterogeneous Methanation: Absence of H_2-D_2 Kinetic Isotope Effect on Ni, Ru and Pt," Journal of Catalysis, Vol. 60 (1979), pp. 167-168.

70. Logan, M.A., and Somorjai, G.A., "Deuterium Isotope Effects on Hydrogenation of Carbon Monoxide over Rhodium," Journal of Catalysis, Vol. 95 (1985), pp. 317-320.

71. Eley, D.D., and Norton, P.R., "Conversion and Equilibration Rates of Hydrogen on Nickel," Faraday Society Discussion, Vol. 41, 135-148 (1966).

72. Ozaki, A., Nozaki, F., Maruya, K.I., "Gas Chromatographic Determination of Reversible Adsorption of Hydrogen I. Reversible Adsorption over a Nickel Catalyst," Journal of Catalysis, Vol. 7 (1967), pp. 234-239.

73. Sachtler, W.M.H., "Elementary Steps in the Catalyzed Conversion of Synthesis Gas," 8th International Congress of Catalysis, Vol. I (1984), pp. 151-173.

74. Nieuwenhuys, B.E., "Adsorption and Reactions of CO, NO, H_2 and O_2 on Group VIII Metal Surfaces," Surface Science, Vol. 126 (1983), pp. 307-336.

75. Wedler, G., Papp, H., and Schroll, G., "The Interaction of Hydrogen and Carbon Monoxide on Polycrystalline Nickel Films at Temperatures up to 353K," Journal of Catalysis, Vol. 38 (1975), pp. 153-165.

76. Horgan, A.M. and King, D.A., Adsorption Desorption Phenomena, (Academic Press, New York 1972).

77. Heal, M.J., Leisegang, E.C., and Torrington, R.G., "Infrared Studies of Carbon Monoxide and Hydrogen Adsorbed on Silica-Supported Nickel Catalysts," Journal of Catalysis, Vol. 42 (1976), pp. 10-19.

78. Primet, M., Dalmon, J.A., and Martin, G.A., "Adsorption of CO on Well-Defined Ni/SiO_2 Catalysts in the 195 - 373 K Range Studied by Infrared Spectroscopy and Magnetic Method," Journal of Catalysis, Vol. 46 (1977) pp. 25-36.

79. Dalmon, J.A. and Martin, G.A., "Kinetics and Mechanism of C-C Bond Formation in CO + H_2 Reaction over Ni/SiO_2," 8th International Congress Catalysis, Berlin, Vol. III (1984), pp. 185-195.

80. Kelley, R.D., Cavanaugh, R.R., and Rush, J.J., "Coadsorption and Reaction of H_2 and CO on Raney Nickel: Neutron Vibrational Spectroscopy," Journal of Catalysis, Vol. 83 (1983), pp. 464-468.

81. Shapiro, B. L., ed., Heterogeneous Catalysis, "Mechanism of Fischer-Tropsch Synthesis by A. T. Bell," (Texas A&M University Press, 1984).

82. Cant, N.W., and Bell, A.T., "Studies of Carbon Monoxide Hydrogenation Over Ruthenium Using Transient Response Techniques," Journal of Catalysis, Vol. 73 (1982), pp. 257-271.

83. Winslow, P., and Bell, A.T., "Studies of Carbon- and Hydrogen-Containing Adspecies Present During CO Hydrogenation Over Unsupported Ru, Ni and Rh," Journal of Catalysis, Vol. 94 (1985), pp. 385-399.

84. Padberg, G., and Smith, J.M., "Chemisorption Rates by Chromatography," Journal of Catalysis, Vol. 12, (1968), pp. 172-182.

85. Dautzenberg, F.M., Helle, J.N., Biloen, P., and Sachtler, W.M.H., "Conversion of n-Hexane Over Monofunctional Supported and Unsupported PtSn Catalysts," Journal of Catalysis, Vol. 63 (1980), pp. 119-128.

86. Wentrcek, P.R., Wood, B.J., and Wise, H., "The Role of Surface Carbon in Catalytic Methanation," Journal of Catalysis, Vol. 43 (1976), pp. 363-366.

87. Araki, J.M. and Ponec, V., "Methanation of Carbon Monoxide on Nickel and Nickel Copper Alloys," Journal of Catalysis, Vol. 44 (1976), pp. 439-448.

88. Bonzel, H.P. and Krebs, H.J., "On the Chemical Nature of the Carbonaceous Deposits on Iron After CO Hydrogenation," Surface Science, Vol. 91 (1980), pp. 499-513.

89. Freel, J., Robertson, S.D., and Anderson, R.B., "The Structure of Raney Nickel III. The Chemisorption of Hydrogen and Carbon Monoxide," Journal of Catalysis, Vol. 18 (1970), pp. 243-248.

90. Dr. D.G. Blackmond's chemisorption measurements are greatfully aknowledged.

91. Uken, A.M., and Bartholomew, C.H., "Borided Metal Catalysis in Methanation of Carbon Monoxide, I. Initial Activity and Conversion-Temperature Behavior of Unsupported Catalysts," Journal of Catalysis, Vol. 65 (1980), pp. 407 - 415.

92. Kester, K.B., and Falconer, J.L., "CO Methanation on Low-Weight Loading Ni/Al_2O_3: Multiple Reaction Sites," Journal of Catalysis, Vol. 89 (1984), pp. 380-391.

93. Goodman, D.W., and Yates, J.T., Jr., "CO Isotopic Mixing Measurements on Nickel: Evidence for Irreversibility of CO Dissociation," Journal of Catalysis, Vol. 82 (1983), pp. 255-260.

94. Kobori, Y., Yamasaki, H., Naito, S., Onishi, T., and Tamaru, K., "Mechanistic Study of Carbon Monoxide Hydrogenation Over Ruthenium Catalysts," Chemical Society London, Journal Faraday Transactions I, Vol.78 (1982) pp. 1473-1490.

95. Yamasaki, H., Kobori, Y., Naito, S., Onishi, T., and Tamaru, K., "Infrared Study of the Reaction of H_2 + CO on a Ru/SiO_2 Catalyst," Chemical Society London, Journal Faraday Transactions I, Vol. 77 (1981) pp. 2913-2925.

96. Goddard, W.A., Walch, S.P., Rappe, A.K., Upton, T.H., Meliu, C.F., "Methanation of CO over Ni Catalyst: A Theoretical Study," Journal of Vacuum Science and Technology, Vol. 14,No. 1 (1977) pp. 416-418.

97. Birkenstock, U., Holm, R., Beinfandt, B., and Storp, S., "Surface Analysis of Raney Catalysts," Journal of Catalysis, Vol. 93 (1985), pp. 55-67.

98. Martin, G.A., Primet, M., and Dalmon, J.A., "Reactions of CO and CO_2 on Ni/SiO_2 Above 373 K as Studied by Infrared Spectroscopic and Magnetic Methods," Journal of Catalysis, Vol. 53 (1978) pp. 321-320.

99. Castner, D.G., Dubois, L.H., Sexton, B.A., and Somorjai, G.A., "Comments on Does Chemisorbed Carbon Monoxide Dissociate on Rhodium?" Surface Science, Vol. 103 (1981), pp. 134-138.

100. Schouten, S.C., Gijzeman, O.L.J., and Bootsman, G.A., "Reaction of Methane with Nickel Single Crystal Surfaces and the Stability of Surface Nickel Carbide," Bulletin Des Societies Chemiques Belges, Vol.88 (1979), pp. 541-547.

101. Rostrup-Nielsen, J.R., "Equilibria of Decomposition Reactions of Carbon Monoxide and Methane over Nickel Catalysts," Journal of Catalysis, Vol. 27 (1972) pp. 343-356.

102. Shelton, J.C., Patil, H.R., and Blakely, J.M., "Equilibrium Segregation of Carbon to a Nickel (111) Surface: A Surface Phase Transition," Surface Science, Vol. 43 (1974), pp. 493-520.

103. Isett, L.C. and Blakely, J.M., "Segregation Isosteres for Carbon at the (100) Surface of Nickel," Surface Science Vol. 58 (1976), pp. 397-414.

104. McCarthy, J.G. and Madix, R.J., "AES and LEED Evidence for Dicarbon Fragments on Ni(110)," Journal of Catalysis, Vol. 48 (1977), pp. 422-426.

105. Zuhr, R.A., and Hudson, J.B., "The Adsorption and Decomposition of Ethylene on Ni(110)," Surface Science, Vol. 66 (1977), pp. 405-422.

106. Coenen, J.W.E., Schats, W.M.T.M., and van Meerten, R.Z.C., "Structure Effects in the Interaction of Hydrogen with Benzene, Cyclopropane and Carbon Monoxide Over Silica Supported Nickel Catalysts," Bulletin Des Societes Chimiques Belges., Vol. 88, No. 7 (1979), pp. 435-452.

107. Bartholomew, C.H., and Vance, C.K., "Effects of Support on the Kinetics of Carbon Hydrogenation on Nickel," Journal of Catalysis, Vol. 91, (1985), pp. 78-84.

108. Vannice, M.A. and Varten, R.L., "Metal-Support Effects on the Activity and Selectivity of Ni Catalysts in CO/H_2 Synthesis Reactions," Journal of Catalysis, Vol. 56 (1979), pp. 236-248.

109. Okamoto, Y., Nitta, Y., Imanaka, T., and Teranishi, S., "Surface State and Catalytic Activity and Selectivity of Nickel Catalysts in Hydrogenation Reactions, III. Electronic and Catalytic Properties of Nickel Catalysts," Journal of Catalysis, Vol. 64 (1980), pp. 397-404.

110. Okamoto, Y., Dukimo, K., Imanaka, T., and Teranishi, S., "Surface State and Catalytic Activity and Selectivity of Nickel Catalysts in Hydrogenation Reactions, IV. Electronic Effects on the Selectivity in the Hydrogenation of 1.3 Butadiene," Journal of Catalysis, Vol. 74 (1982) pp. 173-182.

111. Mustard, D.G. and Bartholomew, C.H., "Determination of Metal Crystallite Size and Morphology in Supported Nickel Catalysts," Journal of Catalysis, Vol. 67, (1981), pp. 186-206.

112. Dalmon, J.A., Mirodatos, C., Turlier, P., and Martin, G.A., "Evidence for Hydrogen Spillover in Partially Reduced Ni Catalysts from Magnetic and Infrared Studies, p. 169," Spillover of Adsorbed Species. Pajonk, G. M., B. J. Teichner and J. E. Germain, editor (Elsevier Science Publishers B.V., Amsterdam, 1983).

113. Tamaru, K., Dynamic Heterogeneous Catalysis, (Academic Press,New York, 1978).

114. Thomas, J.M., and Thomas, W.J., Introduction to the Principles of Heterogeneous Catalysis, (Academic Press, New York, 1967).

115. Happel, J., Cheh, H.Y., Otarod, M., Bajars, L., Hnatow, M.A., and Yin, F., "Transient Isotopic Tracing of Methanation Over Nickel and Molybdenum Sulfide," 8th International Congress of Catalysis, Vol. III (1984), pp. 395-404.

116. Bartholomew, C.H. and Pannell, R.B., "The Stoichiometry of Hydrogen and Carbon Monoxide Chemisorption on Alumina- and Silica-Supported Nickel," Journal of Catalysis, Vol. 65 (1980), pp. 390-401.

117. Pannell, R.B., Chung, K.S., and Bartholomew, C.H., "The Stoichiometry and Poisoning by Sulfur of Hydrogen, Oxygen and Carbon Monoxide Chemisorption on Unsupported Nickel," Journal of Catalysis, Vol. 46 (1977), pp. 340-347.

118. Fang, S.M., White, J.M., Campione, T.J., and Ekerdt, T.G., "CO Hydrogenation and Adsorption Studies on Supported-Nickel SMSI Catalysts," Journal of Ctalysis, Vol. 96 (1985), pp. 491-498.

119. Zagli, A.E., Falconer, J.L., and Keenan, C.A., "Methanation on Supported Nickel Catalysts Using Temperature Programmed Heating," Journal of Catalysis, Vol. 56 (1979), pp. 453-467.

120. Scott, K.F. and Phillips, C.S.G., "Deuterium-Exchange Chromatography on a Nickel/Silica Catalyst," Journal of Catalysis, Vol. 51 (1978), pp. 131-134.

121. Henrici-Olive, G., and Olive, S., The Chemistry of the Catalyzed Hydrogenation of CO, (Springer-Verbag, Berlin, Heidelberg 1984).

122. Christmann, K., Schober, O., Ertl, G., and Neumann, M., "Adsorption of Hydrogen on Nickel Single Crystal Surfaces," Journal of Chemical Physics, Vol. 60, No. 11 (1974), pp. 4528-4540.

123. Peebles, H.C., Peebles, P.E., and White, J.M., "Temperature Induced Structural Changes for Coadsorbed H_2 and CO on Ni(100)," Surface Science, Vol. 125 (1983) pp. L87-L92.

124. Cavanaugh, R.R., Kelley, R.D., and Rush, J.J., "Neutron Vibrational Spectroscopyt of Hydrogen and Deuterium on Raney Nickel," Journal of Chemical Physics, Vol. 77 (1982) pp. 1540-1547.

125. Bianchi, D., Tau, L.M., Borcar, S., and Bennett, C.O., "Nature of Surface Species on Supported Iron During CO/H_2 Reaction," Journal of Catalysis, Vol. 84, (1983), p. 358-374.

126 Margineanu, P., and Oloriu, S., "The Promoting Action of Chromia for Nickel Catalysts," Journal of Catalysis, Vol. 8 (1967), pp. 359-367.

127. Scholten, J.J.F., Pijpers, A.P., and Hustings, A.M.C., "Surface Characterization of Supported and Nonsupported Hydrogenation Catalysts," Catalysis Reviews - Science and Engineering, Vol. 27 (1985), pp. 151-206.

128. Lynch, J.F., Flanagan, T.B., "An Investigation of the Dynamic Equilibrium Between Chemisorbed and Adsorbed Hydrogen in the Palladium/Hydrogen System," Journal of Physical Chemistry, Vol. 77 (1973) pp. 2628-2634.

129. Suprez, D., Mendez, M., and Dalmon, J.A., "Characterization of Nickel Catalysts by Dynamic Volumetry and Magnetic Methods," Applied Catalysts, Vol. 21 (1986), pp. 1-10.

130. Raney, M., "Catalysts From Alloys," Industrial and Engineering Chemistry, Vol. 32, No. 19 (1940) pp. 1199-1203.

131. Kokeo, K.J., and Emmett, P.H., "The Role of Hydrogen in Raney Nickel Catalysts," Journal American Chemical Society, Vol. 81, (1959), pp. 5032-5037.

132. Weatherbee, G.D., and Bartholomew, C.H., "Effects of Support on Hydrogen Adsorption (Desorption Kinetics of Nickel)," Journal of Catalysis, Vol. 87, (1984), pp. 55-65.

133. Christmann, K., Schober, O., Ertl, G., and Neumann, M., "Adsorption of Hydrogen on Nickel Single Crystal Surfaces," Journal of Chemical Physics, Vol. 60, (1974), pp. 4528-4540.

134. McKee, D.W., "Interaction of Hydrogen and Carbon Monoxide on Platinum Group Metals," Journal of Catalysis, Vol. 8, (1967), pp. 240-249.